ECOLE POLYTECHNIQUE
PROMOTION X2004
SAUNIER Lauriane

RAPPORT DE STAGE D'OPTION SCIENTIFIQUE

# Assessment of DEMETER seasonal forecast performance over the Pan-VAMOS region

*Non confidentiel*

Option: Mécanique
Champ de l'option: MEC 591 - Océan, atmosphère et environnement
Directeur de l'option: M. Hervé LE TREUT
Directeur de stage: Mme Celeste SAULO
Dates du stage: du 10/04/2007 au 29/06/2007
Adresse de l'organisme: CIMA
Pab. II, $2^{do}$ piso, Ciudad Universitaria
(1428) Buenos Aires, Argentina

# Abstract

Seasonal forecasts have been a field of active research by many meteorological institutes over the last decade. The applications in social, medical and economical fields for these forecasts are numerous, and improved seasonal forecasting could help reduce the impact of extreme events such as severe droughts or above-normal precipitation on local population. The DEMETER project launched by the European Centre for Medium-Range Weather Forecasts (ECMWF) aimed at developing an improved seasonal prediction system using a multi-model constructed with Europe's state-of-the-art coupled global circulation models.

The goal of this internship was mainly to assess performance in monsoon precipitation seasonal forecasting by the DEMETER multi-model over the North and South American continents. Using the ECMWF DEMETER monthly mean 1-month lead forecasts initialized in May and November for the 1991-2001 period, performance over the North and South American Monsoon Systems were studied for boreal and austral summer. Comparisons between the seven individual model performances for a multi-model constructed as a mean of 63 individual model ensemble members were led for precipitation, 2 meter temperature, sea-surface temperature and 850 HPa circulation. Hindcast performances were assessed with respect to reference datasets available on the Internet, and different statistical scores were used to evaluate model bias, root mean square error, dispersion and their ability to reproduce interannual anomalies and variations.



# Résumé

Les prévisions saisonnières sont un domaine de recherche active de nombreux instituts de météorologie depuis maintenant une dizaine d'années. Les retombées sociales, sanitaires et économiques de ces prévisions sont nombreuses, et l'amélioration des prévisions saisonnières pourraient contribuer à diminuer l'impact d'événements extrèmes comme une secheresse exceptionnelle ou une précipitation au dessus de la normale sur les populations locales. Le projet DEMETER, lancé par le Centre Européen de Prévisions à Moyen Terme (ECMWF) visait à concevoir un système de prévisions saisonnières amélioré en utilisant un multi-modèle, construit à partir des meilleurs modèles globaux couplés européens.

Le but de ce stage d'option est principalement d'évaluer les performances du multi-modèle de DEMETER en matière de prévisions saisonnières de la précipitation en Amérique du Nord et Amérique du Sud. Les performances au dessus des régions touchées par les moussons Nord-Américaine et Sud-Américaine pendant l'été boreal et austral sont étudiées à l'aide des prévisions calculées avec un mois d'avance initialisés en Mai et Novembre de 1991 à 2001. Les résultats des 7 modèles individuels ainsi que du multi-modèle, construit comme la moyenne de 63 prévisions individuelles pour la précipitation, la température à 2 mètres du sol, la température de surface de la mer ainsi que la circulation atmosphérique à 850 HPa d'altitude sont comparés. Les performances des "rétrovisions" sont évaluées par rapport à des banques de données disponibles sur Internet, et différents scores statistiques sont calculés pour évaluer l'erreur, la moyenne quadratique de l'erreur, la dispersion entre modèles et leur capacité à reproduire les variations inter-annuelles et les anomalies.

# Contents

# Part 1

# Introduction

## 1.1 Overview of knowledge on the American Monsoon System

### 1.1.1 Research programs on the American Monsoon System

The North and South American continents present high climate variability due to diverse geographical characteristics and its latitudinal extent from Arctic to Antarctic zones. One of the major issues in weather/climate prediction over the Americas is predictability of precipitation. Some specific areas witness often heavy rains involving floods, whereas others are victims of severe droughts. Both North and South American continents are characterized by a monsoon circulation system which develops during the warm season over low-latitude continental regions, namely the NAMS (North American Monsoon System) and the SAMS (South American Monsoon System). Monsoon systems are a result of thermal contrast between continental and adjacent oceanic regions, and are an important component of warm season precipitation in these regions.

Improving the understanding and prediction of the American Monsoon System is one major goal of the WCRP/CLIVAR/VAMOS (World Climate Research Program/ Climate Variability and Predictability/ Variability of the American Monsoon Systems) program started in 1998. Complementary programs over North and South America, NAME (North American Monsoon Experiment) and MESA (Monsoon Experiment South America) have common objectives over each geographical area, one of them being to improve the monthly-to-seasonal prediction of the monsoon. These projects have led to numerous publications improving theoretical and technical knowledge on the monsoon systems' physical characteristics and predictability.

### 1.1.2 Seasonal evolution of the American Monsoon Systems

The two American Monsoon Systems exhibit a clear annual cycle, with onset, mature and decay phases with symmetry with respect to the equator (figure 1.1 [Vera et al., 2006]). Both NAMS and SAMS exhibit typical characteristics of monsoon systems: a strong land-sea breeze, heavy summer precipitation, an upper-level anticyclone, a low-level trough and intensification of a low-level jet. However, the SAMS characteristics differ from most monsoon systems, since most of the continental portion of South America is mostly situated in the Tropics, therefore reducing seasonal temperature differences. Figure 1.1 shows that SAMS precipitation during the mature phase is much greater than NAMS precipitation, however both monsoons' mature phase accounts for over 50 % of annual precipitation over the continent.

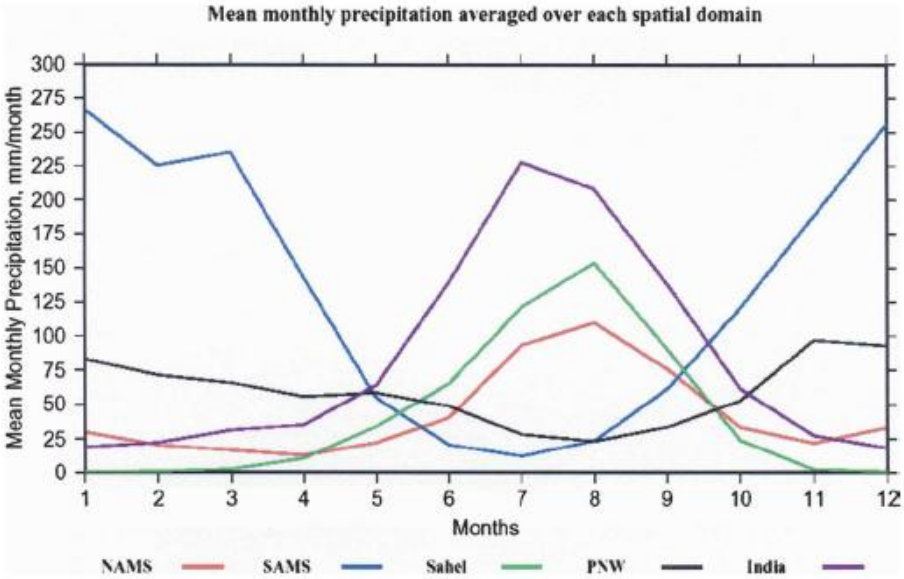


Figure 1.1: *Mean annual cycle of precipitation over several major monsoon areas, figure 1 [Vera et al., 2006].*

The annual cycle of the American Monsoon systems can be described as follows. In May-June, heavy rainfall progresses northward from Mexico into south-western United States beginning of July, accompanied by sudden changes in weather conditions. The NAMS mature phase lasts from July to early September, with the heaviest rains located in Mexico, over the Bay of Campeche (location of the maximum of climatological mean precipitation, see [Vera et al., 2006]). The onset of the South American Monsoon coincides with the decay of the North American Monsoon, when the convection migrates from Central America to equatorial Amazon, from September to October. The mature phase of SAMS occurs from December to February, and the maximum precipitation is located over Central Brazil. A more complete description of the SAMS and NAMS evolutions will be done in the next chapter of this report.

The seasons of interest in this report are boreal and austral summer, respectively June, July and August, and December, January and February, corresponding to each monsoon system's mature phase.

### 1.1.3 Regional circulation features

The monsoonal behavior of rain affects both lower and upper-level circulation over a large area. Figure 1.2 shows regional circulation features for NAMS and SAMS regions. The figures exhibit the main components of each system as well as their differences. The different phases of the monsoon systems are related to variations in position and/or intensity of these regional features. The South American continent has important land-surface areas located in the Tropics, and the presence of the Amazon rainforest provides an important moisture source for the SAMS. The North American system is associated with two low-level jets (LLJ) both east and west of the Sierra Madre, directed northward. These two jets convect warm air from the tropical regions towards cooler sub-tropical regions, therefore increasing precipitation occurence over the regions affected by the jet. In South America, only one LLJ (directed southward) is found east of the Andes, and convects warm

moist air from the Amazon onto the exit zone of the jet over the La Plata Basin.

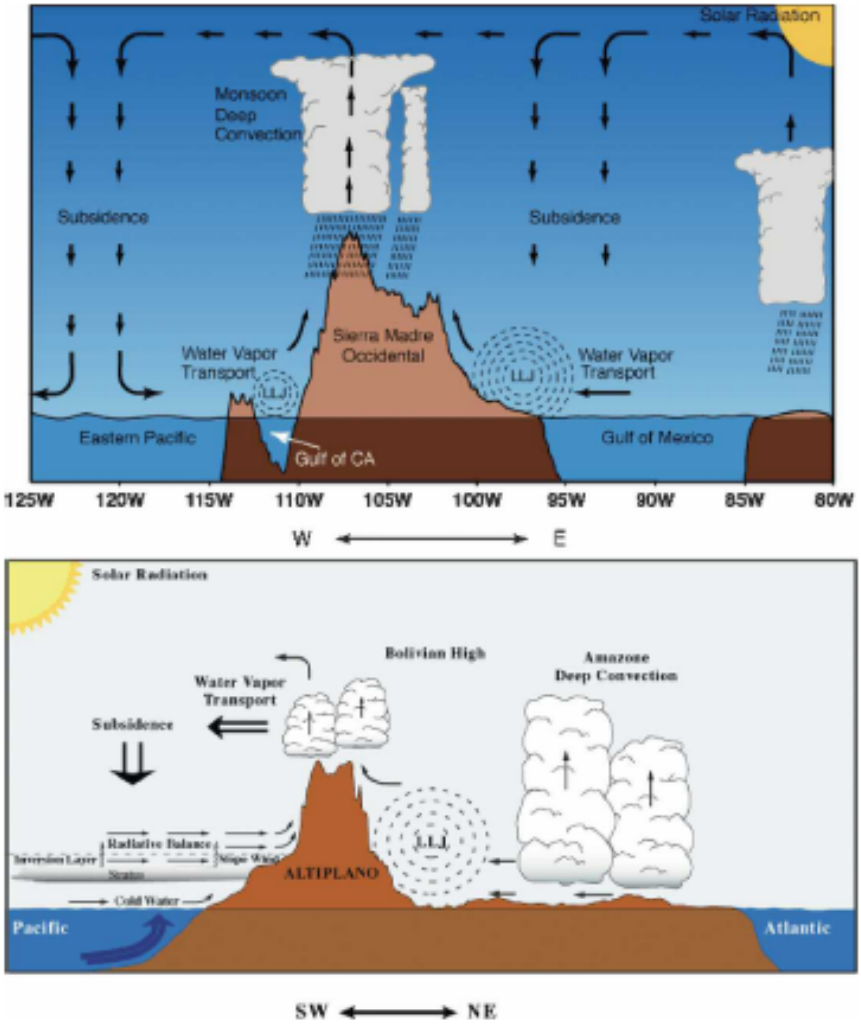


Figure 1.2: *Regional circulation features for NAMS and SAMS. The top figure is a cross-section through the NAMS at 27.5° N, and the bottom figure is a SW-NE cross section showing elements affecting SAMS, figure 3 [Vera et al., 2006].*

In North America, NAMS affects locally precipitation over Mexico and Southwestern United States, but also influences precipitation and circulation patterns over distant regions, such as the US Midwest. The onset of NAMS implies the development of low-level jets (LLJ) over the Gulf of California, and changes in rainfall over regions not directly impacted by the monsoon, such as the Great Plains region where precipitation decreases [Higgins et al., 1997]. Higgins et al. demonstrated that the Great Plains LLJ-related rainfall is controlled by changes in large-scale flow related to the evolution of NAMS.

During austral summer, when SAMS is in its' mature phase, a convection band called SACZ (South Atlantic Convergence Zone) extends from Southern Amazonia to South East Brazil into the Atlantic Ocean. This area of South America witnesses maximum rainfall during the monsoon mature phase, and this phenomena is accompanied by the establishment of the Bolivian High east of the Andes, near 15° S and 65° W ([Marengo et al., 2004]). Intensity of the South American Low Level Jet (SALLJ) is also modulated by SAMS.

## 1.2 Seasonal to inter-annual forecasting over the Pan-VAMOS region

Many meteorology researchers are currently focusing on the issue of seasonal predictions. As explained by Tim Palmer of the European Center for Medium-range Weather Forecasts (ECMWF), "seasonal climate forecasting is of enormous value in its own right. However, as stressed in many of the IPCC assessment reports, seasonal forecasting can also be important as a means of assessing the reliability of climate change predictions". This explains why many research centers have initiated seasonal forecasting projects in the last decade. However, efficient seasonal forecasting relies on global ocean and atmosphere circulation models, and small inaccuracies on short time scales can lead to high errors when it comes to seasonal and intra-seasonal forecasting. As explained by Nobre et al. [Nobre et al., 2006], climate variability at seasonal to inter-annual has two main components: besides the atmospheric variability influenced by daily weather variations and atmospheric conditions, another key component is the external forcing, depending on longer time scale variations of boundary conditions such as sea-surface temperature and soil moisture. These two aspects of the monsoon systems variability are therefore presented in this section.

### 1.2.1 Seasonal and inter-annual variability of the monsoon systems

#### The role of SACZ and ITCZ on intra-seasonal variability

The intensity of SACZ is directly related to the rainfall pattern over the subtropical plains of South America: a strong/weak SACZ implies weakened/enhanced precipitation over the subtropical plains; use of time series of reanalysis data showed evidence of a 10-day see-saw pattern alternating both tendencies [Paegle and Mo, 1997] when the SACZ is displaced toward the Atlantic Ocean. Further research has enabled to determine more precise links between different intraseasonal oscillations such as the Madden-Julian Oscillation and the dipole pattern between precipitation over SACZ or downstream of the SALLJ ([Liebmann et al., 2004] and references therein).

The ITCZ (Intertropical Convection Zone) is a belt of ascending moisture located around the Equator, as part of the Hadley circulation cells. While the Pacific ITCZ's position shifts from the southern hemisphere tropics in austral summer to the northern hemisphere tropics in boreal summer, the Atlantic ITCZ's position shifts less and it is predominantly located north of the equator. ITCZ position plays an important role on precipitation. During boreal summer, the Pacific ITCZ merges with the Core NAM precipitation region over Mexico, and during austral summer, the Atlantic ITCZ shifts southward and weakens, and the Core SAM precipitation region merges with the SACZ. ITCZ position and intensity are closely related to sea surface temperatures over the Pacific and Atlantic oceans.

#### The role of SST on inter-annual variability

Sea-surface temperature (SST) influence on precipitation during the monsoons' mature phase can be local or remote, depending on the regions of interest. Bearing in mind that SSTs are also used as boundary conditions for atmospheric circulation models, it is important to examine its' influence over continental regions. For instance, SST anomalies can modulate the intensity of SACZ and ITCZ, therefore impacting interannual variability of rainfall over tropical South America and Brazil ([Nobre et al., 2006] and references therein).

Several geographical areas are subject to inter-annual SST anomalies, such as El Niño Southern Oscillation (ENSO). These anomalies seem to have some impact on seasonal and inter-annual precipitation and prediction skills ([Vera et al., 2006] and references therein). ENSO impacts will be discussed in Part 2.

#### The role of land surface conditions

Land surface conditions are an example of plausible local precipitation and circulation forcing. In the case of SAMS, soil moisture during spring was shown to have an influence on variation of monsoon precipitation by acting on the moisture flux over Southeast Brazil [Grimm et al., 2007]. Other studies ([Ferreira et al., 2006] and [Collini et al., 2006]) show high sensitivity of circulation and precipitation to changes in land use and soil moisture.

### 1.2.2 Overview of model performances in seasonal forecasting of the AMS

Although many studies have led to a good overall knowledge of the physical processes that modulate the American Monsoon Systems and their seasonal to inter-annual variability, this progress is still difficult to assess in the models' seasonal forecasts. Most models show low to moderate skill when it comes to precipitation, this skill depending highly on the region of interest.

#### Predictability over North and South America

An efficient seasonal prediction should provide reliable mean climate information and reproduce physical influences. State-of-the-art models used today for seasonal predictions encounter difficulties when it comes to representing the amplitude of intraseasonal variability and importance of teleconnections and physical forcing mechanisms.

A study of seasonal to decadal predictability of South American climate by atmospheric global circulation models (AGCMs) [Nobre et al., 2006] shows that AGCM skill in predicting precipitation over South America depends greatly on the region: indeed, results presented demonstrate the models' ability to predict seasonal rainfall over the Brazilian Nordeste region and poor results over the South East Brazil region. A physical explanation is that the prediction skill of non-coupled models depends on two components: the internally forced variations (atmospheric circulation) and externally forced variations (boundary conditions including sea surface temperature). Different regions face different types of external forcing: in the Tropics, rainfall variance is more affected by SST anomalies whereas land-atmosphere feedback plays a more significant role in rainfall variance over southeast Brazil and the SAM core precipitation zone. According to Nobre et al., 2006, climate prediction over South America therefore depends on effective forecasting tools for the external parameters used in AGCMs, such as SST or land-surface feedback, or on the development of coupled models including ocean, atmosphere and surface feedbacks.

As part of the NAME project, global and regional circulation model performances in monsoon precipitation prediction were evaluated [Gutzler et al., 2005]. The global models were shown to encounter difficulties in forecasting the monsoon onset date, and although they represented the geographical spread of precipitation

patterns from June to August quite well, they failed to capture the maximum precipitation period, placing it in August instead of July over the Core NAM region. Global models were later shown to have problems in constraining surface quantities such as temperature or heat fluxes, and reproducing linkages between low-level jets and precipitation. As over South America, prediction skill depends on model ability in reproducing internal and remotely forced variations. The effect of the Madden-Julian Oscillation (an intraseasonal fluctuation modulating tropical rainfall patterns), ENSO and land surface conditions on boreal summer NAM precipitation is discussed by [Higgins and Gochis, 2007] and references therein.

**DEMETER and ensemble forecasting**

Ensemble forecasting is a method used in weather prediction models since the early 1990s. It has been an alternative to represent the diverse states that the atmosphere can develop from slightly different initial conditions, as discovered by Lorenz (1963). This discovery encouraged researchers to use perturbations in initialization of models when predicting weather for long time scales, constructing what is called "ensembles". These perturbations can contain the natural dynamical perturbations that develop with time, and in longer time scales, the ensemble average forecast has higher performance than the zero-perturbation forecast, since some uncertain components average out. Another advantage of ensemble forecasting is showing different outcome possibilities for one initial state. Using different ensembles can illustrate the probability of a particular event and the uncertainty of the zero-perturbation forecast [Kalnay, 2003]. This development enabled researchers to extend forecasts further than the two-week empirical limit, and start focusing on monthly to seasonal time periods.

An inventory of state-of-the-art European coupled models was made very recently by ECMWF (European Centre for Medium-Range Weather Forecasts) as part of the DEMETER project (**D**evelopment of a **E**uropean **M**ultimodel **E**nsemble system for seasonal to in**TER**annual prediction). This project aims to improve seasonal weather predictions by developing a multi-model ensemble forecast system [Palmer et al., 2004]. Improvements in precipitation forecasting using the multi-model ensembles has been proven using various statistic and probabilistic scores, but no specific study of the American Monsoon System is available neither on the DEMETER website nor in the literature.

Although the models used in this project are amongst the best models available, all contain systematic errors characteristic of coupled GCMs that considerably affect forecasting skill over some regions, such as errors in El Niño simulation, ITCZ position and Atlantic SSTs. Figure 1.3 shows all individual models of the DEMETER projects' mean hindcasts for austral summer (DJF) 1991-1992 to 2001-2002, and mean precipitation values obtained by CMAP data for the same period. This figure illustrates the fact that models tend to predict different precipitation values and place precipitation regions differently, and shows the interest of combining models to reduce error: this technique is called the multi-model ensemble approach, or MME.

The MME aims to reduce some of these systematic errors by combining the different coupled GCM outputs into one multi-ensemble mean forecast. The seven models used as part of the DEMETER project are the CERFACS (Centre Européen de Recherche et de Formation Avancée en Calcul Scientifique, France), ECMWF (European Center for Medium-Range Weather Forecasts, international organization), INGV (Instituto Nazionale de Geofisica e Vulcanologia, Italy), LODYC (Laboratoire d'Océanographie Dynamique et de Climatologie, France), CNRM (Centre National de Recherches Météorologiques, Météo-France, France), MetOffice (The Met Office, UK) and MPI (Max Planck Institut für Meteorologie, Germany). From now on the models will be referred to by their abbreviations. The different models and their characteristics are shown in table 1.4 taken from [Palmer et al., 2004].

For each model, nine different ensemble "hindcasts" (retrospective forecasts) generated every three months (February, May, August and November) are available online for the 1980-2001 time period. Ensemble gener-

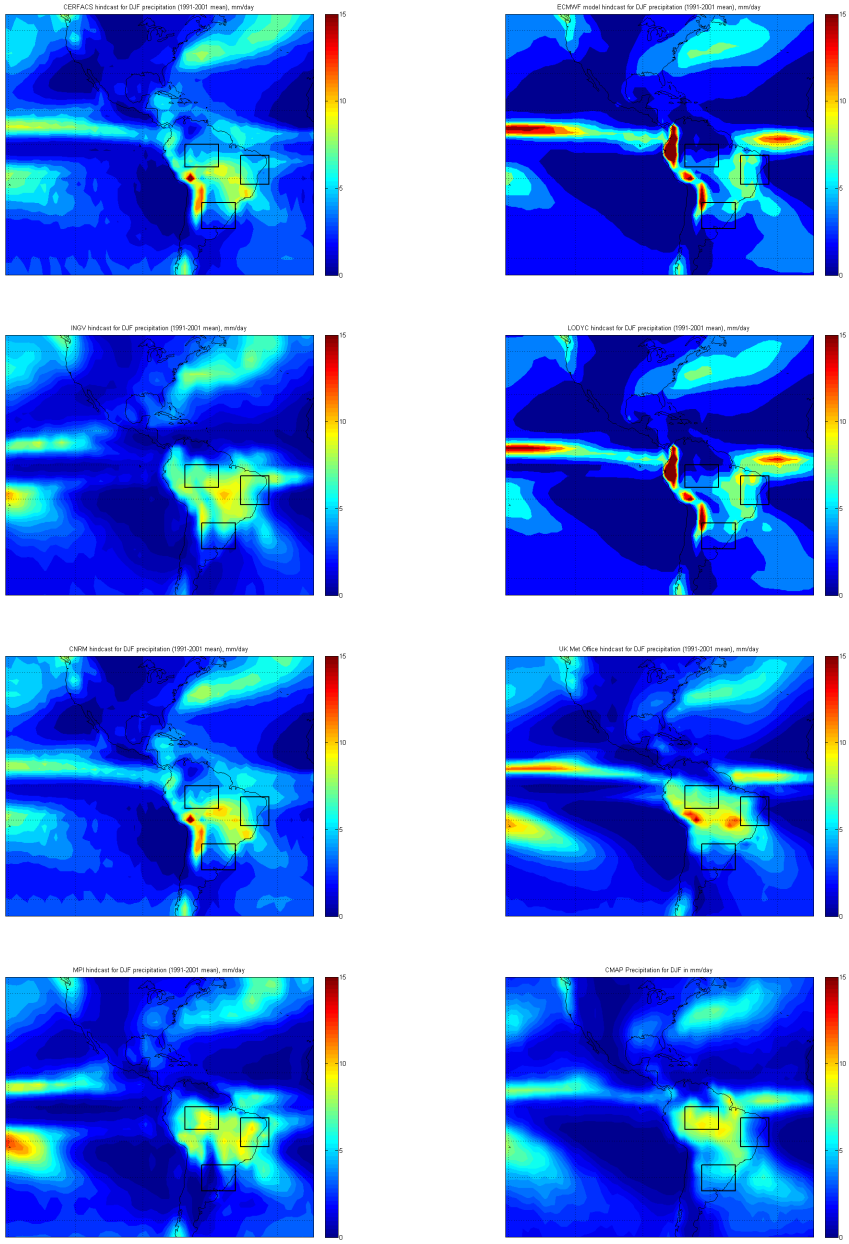


Figure 1.3: *Mean daily precipitation (mm/day) hindcasts for December, January and February (DJF) 1991-1992 to 2001-2002 for all DEMETER individual models, and CMAP reference precipitation data for the same period (bottom right). Models from left to right and top to bottom: CERFACS, ECMWF, INGV, LODYC, CNRM, MetOffice, MPI.*

| | CERFACS | ECMWF | INGV | LODYC | Météo-France | Met Office | MPI |
|---|---|---|---|---|---|---|---|
| atmosphere component | ARPEGE | IFS | ECHAM-4 | IFS | ARPEGE | HadAM3 | ECHAM-5 |
| resolution | T63<br>31 Levels | T95<br>40 Levels | T42<br>19 Levels | T95<br>40 Levels | T63<br>31 Levels | 2.5° x 3.75°<br>19 Levels | T42<br>19 Levels |
| atmosphere initial conditions | ERA-40 | ERA-40 | coupled AMIP-type experiment | ERA-40 | ERA-40 | ERA-40 | coupled run relaxed to observed SSTs |
| reference | Déqué 2001 | Gregory et al. 2000 | Roeckner 1996 | Gregory et al. 2000 | Déqué 2001 | Pope et al. 2000 | Roeckner 1996 |
| ocean component | OPA 8.2 | HOPE-E | OPA 8.1 | OPA 8.2 | OPA 8.0 | GloSea OGCM, based on HadCM3 | MPI-OM1 |
| resolution | 2.0° x 2.0°<br>31 Levels | 1.4° x 0.3°-1.4°<br>29 Levels | 2.0° x 0.5°-1.5°<br>31 Levels | 2.0° x 2.0°<br>31 Levels | 182 GP x 152 GP<br>31 Levels | 1.25° x 0.3°-1.25°<br>40 Levels | 2.5° x 0.5°-2.5°<br>23 Levels |
| ocean initial conditions | ocean analyses forced by ERA-40 | ocean analyses forced by ERA-40 | ocean analyses forced by ERA-40 | ocean analyses forced by ERA-40 | ocean analyses forced by ERA-40 | ocean analyses forced by ERA-40 | coupled run relaxed to observed SSTs |
| reference | Delecluse and Madec 1999 | Wolff et al. 1997 | Madec et al. 1998 | Delecluse and Madec 1999 | Madec et al. 1997 | Gordon et al. 2000 | Marsland et al. 2002 |
| ensemble generation | windstress and SST perturbations | windstress and SST perturbations | windstress and SST perturbations | windstress and SST perturbations | windstress and SST perturbations | windstress and SST perturbations | 9 different atmospheric conditions from the coupled initialization run (lagged method) |

Figure 1.4: *DEMETER coupled GCM characteristics for atmosphere and oceanic components and initialization procedures. Table 1 [Palmer et al., 2004].*

ation is done using the following method to construct 9 different ocean initial conditions: for every hindcast initialization, the reference initial ocean state (control) referred to as "ensemble 0" is provided by ERA-40 reanalysis (ECMWF 40 year Re-Analysis) data for momentum, heat flux and mass flux. Then, perturbed states are constructed by adding/subtracting randomly selected daily positive/negative wind stress perturbations and adding/subtracting SST perturbations to the ocean analyses. This forms a total of 8 perturbed initial states [Palmer et al., 2004]. This initialization procedure is used for 6 of the 7 models in the DEMETER project. For the MPI model, 9 different atmospheric initial conditions are used.

The DEMETER data used in this project was provided by the ECMWF-DEMETER data server on the ECMWF website, interpolated over a 2.5° latitude by 2.5° longitude grid.

## 1.3 Project aim and methodology

### 1.3.1 Project aim

The aim of this project is to assess the performance of seasonal forecasts over the Pan-VAMOS region, specifically during the summer monsoon period. The forecasts used in this project are those made available by the ECMWF DEMETER project. They are "hindcasts" of monthly means of different fields (such as surface temperature or precipitation) from 1991 to 2002 achieved by merging the seven different DEMETER coupled global circulation models. The hindcasts referred to as "multi-model" hindcasts were obtained by computing the mean of all model ensembles, therefore averaging a total of 63 ensemble members. So as to estimate the forecast performance, these hindcasts are compared to public analyzed datasets.

### 1.3.2 Methodology

#### Choice of specific regions

Specific regions greater than 35 grid points in size were chosen in order to examine core monsoon regions, regions of high predictability and regions of poor predictability or peculiar rainfall variability. Region names and geographical limits are shown in table 1.1.

| | **Region name** | **Geographical coordinates** |
|---|---|---|
| SAMS | Core Amazon Region | [10° S - 0° N, 57.5° W - 70° W] |
| SAMS | Northeast Brazil (Nordeste) | [16° S - 5° S, 35° W - 45° W] |
| SAMS | La Plata Basin | [25° S - 33° S, 50° W - 62.5° W] |
| NAMS | US Southwest and Northern Mexico | [22° N - 35° N, 105° W - 115° W] |
| NAMS | Inter-Americas zone | [10° N - 22.5° N, 107.5° W - 117.5° W] |
| NAMS | Great Plains region | [30° N - 40° N, 85° W - 100° W] |

Table 1.1: *Different regions of study used for the DEMETER model hindcast skill assessments.*

For the SAMS region, the regions of interest were chosen in reference with the bibliography. Specific studies of regional and global atmospheric circulation model performances in predicting precipitation over similar regions have been led. The regions chosen here are similar to those studied by Seth et al. [Seth et al., 2007] to assess regional model climatology performances. The Core Amazon Region chosen in this project is the region of maximum precipitation during the SAMS mature phase, and is a primordial region for its land surface feedback importance in moisture transport over the South American continent. Therefore, performance in fields such as temperature can be of particular interest over this region. The Nordeste (Brazilian Northeast) region was chosen as a "reference" region for model performance, since this region is commonly cited as a high predictability area, at least when it comes to high resolution regional models. The La Plata Basin region was chosen as the exit region of moisture transported by the SALLJ. It is also a region of high intra-seasonal precipitation variability and where models commonly encounter some predictability problems.

For the NAMS region, regions were chosen following similar criteria. The Core NAMS region is the US Southwest and Northern Mexico area, where even regional models have trouble representing precipitation evolution during the NAMS mature phase [Mo et al., 2005]. The Great Plains region is the North American "equivalent" to the La Plata Basin, since it is also influenced by a low-level jet, even if precipitation regimes and geographical characteristics are different. Finally, the Inter-Americas zone was chosen for its geographical

situation in the Tropics, where precipitation amounts are considerable and global models generally tend to have higher performance.

#### Choice of fields of study

The first parameter of interest in this study of the American Monsoon System forecasts was total precipitation. Comparing DEMETER hindcasts to monthly precipitation datasets for the same time period highlight strengths and weaknesses of these models over different regions of North and South America.

The next step of this project was to analyze other parameters physically related to rainfall, in order to enhance comprehension of model performance over the specific regions, and uncover links between these parameters and rainfall prediction.

### 1.3.3 Reference Datasets

#### The CPC Merged Analysis of Precipitation Data (CMAP)

The Climate Prediction Center's Merged Analysis of Precipitation (CMAP) data is issued from a technique combining raingauge observations and precipitation estimations obtained from satellite measures in infrared and microwave wavelength. Data is placed on a 2.5 by 2.5 latitude/longitude grid, enabling easy comparison with DEMETER precipitation hindcasts. CMAP data starts in 1979, and input data sources have evolved since then, but the estimates used for the period of interest in this project (1991 to 2001) are issued from the same satellites. Two datasets are available, one using additional numerical model predictions in the merged analysis, one based only on observations. The version without numerical model predictions was chosen in order to have a clear distinction between prediction and observation. CMAP data is available as monthly mean precipitation in mm/day.

More precisions on the CMAP merging technique can be found in the bibliography [Xie and Arkin, 1996].

#### ERA-40 Re-analysis Data (ERA-40)

ERA-40 (ECMWF 40 year re-analysis) is another project of the European Center for Medium-Range Weather Forecasts (ECMWF). This project's goal was to provide global analyses of atmospheric, surface and land conditions for the 1957-2002 period. More information on the project can be found in the literature [Uppala et al., 2005]. The ECMWF ERA-40 website provides daily and monthly mean fields computed every 6 hours and monthly mean daily fields. The ERA-40 fields used in this report were the monthly mean daily 2 meter temperature fields and the monthly mean 0:00 GMT 850 HPa circulation fields, both with 2.5 by 2.5 degree latitude/longitude resolution, so as to match with the DEMETER project hindcasts.

#### The NCEP Reynolds Optimally Interpolated SST datasets (Reynolds SST)

The NCEP (National Centers for Environmental Prediction) Reynolds O.I. version 2 SST dataset provides weekly and monthly means of global sea surface temperature fields. The data is issued from in-situ observations (buoys and boats) as well as satellite data provided by NOAA Advanced Very High Resolution Radiometer, optimally interpolated using an algorithm developed by R.W. Reynolds [Reynolds et al., 1994]. The radiometer is carried by four NOAA polar orbiting satellites, and measures emitted and reflected radiation from Earth in two visible and three infrared channels.

Grid size is 1 degree longitude by 1 degree latitude. This implies that additional interpolation had to be computed in order to adapt the data to the DEMETER grid size. This was done using bilinear interpolation.

# Part 2

# Initial study of the American Monsoon System

In this chapter, a study of the American Monsoon System is done using the reference datasets, and an initial comparison is made with the DEMETER multi-model hindcasts so as to demonstrate their performance over the American continents and over regions of particular interest for further study. Mean fields over the 1991 to 2001 period are presented for boreal and austral summer, as well as fields for particular years. A "reference" year of 1993-1994 was chosen so as to illustrate evolution of precipitation in various regions. 1993-1994 was a year with no particular ENSO anomaly with average values for all of the fields studied.

## 2.1 Summer monsoon precipitation in North and South America

### 2.1.1 SAMS Precipitation during austral summer

As shown by figure 1.1 in the introduction of this report, the SAMS brings stronger precipitation than the NAMS, with monthly means during its peak comparable to those measured in India during the monsoon season.

Figure 2.1 page 16 shows mean daily precipitation during austral summer season (December to February) over North and South America. This mean daily precipitation was calculated using CMAP data for December 1991 to February 2002. This eleven-year period is used as the reference climatology for this study. The strongest precipitation is found in the Core Amazon Region, south of the equator, where daily rainfall amounts reach more than 9 mm/day. Over the Atlantic, strong precipitation (5 mm/day and above) can be seen just north of the Equator, associated with the Intertropical Convergence Zone (ITCZ) and another area that extends toward the South East Atlantic referred to as the South Atlantic convergence zone (SACZ).

It is important to notice that precipitation is close to zero in the Intra-Americas zone and in the Southwest of the United States, which will be of use when studying NAMS.

#### Evolution of SAMS as shown by CMAP precipitation data

In order to better grasp the evolution of SAMS, monthly means of daily precipitations were used, so as to give further detail on the geographical distribution and intensity of precipitation during the onset and peak

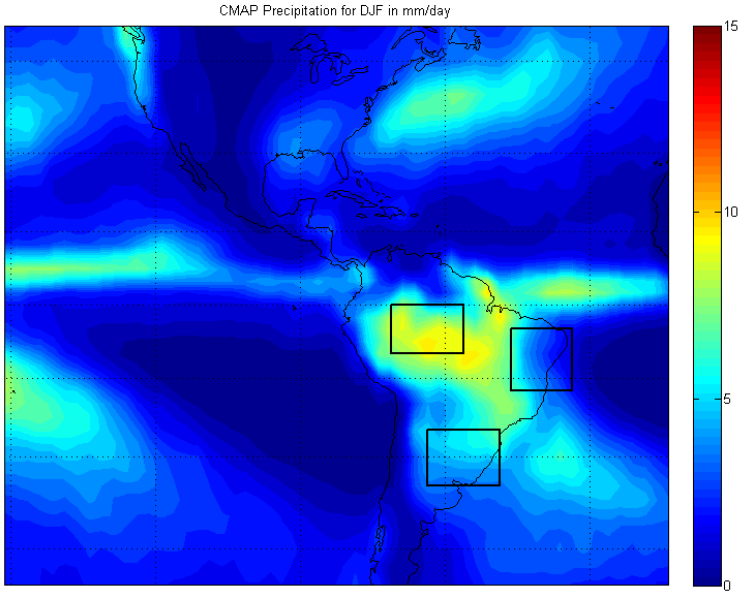


Figure 2.1: *Mean daily precipitation for December, January and February over the PAN-Vamos region, according to CMAP precipitation data averaged from 1991-1992 to 2001-2002 (mm/day).*

phases of the SAMS. The 1993-1994 period has been selected to show this evolution. Figures 2.2 page 17 show monthly means of daily precipitation (mm/day) from October 1993 to March 1994.

During October and November ([a] and [b]), precipitation moves progressively south as the Pacific ITCZ moves southward and produces less precipitation. The Atlantic ITCZ becomes very active, with precipitation reaching 15 mm/day in some regions. Strong precipitation (over 5 mm/day) appears over the La Plata Basin region and the Core Amazon. The SAMS exhibits it's mature phase from November to February ([b] to [e]) and is characterized by a progression of the precipitation south eastward, and the formation of the SACZ. Though not completely evident from these figures, a tendency of enhanced/weakened precipitation over SACZ can be associated with less/more precipitation over La Plata Basin. This observation is consistent with the dipole in the monsoon precipitation regime documented by Paegle and Mo [Paegle and Mo, 1997]. In December, precipitation is important over the entire southern tropical region, save North East Brazil, ranging from 5 to 8 mm/day. Precipitation over the equatorial Atlantic is very strong, reaching more than 10 mm/day. In January, precipitation is intensified over the Core Amazon Region and Northern Brazil, and the zone of rainfall over 6 mm/day that reached into the La Plata Basin region has pulled back into Central Brazil. In February, very strong rainfall is observed over the Core Amazon Region (between 10 and 15 mm/day), while heavy precipitation is also measured in the northern La Plata Basin area (over 10 mm/day). March ([f]) marks the beginning of the monsoon decay phase. While heavy rains are still measured over Brazil and the Western Amazon, precipitation over the La Plata Basin is reduced to less than 5 mm/day.

These observations are coherent with climatologies of SAMS, and illustrate the progress of the SAMS over

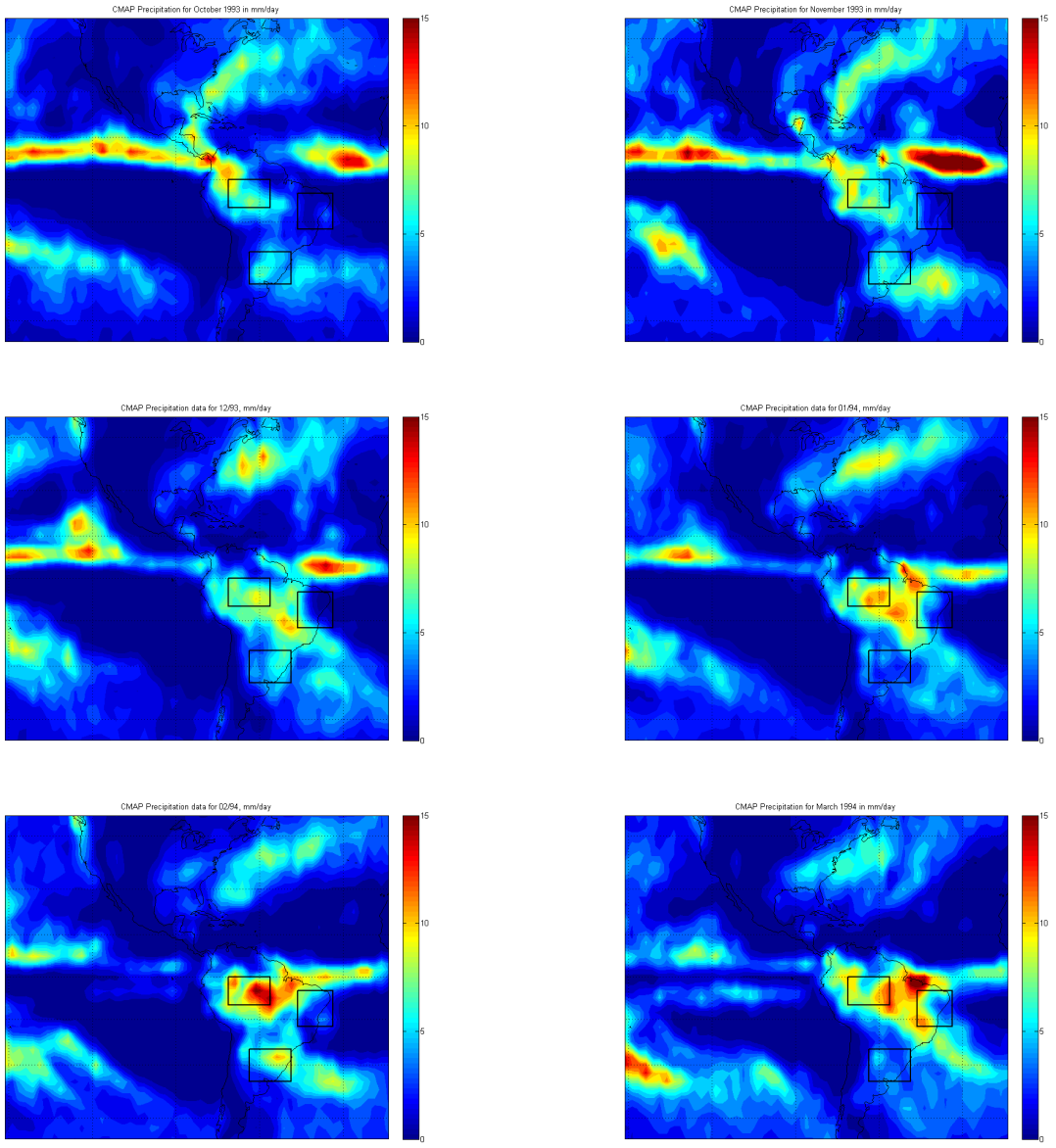


Figure 2.2: *Mean daily precipitation (mm/day) from October 1993* [a], top left *to March 1994* [f], bottom right *as provided by CMAP precipitation data. Peak SAM precipitation occurs during austral summer, from December* [c] to February [e].

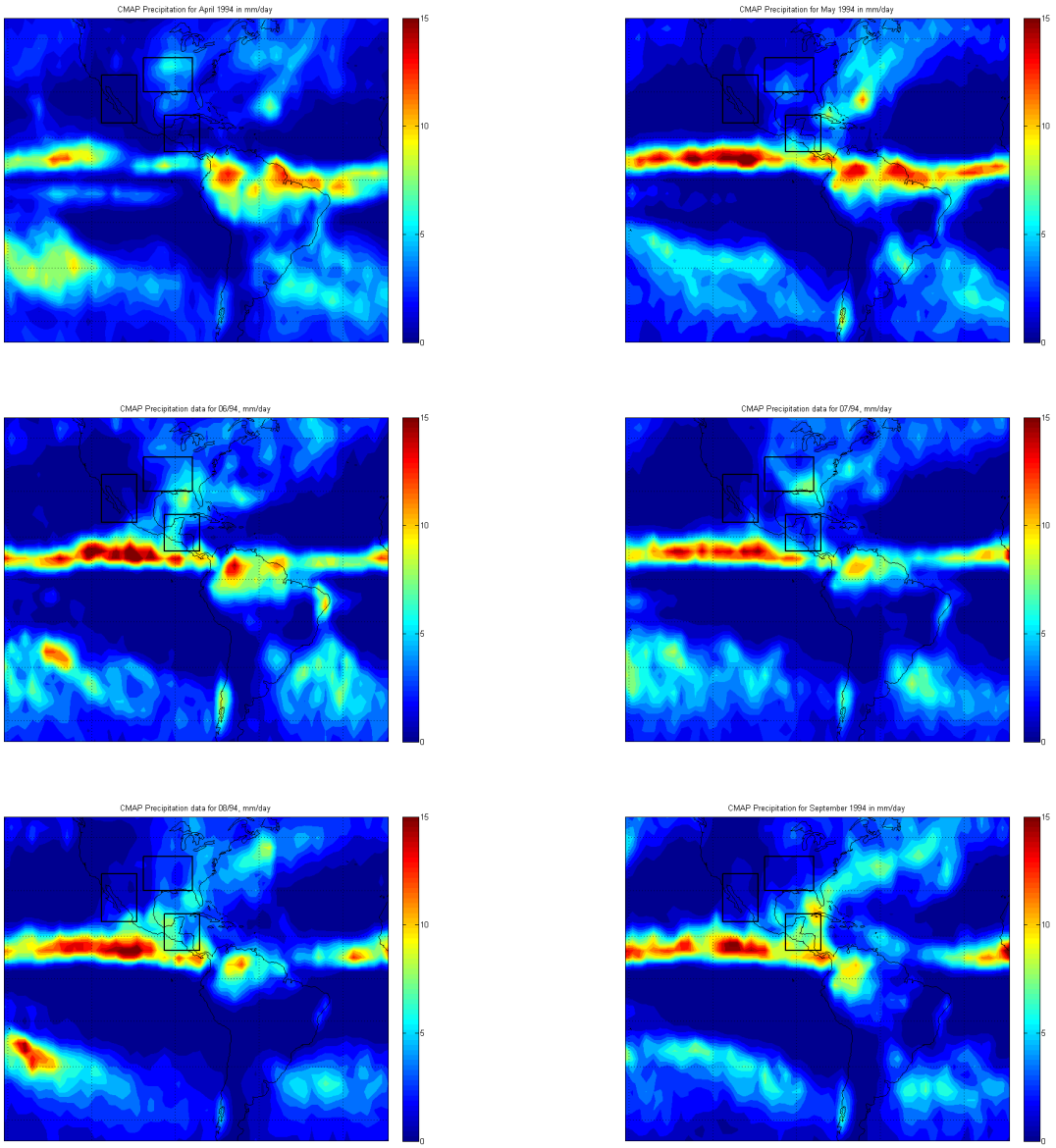


Figure 2.3: *Mean daily precipitation (mm/day) from April* [a], top left *to September 1994* [f], bottom right *as provided by CMAP precipitation data. Peak NAM precipitation occurs from late June to early September, and the boreal summer period studied here is June, July and August* [c] [d] and [e].

the South American continent [Vera et al., 2006].

**Performance and limitations of the DEMETER multi-model**

After a study of the evolution of precipitation during the SAMS onset and peak season, the DEMETER project models' skill in recognition and prediction of the SAMS characteristics was examined. So as to study seasonal predictions of the SAMS, one to three-month hindcasts started in November from 1991 to 2001 (predicting monthly means for December to February) were used. Figure 2.4 page 20 shows the mean multi-model hindcast of austral summer precipitation averaged over eleven years of hindcasts, and it's bias with respect to CMAP precipitation data. The multi-model misplaces the area of maximum precipitation south-east of the actual core SAMS region, therefore over-estimating precipitation over North-East Brazil (up to 3 mm/day difference) and underestimating precipitation over the Core Amazon Region (up to -5 mm/day difference). Over the La Plata Basin area, precipitation is underestimated by 1 to 2 millimeters per day. Independent studies of mean hindcasts for December, January and February for the same time period show the same tendencies, with errors growing from one month to the next.

High overestimation of precipitation over the Andes is also visible, but cannot be accounted for considering the difficulty of obtaining accurate rain gauge measures of precipitation over such regions. However, some models perform better than others over high topography. Some models such as the LODYC model overestimate precipitation over Peru and the Bolivian Altiplano. All models tend to contribute to the multi-models' error in the SAMS core region location, and most models overestimate precipitation over North East Brazil and underestimate precipitation over the Core Amazon Region, but this behaviour depends on the year and the model studied.

So as to further examine the performance of the multi-model in forecasting precipitation, spatial root mean square errors over the three regions of study were calculated for December, January and February of each year. For each month, the spatial root mean square error is defined by equation 2.1, where n is the number of grid points in the domain, $F_i$ is the forecast and $O_i$ the observed precipitation for grid point i.

$$RMSE = \sqrt{\frac{\sum_{i=1}^{n} (F_i - O_i)^2}{n}} \tag{2.1}$$

Bias and root mean square error with respect to CMAP data over La Plata Basin in February are shown in figure 2.5 page 21. Results for December and January are similar (not shown). For most years, the multi-model underestimates mean precipitation. This is consistent with the mean 1991-2001 bias observed earlier. The bias scores (figure [a]) for the multi-model are not as good as some models, due to high bias for the MPI model. Observing figure [b], one sees the differences in performance between the models used in the DEMETER project over this particular region, and the overall improvement of root mean square error scores achieved by using the multi-model. Indeed, most models behave similarly, save the LODYC and ECMWF models (who both use the same atmospheric component in their models) who have overall higher but more constant root mean square error. Most models, and therefore the multi-model, seem to follow at times the mean precipitation evolutions from one year to the next. This is most striking during the warm ENSO year 1997-1998, where higher than average precipitation over the La Plata Basin induces higher than average root mean square error for most models in December 1997 and January 1998 (not shown) and for all models in February 1998. One important fact shown in these figures is that the root mean square error is inferior to the mean precipitation amounts by less than 2 mm/day in average for the multi-model, and ranges from 2 to 4 mm/day. This confirms that negative and positive biases are compensated and the DEMETER models face some difficulties when it comes to precipitation forecasting over this region.

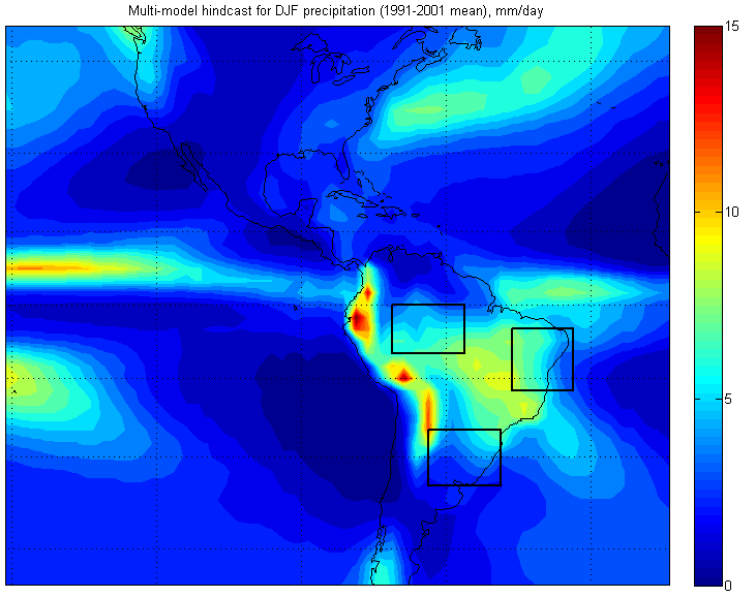


[a]

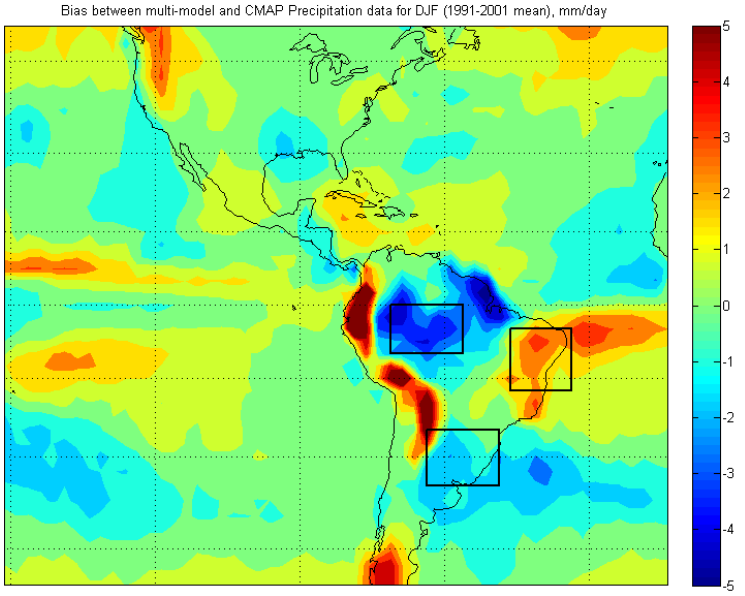


[b]

Figure 2.4: *DEMETER multi-model hindcast of mean daily precipitation for austral summer (DJF) over the PAN-Vamos region (mm/day). Mean hindcast from 1991 to 2001* [a]. *Bias of the multi-model with respect to CMAP precipitation data for the same period (DJF 91-92 to 2001-2002) (mm/day)* [b].

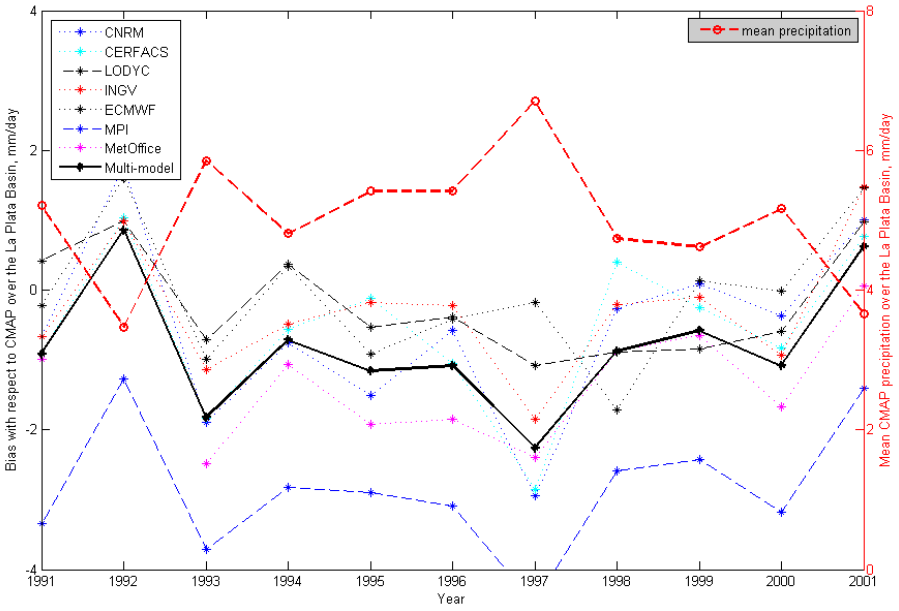


[a]

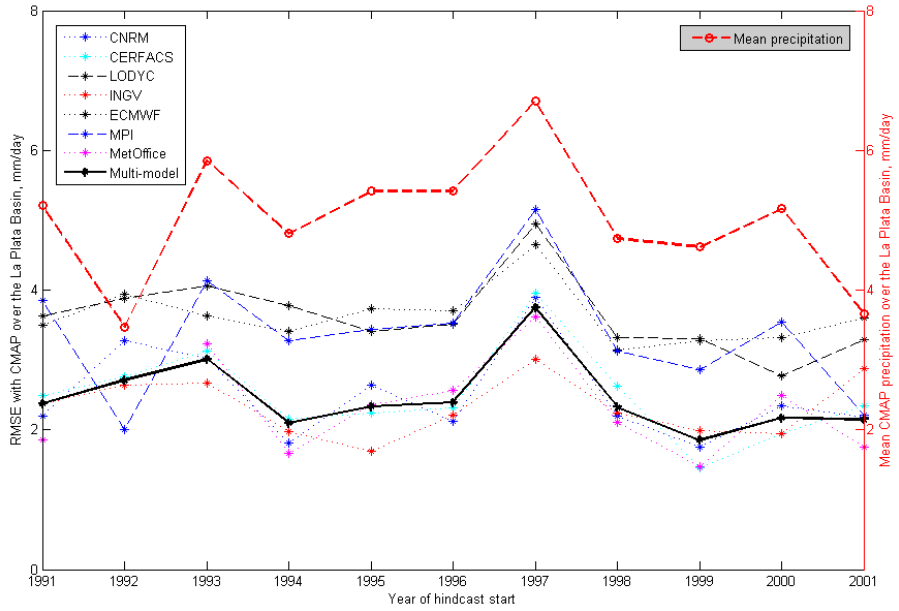


[b]

Figure 2.5: *DEMETER hindcasts of mean daily precipitation bias* [a] *and root mean square errors* [b] *with respect to CMAP precipitation data over the La Plata Basin area for February for hindcasts started in November 1991 to 2001 (units are mm/day). The mean precipitation over the La Plata Basin for the same month is shown in red (same units).*

Over the Amazon region, similar performances are observed when it comes to root mean square error (not shown). In December the multi-model always has less root mean square error than the other models, and values don't reach half of the mean precipitation values. In January, the multi-model root mean square errors are higher than in December, due to poorer performance of the LODYC and ECMWF models. This behaviour is also observed for the February hindcasts.

In what follows, DEMETER hindcasts for boreal summer precipitation over the NAMS region will be examined to document if a similar behaviour is found.

### 2.1.2 NAMS Precipitation during boreal summer

Figure 2.6 page 22 illustrates mean precipitation over North and South America during boreal summer (June, July and August), using CMAP mean precipitation from 1991 to 2001. The NAMS is at it's peak period from late June until early September, with maximum precipitation over the North American continent located over Mexico in the Bay of Campeche [Vera et al., 2006]. Very strong precipitation occurs just north of the equator in northern South America (over 10 mm/day) and over the northern tropical Pacific Intertropical Convergence Zone (ITCZ) (over 15 mm/day in some areas). This region is also active during austral summer (see figure 2.1 page 16) but with much less precipitation. Strong precipitation (over 5 mm/day) is also present over Florida.

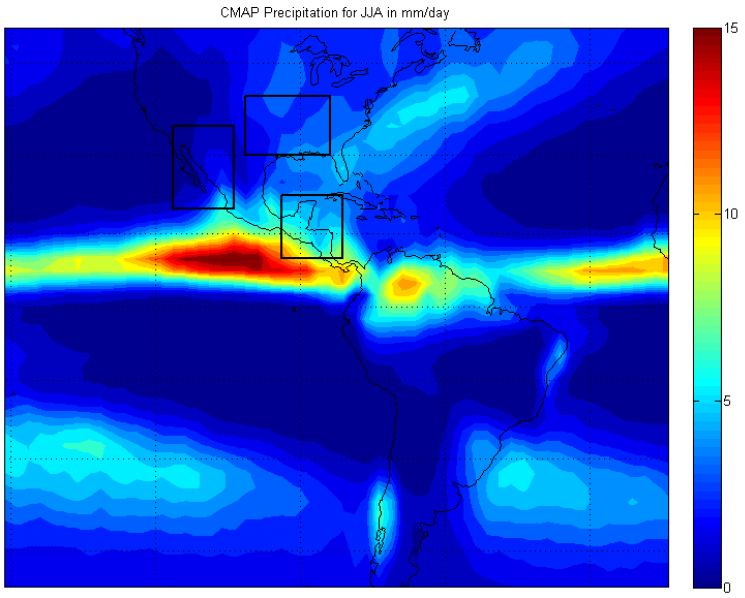


Figure 2.6: *Mean daily precipitation from June to August over the PAN-Vamos region, according to CMAP precipitation data averaged for 1991 to 2001 (mm/day). Boxed regions will later be referred to as the US Southwest and Northern Mexico region* [22° N - 35° N, 105° W - 115° W] *, the Great Plains region* [30° N - 40° N, 85° W - 100° W] *, and the Inter-Americas zone* [10° N - 22.5° N, 107.5° W - 117.5° W].

**Evolution of NAMS as shown by CMAP precipitation data**

Once again, in order to study more precisely the spatial and temporal evolution of the NAMS, monthly means for CMAP precipitation data were examined, using the "reference" period of April to September 1994. These are shown in figure 2.3 page 18. During April and May (NAMS onset period, [a] and [b]), precipitation intensifies over the ITCZ and northern South America, and appears over Mexico. June (figure [c]) is the last month of the NAMS onset, and heavy rains occur over the Tropics. Over the US Southwest and Northern Mexico region, rain is still scarce, with some regions having close to 0 mm/day rainfall in June. Precipitation over the Great Plains region depends greatly on the geographical region, with precipitation increasing with distance from the Rocky Mountains and decreasing with distance from the Gulf of Mexico. In the Inter-Americas zone, precipitation over land surpasses 5 mm/day whereas precipitation over sea is significantly less important. In July, the NAMS moves Northward west of the Sierra Madre, and extends into Arizona and New Mexico. This is demonstrated by the figure 2.3 [d], where precipitation in the US Southwest region has increased and moved northward compared to June. The geographical distribution of precipitation shifts slightly over the Great Plains region but precipitation amounts are sustained. Precipitation over the Inter-Americas zone decreases by 1 or 2 mm/day depending on the region. This phenomena is visible for other years of the 1991-2001 period. In August, the NAMS has moved yet more to the North, and most of the US Southwest region witnesses rainfall during this month. Precipitation over the Great Plains area slightly decreases, whereas precipitation over the Inter-Americas zone is comparable to that of June. In both July and August, precipitation over the Tropical Pacific and over northern South America slightly decreases compared to June. The NAMS mature phase ends by the beginning of September (figure [f]), and precipitation moves southward. This marks the beginning of the onset phase of SAMS (see figure 2.2 page 17).

**Performance and limitations of the DEMETER multi-model**

The NAMS involves less precipitation than the SAMS, meaning that the DEMETER models may react completely differently to both systems. Furthermore, the South American continent is essentially located in the Tropics, whereas the tropical areas of North America are very limited, and Inter-American geography may cause some model difficulties due to resolution of land-sea interfaces. Therefore, studying both regions can be of use to understand performances of the DEMETER models better, and the model reactions may be totally different in both cases.

The DEMETER hindcasts used for the NAMS study were those generated in May 1991 to 2001. The hindcasts were for June, July and August of each of these years, so as to have the same time span than for the austral summer study (1 to 3 month in advance hindcast for the monthly means). Figure 2.7 page 24 presents the mean of all multi-model ensembles hindcasts for June, July and August 1991 to 2001, and it's bias with respect to CMAP precipitation data for the same period.

The multi-model captures quite well the progress of the NAMS in the US Southwest region, as well as the precipitation patterns over the Great Plains, but with some errors of precipitation values. Indeed, precipitation over the Great Plains region is slightly underestimated, as well as over California. In the southern half of the Inter-Americas zone, precipitation is constantly considerably overestimated by the multi-model, whereas the strong precipitation pattern over northern South America is too weak in the hindcast, therefore leading to underestimation over most of northern South America during boreal summer. Therefore, the model seems to work better over the northern subtropical zones such as the Great Plains area than over the tropics. However, it should also be emphasized that the Core NAM precipitation exhibits a strong dependence on resolution, which is an aspect that cannot be analyzed with the datasets used in this study. Indeed, low-resolution models are known not to resolve the Gulf of California area correctly, implying lower

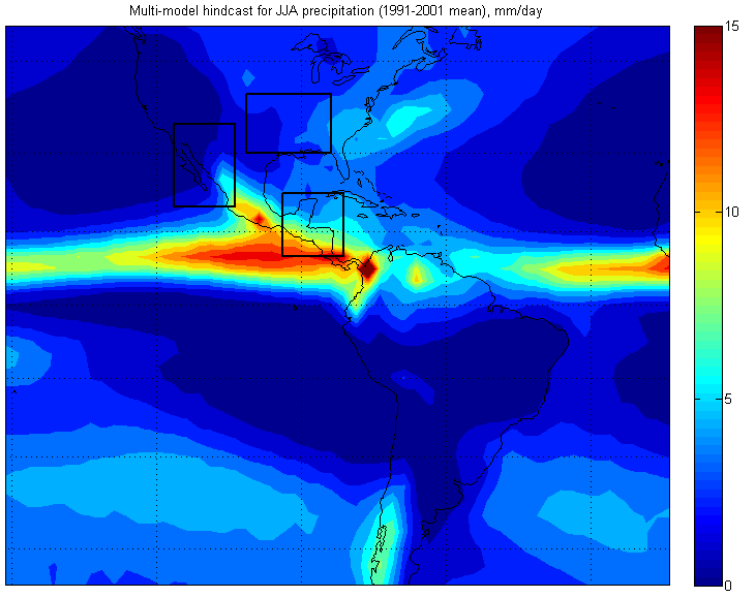


[a]

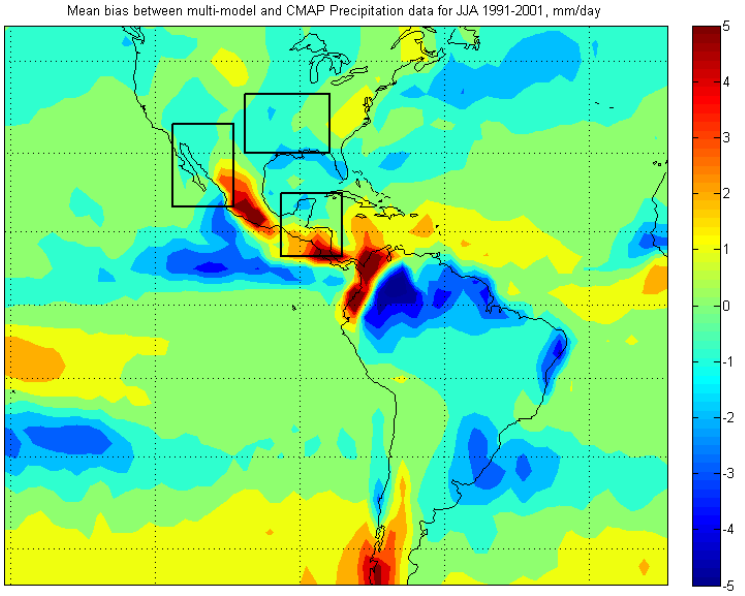


[b]

Figure 2.7: *DEMETER multi-model hindcast of mean daily precipitation for boreal summer (JJA) over the PAN-Vamos region (mm/day), averaged from 1991 to 2001* [a]. *Bias of the multi-model with respect to CMAP precipitation data for the same period (mm/day)* [b].

skill than higher-resolution models [Mo et al., 2005]. This resolution problem is also present in the case of the reference datasets, which could explain the apparent better results found for summer precipitation predictions over the area. In order to further examine model performance, mean bias for June, July and August precipitation with respect to CMAP and spatial root mean square errors were computed over each region.

Results over the Great Plains area for August (mean bias and root mean square error) are shown in figure 2.8 page 26. The multi-model bias is in most years negative (save 1999 and 2000) and closer to zero than most of the independent model biases. In fact, some models such as MPI and INGV have systematic positive biases that reach one third of the total precipitation over the region, whereas others such as ECMWF and LODYC have systematic negative biases with similar amplitudes. These four models also have the highest root mean square error. The antisymmetry between the mean precipitation pattern and the multi-model's bias with respect to CMAP data is striking when looking at figure [a]. Figure [b] demonstrates the multi-models' better performance over individual models, since root mean square error is lower for the multi-model nearly every year. However, the root mean square error oscillates around the value of 1 and is therefore much higher than the mean bias, indicating that positive and negative bias values cancel out. Over the Core NAM region, bias is relatively low for the multi-model in June, and bias values for the multi-model range mostly from -0.5 to 0.5 mm/day. This bias increases and is positive for July and August, reaching values of 1.25 mm/day (not shown). This is also noted over the Inter-Americas region, where individual model biases reach 5 mm/day. In the case of the Inter-Americas zone, the multi-model doesn't have the lowest bias of all models, since model dispersion is high and some models such as the ECMWF and LODYC models have very high bias whereas others such as the Met Office model perform quite well over the region (not shown). In all cases, an overall reduction of root mean square errors is obtained by using the multi-model.

Although the multi-model seems to perform generally better than individual models over the regions of study, it faces some difficulties in precipitation prediction. Further evaluation of model performance will be done using other statistical scores later on in this report.

## 2.2 Study of other parameters linked to precipitation

Other parameters predicted by DEMETER hindcasts are physically linked to precipitation. Therefore, in order to possibly explain links between precipitation prediction errors and other errors, a study of other fields was necessary.

### 2.2.1 2 m surface temperature

#### 2 m surface temperature prediction during austral summer

Figures 2.9 page 27 and 2.10 page 28 show 2 meter mean surface temperature obtained by ERA-40 reanalysis data (figure 2.9), the multi-model (figure 2.10 [a]) and the multi-model's bias with respect to ERA-40 ([b]) for austral summer (DJF) 1991-1992 to 2001-2002. Mean temperatures over the Core Amazon Region (averaged over the entire day) and North East Brazil are very well estimated by the DEMETER multi-model, with errors ranging from -1 to 1 degrees only. On the other hand, temperatures are highly overestimated over the La Plata Basin area. This behaviour of model predictions is similar from one month to the next, with the same sign in bias. The bias sometimes increases between December and February (not shown).

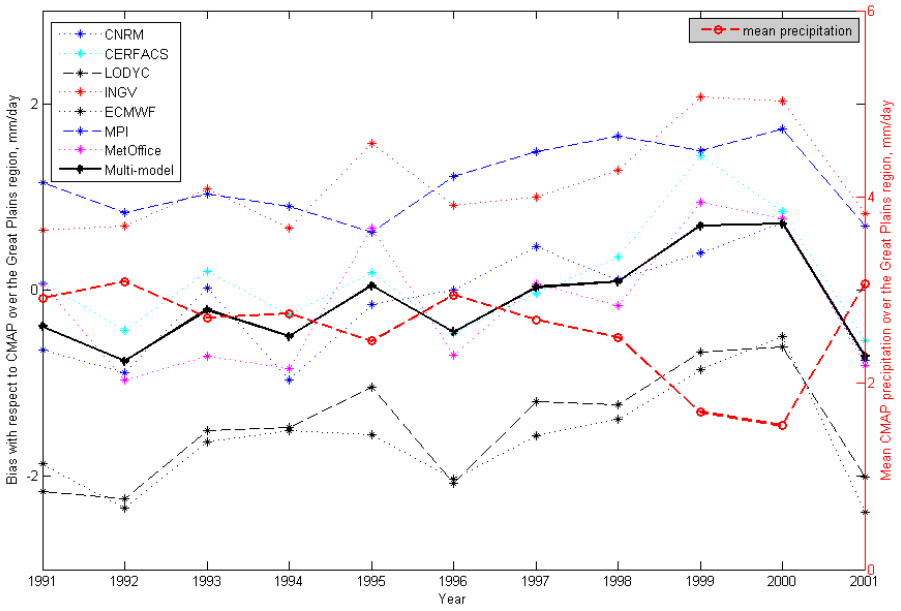


[a]

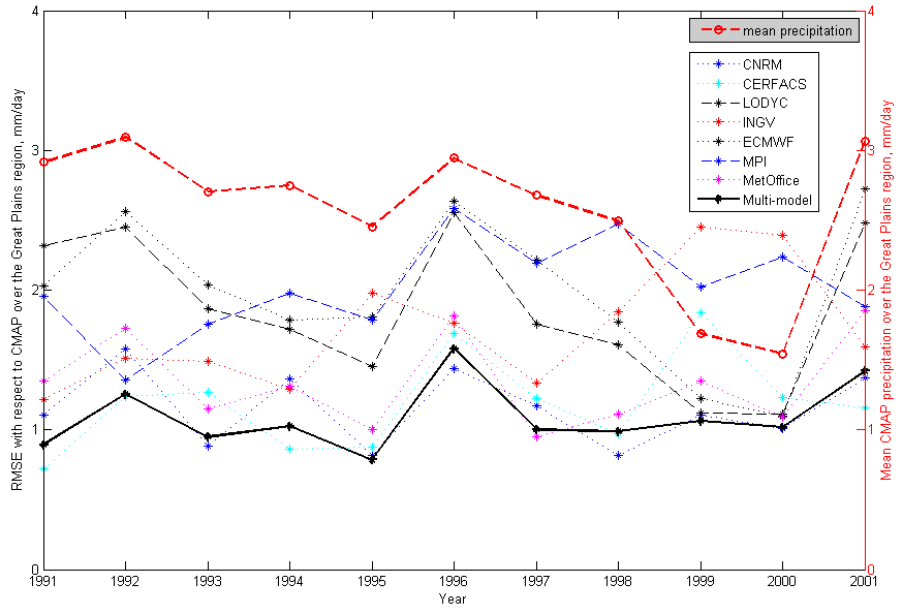


[b]

Figure 2.8: *DEMETER hindcasts of mean daily precipitation bias* [a] *and root mean square errors* [b] *with respect to CMAP precipitation data over the Great Plains area for August for hindcasts started in May 1991 to 2001 (units are mm/day). The mean precipitation over the Great Plains area for the same month is shown in red (same units).*

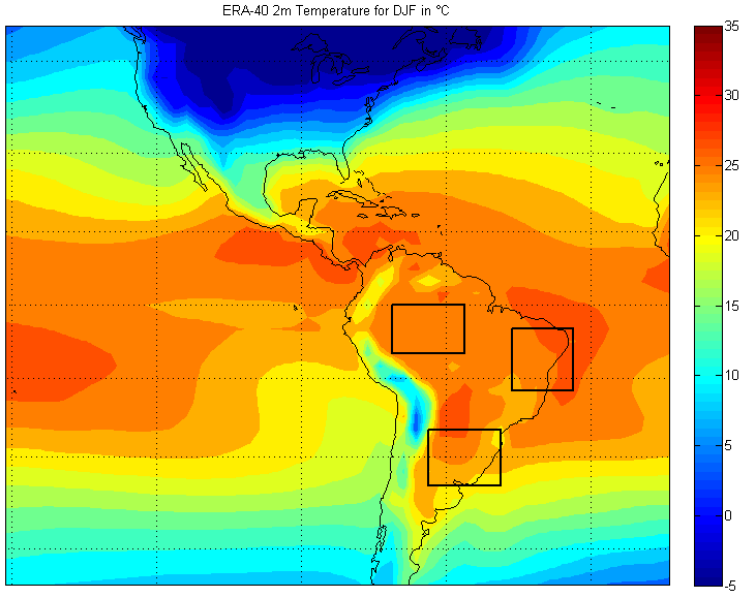


Figure 2.9: *ERA-40 data for mean 2m temperature for austral summer (DJF) 1991-2001 over the PAN-Vamos region (degrees Celsius)*

**Surface temperature evolution and prediction during boreal summer**

Figure 2.11 shows average 2m temperature for boreal summer (JJA) as given by ERA-40 analysis data, and figure 2.12 page 30 shows the multi-model mean predictions ([a]) and bias with respect to ERA-40 ([b]) for the 1991-2001 time period. The DEMETER multi-model clearly overestimates temperature over the Great Plains Region, with errors of over 4 degrees. Performance over the Inter-Americas region is quite good, with an underestimation of 1 degree over most of the area. Model predictions over the Southwest US and Northern Mexico region show dipolar behaviour: temperature is overestimated over the state of California in the United States and Baja California in Mexico, whereas it is systematically underestimated over continental Sonora. This could be due to model resolution, and should be kept in mind when studying hindcast performance over this region.

### 2.2.2 Prediction of 850 HPa circulation during summer

Given the prominent role of low-level jets as effective means of moisture transport, it was considered of interest to analyze low-level circulation. Viewing how the multi-model predicts the 850 HPa wind velocities and directions provides additional information on the multi-model's performance in precipitation forecasting.

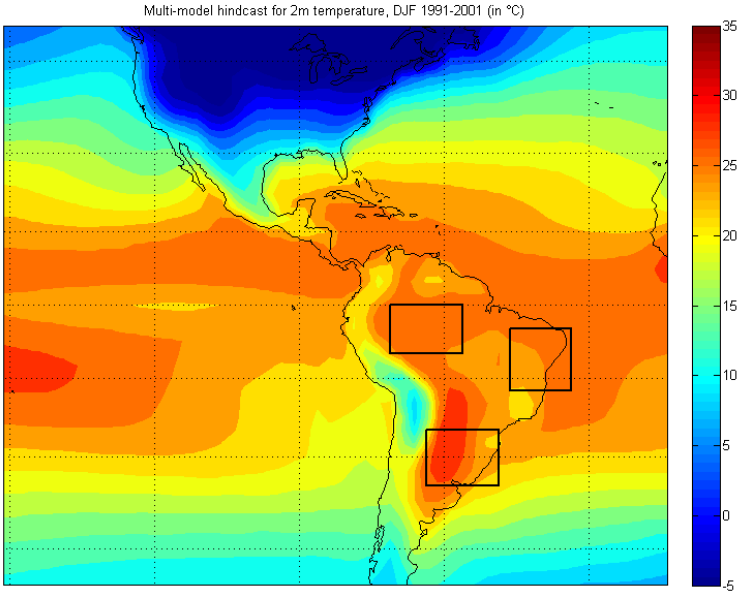


[a]

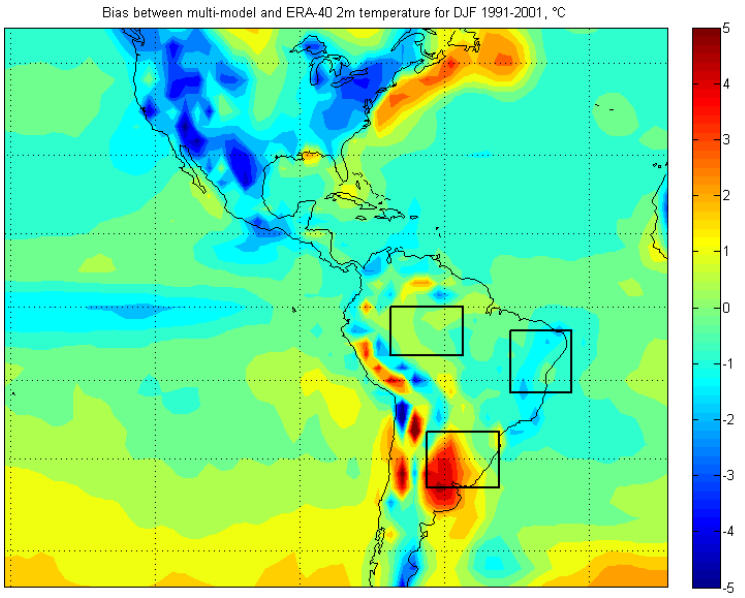


[b]

Figure 2.10: *ERA-40 data for mean 2m temperature from December 1993 to February 1994 over the PAN-Vamos region (degrees Celsius)* [a]. *Bias of the multi-model with respect to ERA-40 data for the same period (degrees Celsius)* [b].

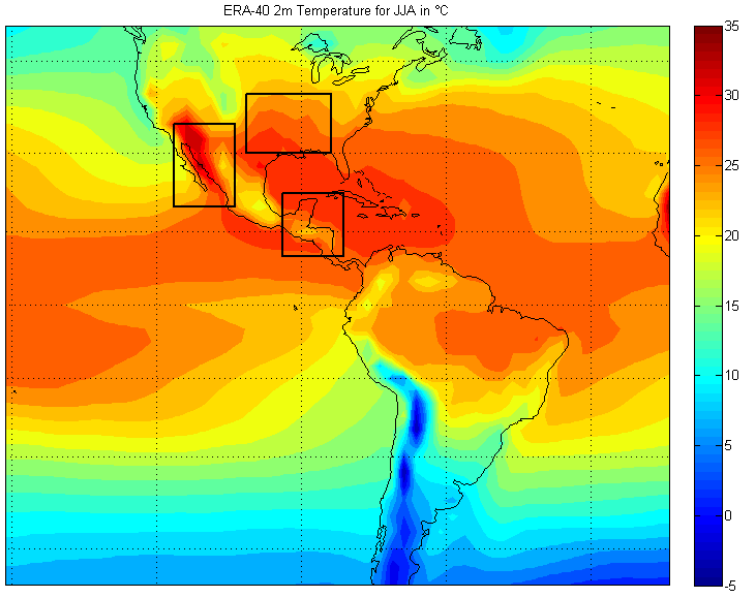


Figure 2.11: *ERA-40 data for mean 2m temperature for boreal summer (JJA) 1991-2001 over the PAN-Vamos region (degrees Celsius)*

### 850 HPa circulation during austral summer

Figure 2.13 page 31 shows mean 850 HPa circulation at 0:00 GMT and mean precipitation for austral summer (DJF) of the period of study (1991-1992 to 2001-2002). A first glance at both figures shows that the multi-model correctly represents the global 850 HPa height circulation patterns. Over South America, easterly tropical winds arrive over the continent north of Brazil and are abruptly deflected southward due to the presence of the Andes. This continental circulation is reproduced by the multi-model, however, some problems in forecasting wind velocities are encountered, for example over the La Plata Basin and south-eastern Brazil, where easterly wind velocities are overestimated.

These conclusions are confirmed by examining the bias of the multi-model winds with respect to ERA-40 data for the same time period, shown in figure 2.14. The multi-model has some error in wind velocity and also in wind directions over some regions of the South American continent. A bias ranging from 2.2 to 2.5 m/s is found just north-east of the La Plata Basin region, and over the SALLJ region northerly winds are underestimated by 1 to 2 m/s. Between the Amazon region and North East Brazil region studied in this report, the multi-model overestimates north-eastern winds arriving from the Atlantic. Over the La Plata Basin, mean precipitation is underestimated by the multi-model, and 2 meter temperature is highly over estimated. The misrepresentation of circulation over this region could imply that synoptic-scale phenomena such as the South American Low Level Jet (SALLJ) are poorly captured by the global models. The SALLJ is strongest at altitudes ranging from 900 HPa to 850 HPa depending on the season, and the warm season SALLJ exhibits strong moisture content [Marengo et al., 2004]. SALLJ is an important source of moisture

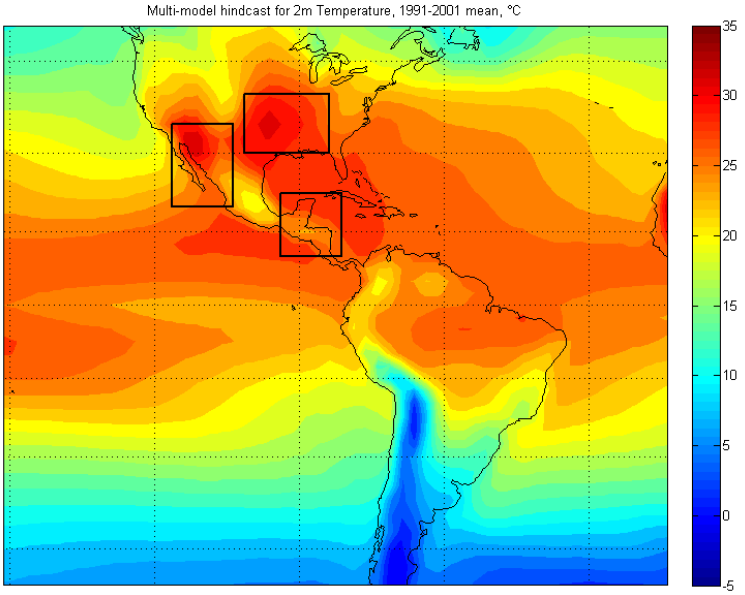


[a]

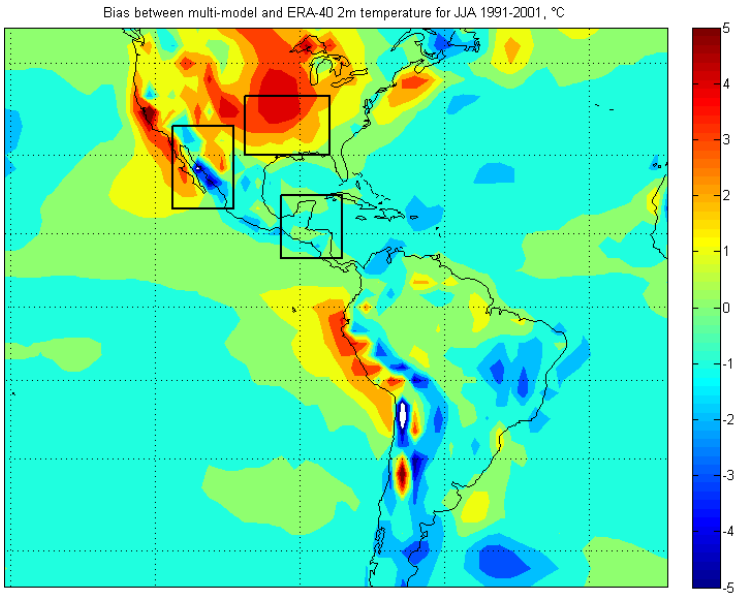


[b]

Figure 2.12: *Mean DEMETER multi-model hindcast for 2m temperature from June to August over the PAN-Vamos region (degrees Celsius), averaged from 1991 to 2001* [a]. *Bias of the multi-model with respect to ERA-40 data for the same period (degrees Celsius)* [b].

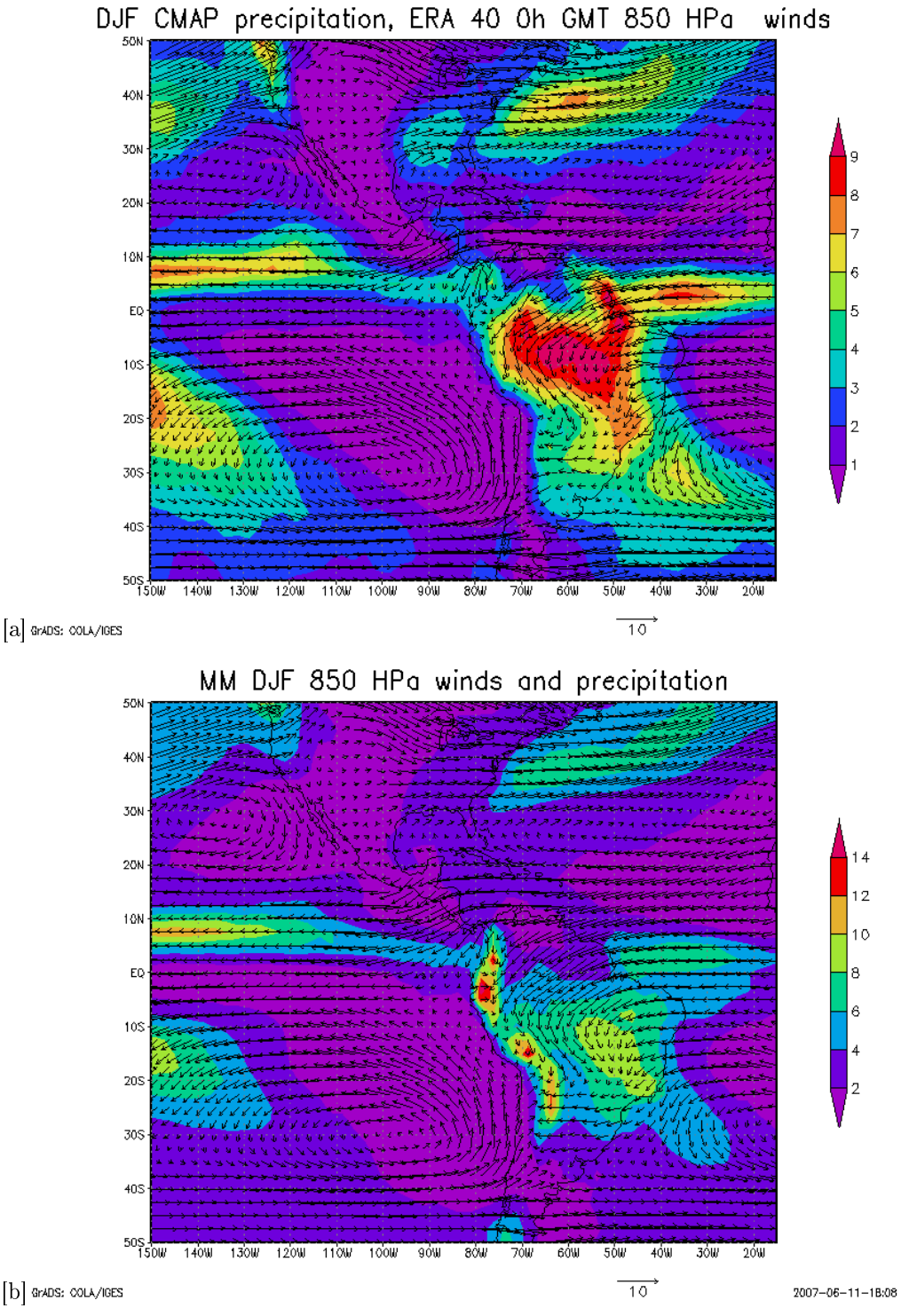


Figure 2.13: *DJF 1991-2001 climatology for precipitation (CMAP data, in mm/day) and 0:00 GMT 850 HPa winds (ERA-40 data, reference vector 10 m/s)* [a]. *Multi-model mean hindcast for the same fields* [b]. *Note that the precipitation scale is different from one graph to the next.*

over the La Plata Basin, and a misrepresentation of SALLJ, particularly an underestimation of lower level winds, could explain the multi-models' precipitation deficit with respect to CMAP data for austral summer. However, to verify this hypothesis, a detailed study using daily hindcasts should be led. This is beyond the scope of this report.

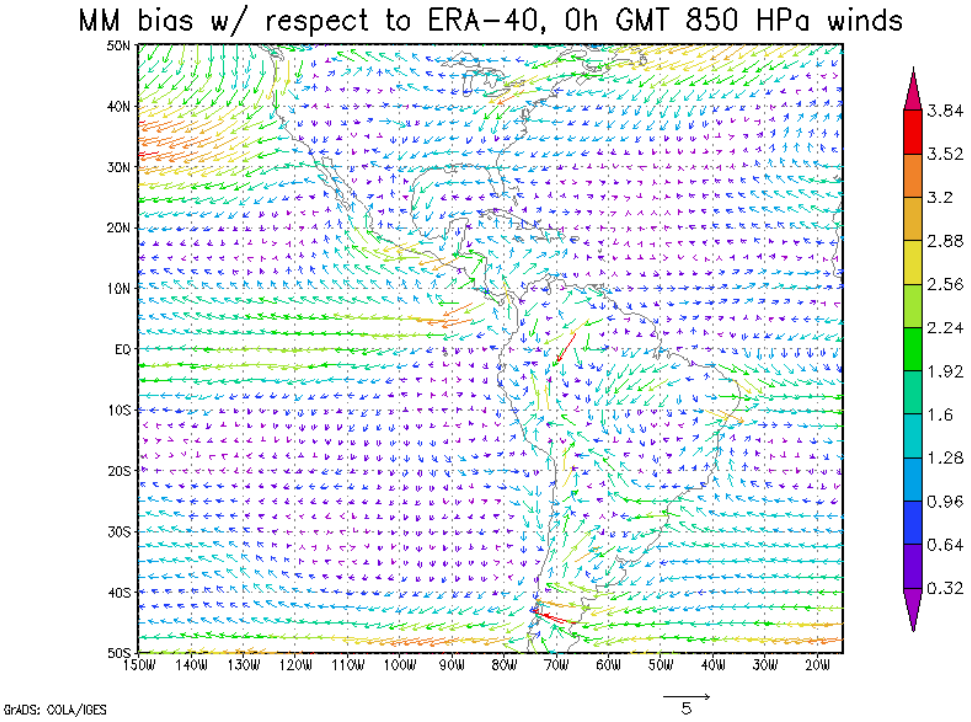


Figure 2.14: *DJF 1991-2001 multi-model mean hindcast bias with respect to ERA-40 data for 850 HPa circulation (reference vector 5 m/s). Colors indicate the magnitude of the wind bias for each grid point.*

### 850 HPa circulation during boreal summer

Boreal summer 850 HPa circulation and mean precipitation values from the reference data (CMAP and ERA-40) and as hindcasted by the multi-model for the 1991-2001 time period are shown in figure 2.15 page 33. As for austral summer, the multi-model represents global circulation correctly. Some visible difference is noted over Southwest US (wind direction) and over the Inter-Americas zone (wind velocity).

Further assessment of circulation field differences between the multi-model hindcasts and the ERA-40 reanalysis data is done by calculating the difference between both vector fields, presented in figure 2.16. A first conclusion while looking at the figure is that bias over the SALLJ area higher in austral winter than in austral summer (see previous section). Concerning boreal summer predictions, the highest bias over land is found over the Inter-Americas zone. This bias is due to an underestimation of wind velocities, since the wind directions over the area are similar (see figure 2.15). Winds in the northeast corner of the US Southwest region are predicted as westerly winds instead of southwesterly, leading to a velocity bias of over

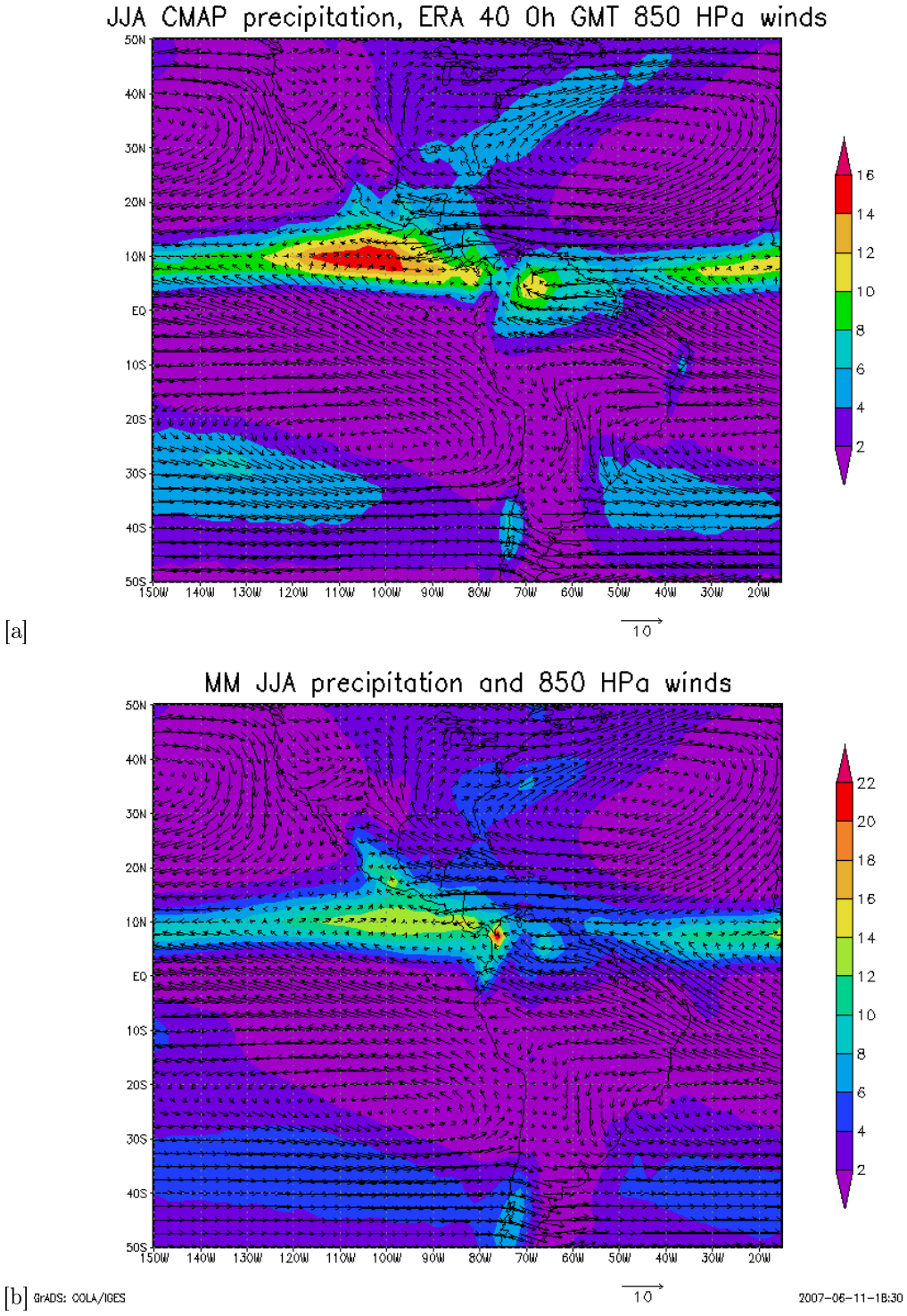


Figure 2.15: *JJA 1991-2001 climatology for precipitation (CMAP data, in mm/day) and 850 HPa winds (ERA-40 data, reference vector 10 m/s)* [a]. *Multi-model mean hindcast for the same fields* [b]. *Note that the precipitation scale is different from one graph to the next.*

1.5 m/s at some grid points of the region. Some underestimation of wind velocities and slight errors in wind directions lead to biases higher than 2 m/s over the eastern half of the Great Plains region. This could hint that models also encounter difficulties in accurately predicting the Great Plains LLJ intensity, but linkages between precipitation, circulation and temperature forecasting over this region may be different than in the case of the La Plata Basin because models tend to overpredict the Great Plains LLJ.

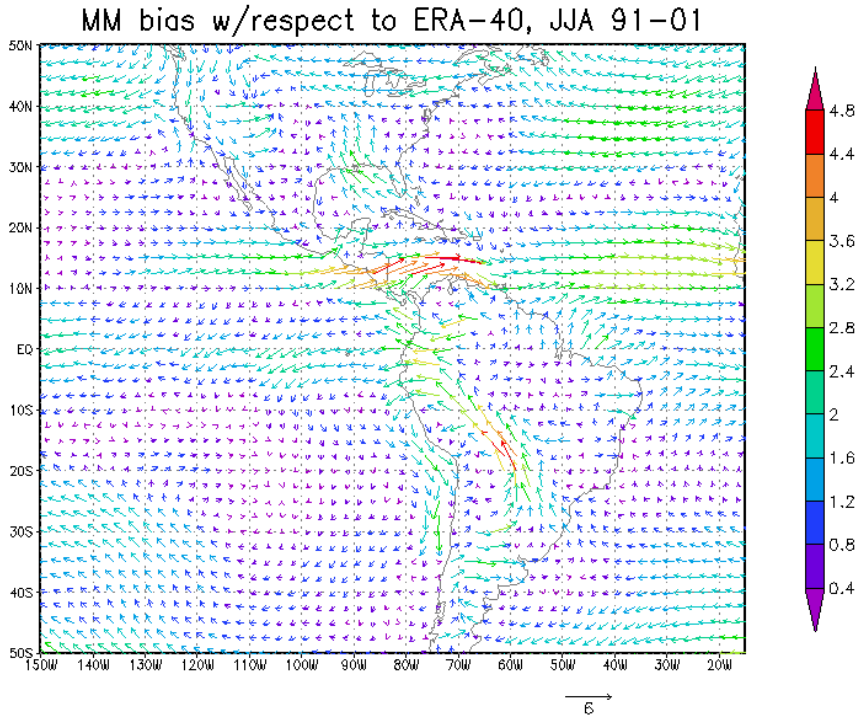


Figure 2.16: *JJA 1991-2001 multi-model mean hindcast bias with respect to ERA-40 data for 850 HPa circulation (reference vector 6 m/s). Colors indicate the magnitude of the wind bias for each grid point.*

### 2.2.3 Prediction of sea surface temperature and ENSO during austral summer

Some fields such as 2 meter temperature or convection exert local forcing on precipitation, whereas others exert both local and remote influence. One example is SST: warm or cold SST anomalies over the equatorial Pacific Ocean can considerably change general circulation patterns and therefore influence precipitation over distant regions such as North or South America. This phenomena is part of the El Niño Southern Oscillation, or ENSO.

The ENSO cycle is the year-to-year variations in SSTs, convection, sea-level pressure and circulation over the equatorial Pacific Ocean. Extreme events are El Niño (warm extremes) and La Niña (cold extremes). Figures 2.17 page 36 show a schematic of the circulation systems over the Pacific Ocean during neutral [a], El Niño [b] and La Niña [c] phases, including the position of the oceanic thermocline and SSTs. Figure [a] shows the average Walker circulation over the Pacific Ocean. A high pressure system over the eastern Pacific

and a low pressure system over Indonesia causes easterly trade winds and upwelling of cold ocean water off the coasts of Peru and Equator.

During El Niño [b], the Walker circulation is weakened, due to higher SSTs over the equatorial Pacific Ocean. The thermocline therefore shifts to a more horizontal position, and easterly trade winds are weakened over the east Pacific and changed to westerly over the west Pacific, while convective rainfall is shifts from Indonesia to the eastern half of the Pacific Ocean. These changes affect precipitation patterns over parts of North and South America. During La Niña [c], opposite changes are observed. The Walker circulation is enhanced due to cooler SSTs over the equatorial Pacific Ocean, and convective rainfall over the eastern Pacific Ocean is suppressed.

El Niño/La Niña episodes occur every 3 to 5 years, however the period can vary from 2 to 7 years. One way to monitor ENSO variations is to measure SSTs over the Equatorial Pacific Ocean. El Niño/La Niña events are defined by the NOAA as a positive/negative SST anomaly averaged over 3 consecutive months greater or equal to 0.5 degrees Celsius with respect to 1971-2000 climatology in the El Niño 3.4 region. The El Niño 3.4 region is a critical region containing a band of cool water, and departures from average in this region are known to trigger changes in precipitation and temperature patterns around the world. Figure 2.18 shows El Niño 3.4 mean SSTs from 1982 to today. The figure shows the variability in warm and cold episode lengths and intensity.

During the 1991-2001 period studied in this report, ENSO warm events occurred in 1991-1992, 1994-1995 and 1997-1998, and cold events occurred in 1995-1996 and from 1998 to 2000. The 1997-1998 El Niño event was the strongest in the decade, with SST anomalies over El Niño 3.4 reaching 2.5 degrees Celsius, and is the second strongest El Niño event after 1982-1983 in the last 50 years (source: [IRI website]). This makes 1997 austral spring and winter SSTs an interesting field of study to examine model response to changes in SST.

In this section a first evaluation of model performance in austral summer SST prediction in presented. Reynolds SST data is used as reference data, and after a general study of the 1991-2001 period, performance for the El Niño 1997-1998 austral summer is assessed. Many papers assess a remote influence of the El Niño 3.4 region SSTs on precipitation over South America ([Paegle and Mo, 2002]) as well as local influence of South Atlantic SSTs on specific regions of South America ([Doyle and Barros, 2002]). The following study will therefore focus on the Niño 3.4 region and the Western Subtropical South Atlantic to further examine model performance.

#### 1991-2001 mean SSTs and forecasts

Figure 2.19 page 38 shows mean Reynolds sea-surface temperature in both the Pacific and Atlantic Oceans during the austral summer season, averaged from 1991 to 2001. Figure 2.20 [a] and [b] show the mean of all ensembles multi-model hindcast for the austral summer SSTs during the 1991-2001 period, and it's bias with respect to Reynolds SST data. A positive bias with respect to Reynolds data is blatant in the South Atlantic and South Pacific areas, whereas the multi-model tends to underestimate SSTs by 1 or 2 degrees in the Niño 3.4 area, but more generally over the tropical and North Pacific and the North Atlantic.

A more detailed study of bias and root mean square errors over the El Niño 3.4 region was carried out for austral summer of every year, so as to see performances of individual models and year to year variations. Results for December are shown figure 2.21 page 40. Every year, the multi-model underestimates slightly SSTs over the El Niño 3.4 region, but root mean square error remains reasonable (around 1 degree Celsius). Although most models show similar skill than the multi-model, the MPI model faces some problems in predicting accurately SST over this region. This difference between the MPI model and others amplifies in January and February, where MPI hindcast bias with respect to Reynolds data reaches -5 degrees in February 1992 (not shown). This could be due to the fact that the MPI coupled model is not initialized using the same

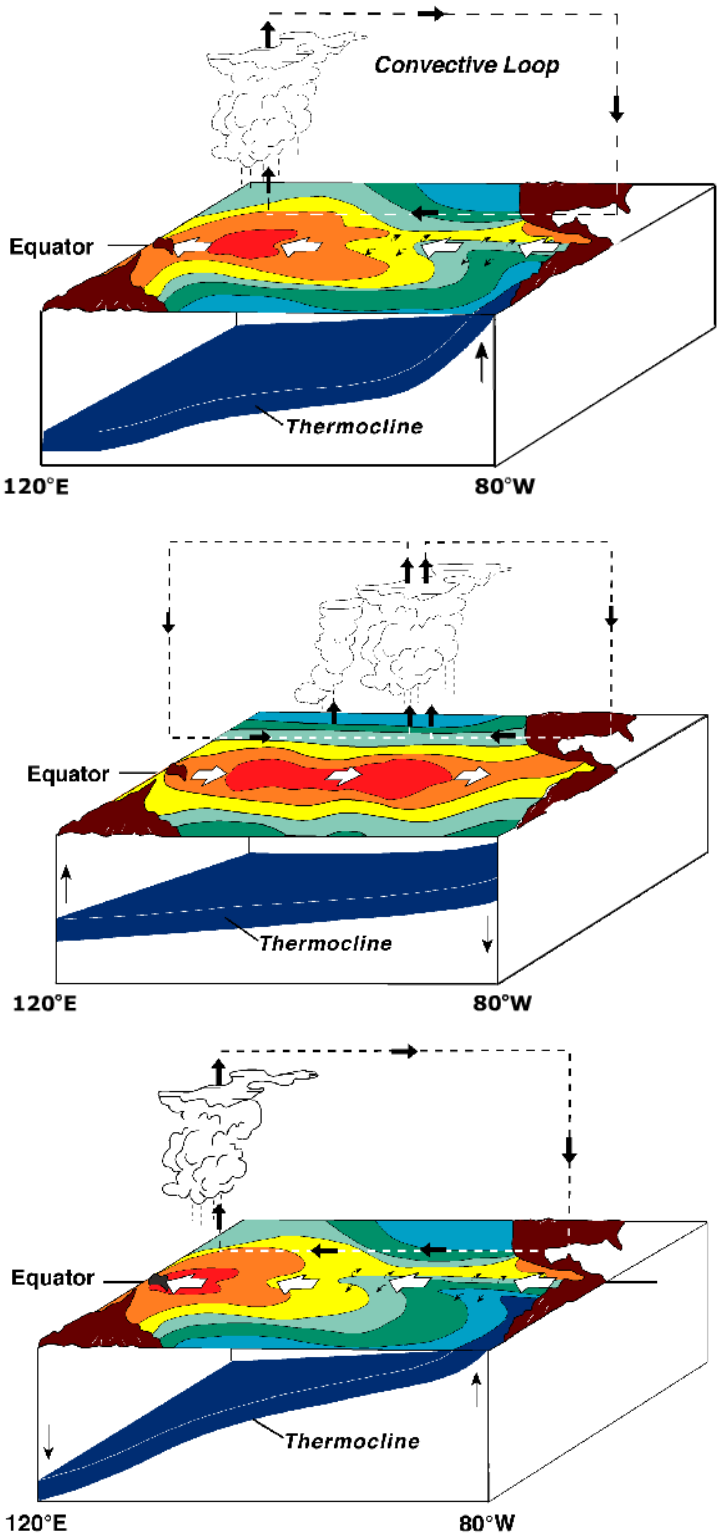


Figure 2.17: *Convection, ocean thermocline, SSTs and main atmospheric winds during the ENSO neutral* [a], *El Niño* [b], *and La Niña* [c] *phases. Source: NOAA/Wikipedia.*

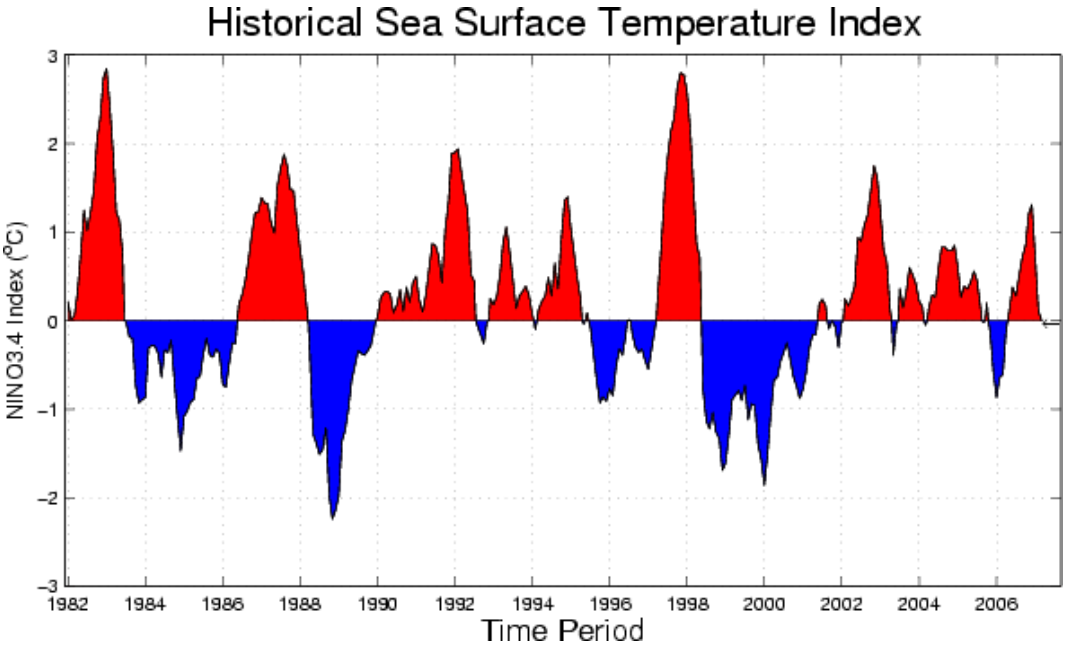


Figure 2.18: *Mean SSTs over the El Niño 3.4 region from 1982 to today, in degrees Celsius. Source: [IRI website]*

procedure as in other models of the DEMETER project that use ERA-40 reanalysis data to initialize ocean and atmospheric states [Palmer et al., 2004]. The multi-models' performance is affected by this large bias, and in February some individual models have lower bias and root mean square error than the multi-model over the region.

It is also interesting to notice that forecast performance for 1997 (the strongest El Niño event in the time period) is the highest for most models, with close to zero bias and low root mean square errors. There is however no visible pattern between ENSO warm or cold events and hindcast performance in general, some El Niño years corresponding to higher SST bias and others to relatively lower bias for the multi-model.

Many papers in the bibliography have studied links between spring SST conditions and summer precipitation ([Vera et al., 2006] and references therein). This justifies the following study of model performance in SST predictions for the austral spring season.

### 2.2.4 Prediction of SSTs and ENSO during austral spring

Figure 2.22 shows mean Reynolds SST data for austral spring, averaged from 1991 to 2001. SSTs are notably warmer over the Tropical North Atlantic and Pacific than in austral summer, but little change over the El Niño 3.4 region is seen. Figures 2.23 page 42 show multi-model mean hindcasts and bias with respect to Reynolds data over the Pan VAMOS region and Pacific Ocean for austral spring. As in austral summer, the multi-model underestimates SSTs over the El Niño 3.4 region, but mean bias is higher than for austral summer. Over the Western Subtropical South Atlantic, bias in spring is negative, whereas positive in summer.

Further evaluation of model performance was done by computing year after year bias and root mean

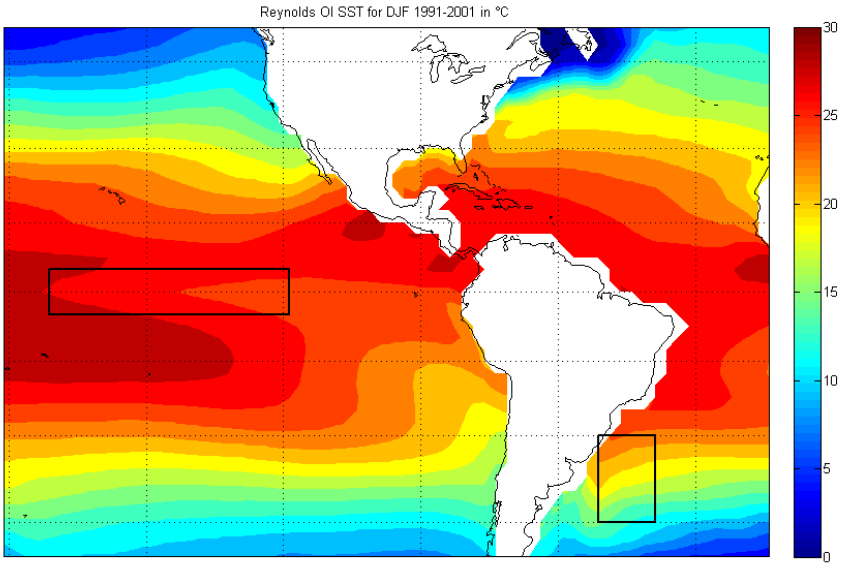


Figure 2.19: *Reynolds OI SST data for austral summer (JJA) 1991-2001 over the PAN-Vamos region and Pacific Ocean (degrees Celsius)*

square error over the chosen regions. Results for the month of September over the El Niño 3.4 region are shown in figure 2.24 page 43. Once again the MPI model's performance alters the multi-model's bias and root mean square error so that some individual models (CNRM, LODYC, ECMWF) have better scores over the El Niño 3.4 region. The multi-models' bias is lowest in September 1997, due to a close to zero bias for the MPI model and overall good performance of the other models. Bias and root mean square errors are comparable with those calculated for austral summer, even if root mean square error is sometimes slightly higher for spring hindcasts. The same evolution between September and November is observed as between December and February: model biases and root mean square errors tend to increase. Although the multi-model bias increases little, it's root mean square error increases much more due to high root mean square error for the MPI model and increasing root mean square error for other models.

This analysis of SST forecasting by the DEMETER models and multi-model shows that one-month lead hindcasts perform very well over the El Niño 3.4 region and models reproduce well ENSO. This could be due to the fact that the hindcasts studied are one-month lead hindcasts (started in November), meaning the ENSO signal is already included in the ocean initial conditions for the models. The fact that the only model that isn't initialized using reanalysis data is the one with the highest bias tends to confirm this hypothesis.

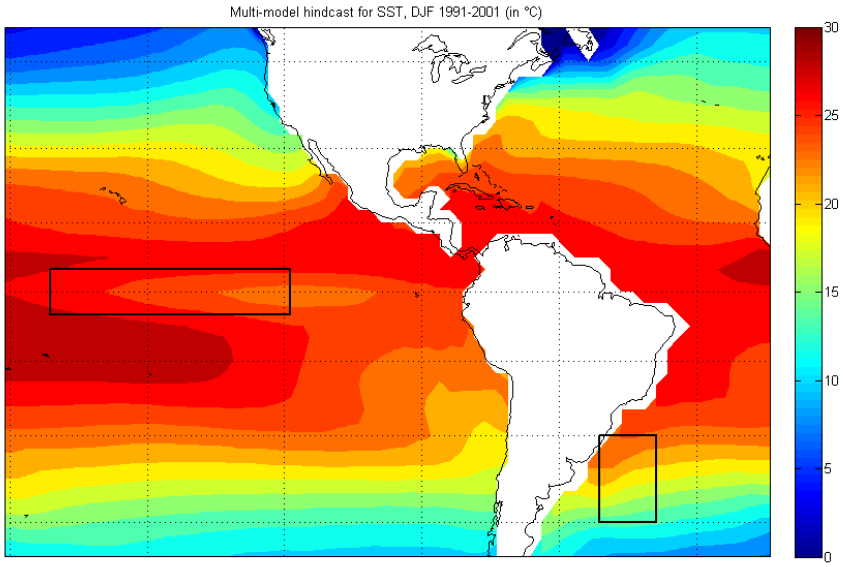


[a]

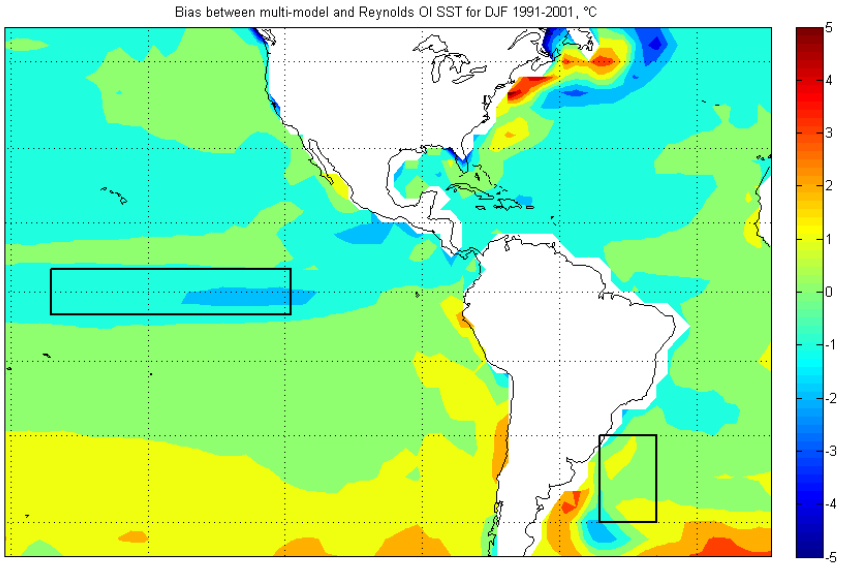


[b]

Figure 2.20: *Mean multi-model hindcast for 1991-2001 austral summer SSTs over the Pacific and Atlantic oceans (degrees Celsius)* [a]. *Bias of the multi-model with respect to Reynolds OI SST data for the same period (degrees Celsius)* [b]. *Boxed areas are the Niño 3.4 area* [5° S - 5° N, 170° W - 120° W] *and the Western Subtropical South Atlantic area* [30° S - 45° S, 45° W - 55° W].

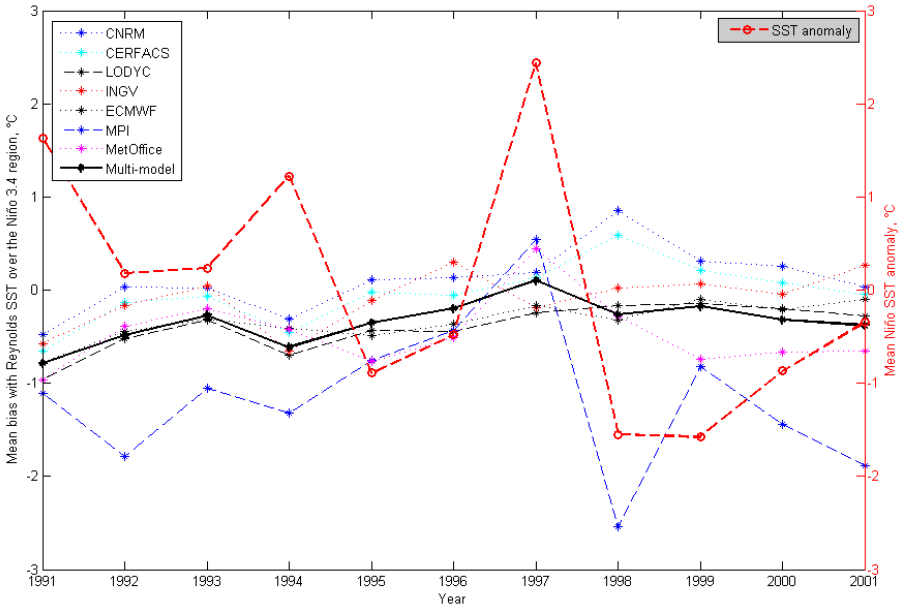


[a]

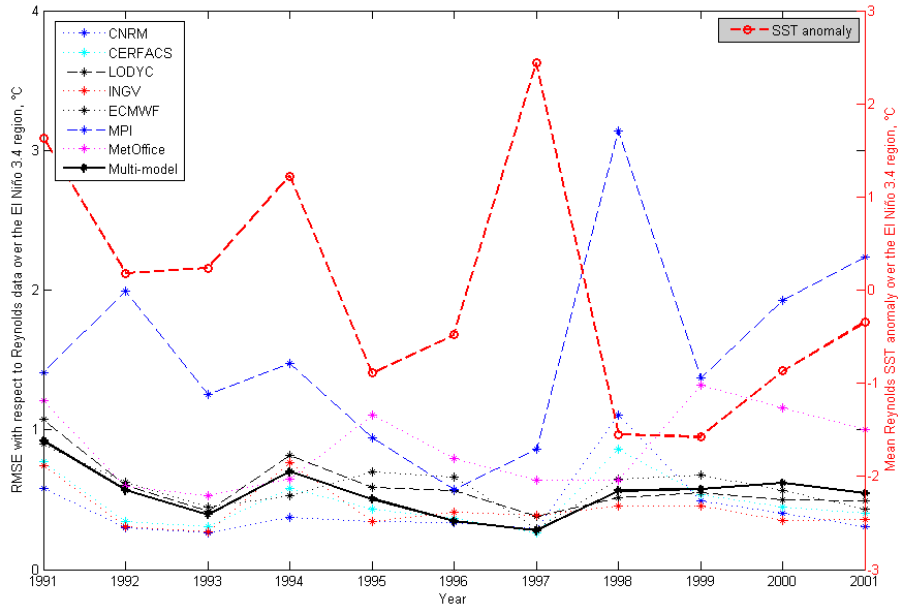


[b]

Figure 2.21: *Year by year hindcast mean bias* [a] *and spatial root mean square error* [b] *with respect to Reynolds data over the El Niño 3.4 region for the month of December, in degrees Celsius.*

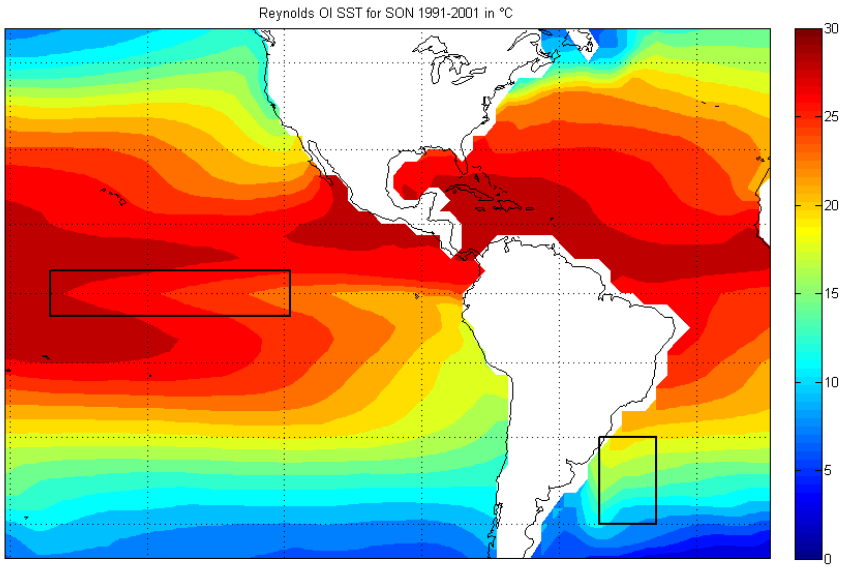


Figure 2.22: *Reynolds OI SST data for austral spring (SON) 1991-2001 over the PAN-Vamos region and Pacific Ocean (degrees Celsius)*

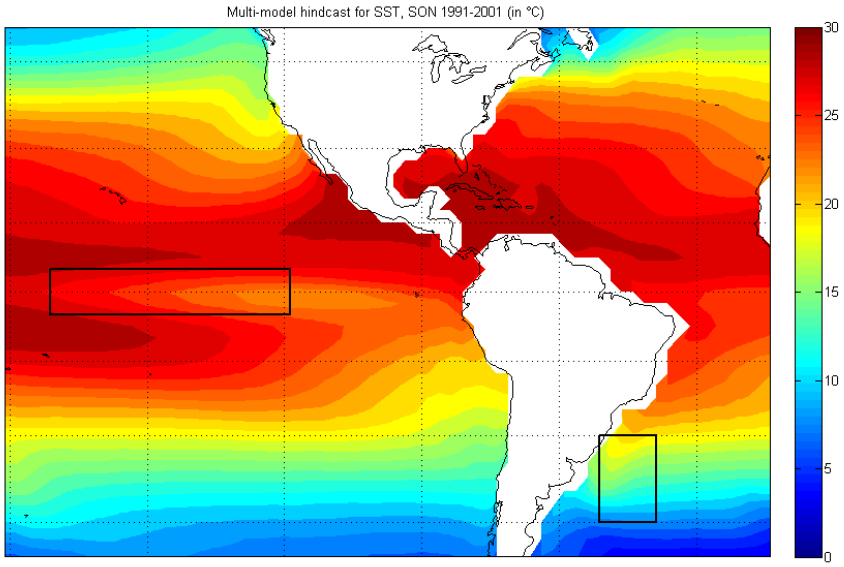


[a]

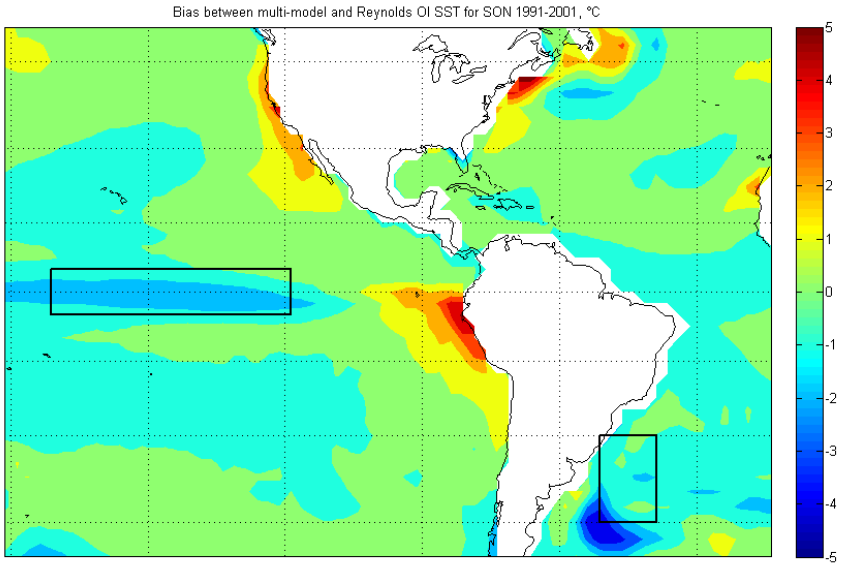


[b]

Figure 2.23: *Mean multi-model hindcast for 1991-2001 austral spring SSTs over the Pacific and Atlantic oceans (degrees Celsius)* [a]. *Bias of the multi-model with respect to Reynolds OI SST data for the same period (degrees Celsius)* [b]. *Boxed areas are the Niño 3.4 area* [5° S - 5° N, 170° W - 120° W] *and the Western Subtropical South Atlantic area* [30° S - 45° S, 45° W - 55° W].

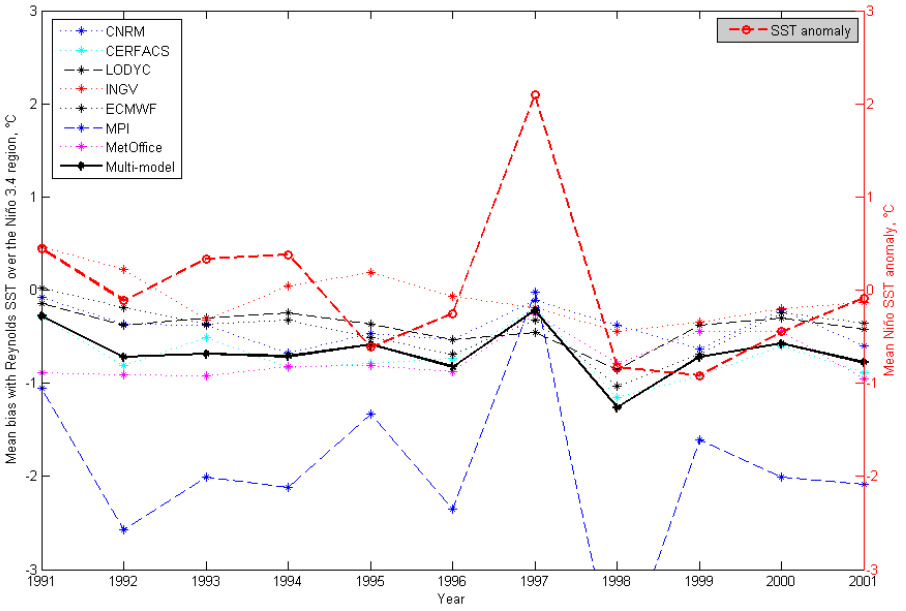


[a]

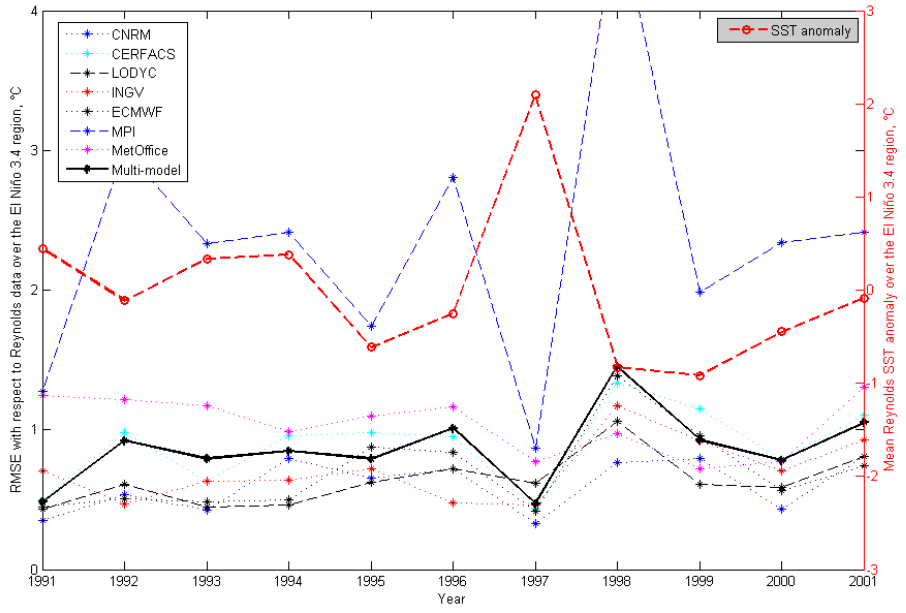


[b]

Figure 2.24: *Year by year hindcast mean bias* [a] *and spatial root mean square error* [b] *with respect to Reynolds data over the El Niño 3.4 region for the month of September, in degrees Celsius.*

# Part 3

# Assessment of DEMETER model performances using statistical scores

In the previous section, an initial study of different fields linked to monsoon peak season precipitation and the performance of the different models of the DEMETER project were presented. Further evaluation of model performance during the American monsoon peak seasons is shown in this section, using complementary statistical scores. A first study is led for precipitation forecasts, and the forecast accuracy for other fields related to precipitation is also studied.

## 3.1 Model performance for precipitation hindcasts

### 3.1.1 Evaluation of model dispersion

In this paragraph, insight on the DEMETER models' behaviour as a multi-model ensemble system is given by comparing monthly model dispersion with interannual standard deviation of precipitation over the areas of interest in this project. Calculations are detailed in equations 3.1 and 3.2. m is the number of models in the multi-model (m=7), $M_j^y(i)$ is model number j's monthly mean hindcast value, $\overline{M^y(i)}$ is the multi-model hindcast for grid point i and year y, $O^y(i)$ is the observed precipitation, and $\overline{O(i)}^y$ is the mean observation over the 1991-2001 period for the month of interest.

$$Mdisp^y(i) = \sqrt{\frac{\sum_{j=1}^{m}\left(M_j^y(i) - \overline{M^y(i)}\right)^2}{m}} \tag{3.1}$$

$$CMAPstd(i) = \sqrt{\frac{\sum_{y=1991}^{2001}\left(O^y(i) - \overline{O(i)}^y\right)^2}{11}} \tag{3.2}$$

Comparing these values give an idea of how robust the signal (i.e. what is forecasted, here the seasonal anomaly) may be with respect to the noise (i.e. the variability between models), which in some way leads to uncertainty in the forecast. Dispersion between models should also be viewed along with mean precipitation

values for the regions of study, since a root mean square dispersion of 2 mm/day over the ITCZ doesn't have the same impact on the multi-model's performance than if over a region with low average precipitation.

**Model dispersion for austral summer hindcasts**

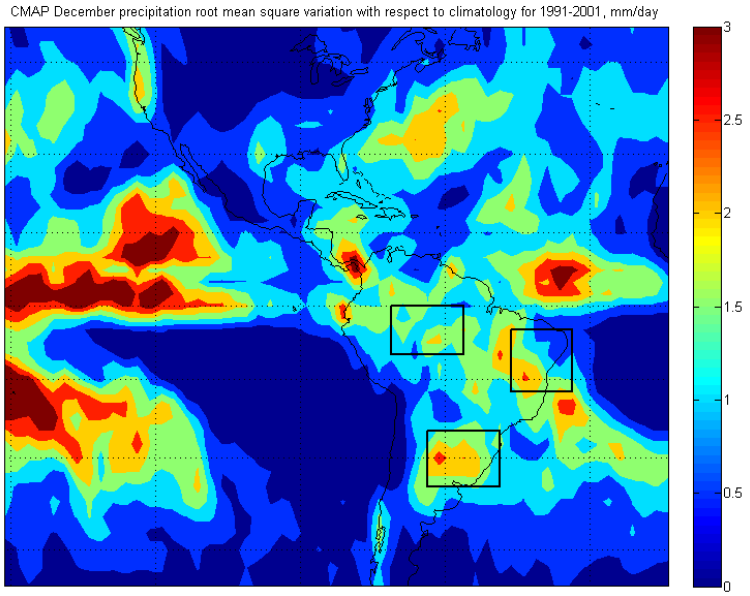


Figure 3.1: *CMAP interannual standard deviation for December precipitation over the Pan-VAMOS region, from 1991 to 2001, in mm/day.*

Before viewing the models' dispersion, the CMAP interannual standard deviation for December 1991 to 2001 is presented in figure 3.1. Comparing this figure with CMAP precipitation means, one sees that interannual standard deviation is highest mostly over the regions with strongest precipitation. The ITCZ and SACZ regions are particularly visible on this map. Standard deviation is also high over the La Plata Basin, meaning that December precipitation means vary a lot from one year to the next: the standard deviation is higher than half of the mean precipitation value over some areas of the La Plata Basin region. This is also true for the Brazilian Nordeste. Precipitation interannual standard deviation is comparatively lower over the Core Amazon Region, where mean precipitation values are higher. This first aspect of model behavior gives a possible explanation as to why models don't perform as well over the La Plata Basin and Nordeste regions as over other regions.

Figure 3.2 shows the different DEMETER models' root mean square dispersion (Mdisp value) over the Pan-VAMOS region for December 1993. Results for hindcasts started in 1993 are similar to other years, as will be shown later. Figure 3.2 can be compared to figure 2.2 [c] which shows CMAP mean precipitation for the same month. Model dispersion is particularly high over northern Peru and Equator, as well as regions of the Andes and the ITCZ. Of the three regions of interest, part of the Nordeste region is where the model

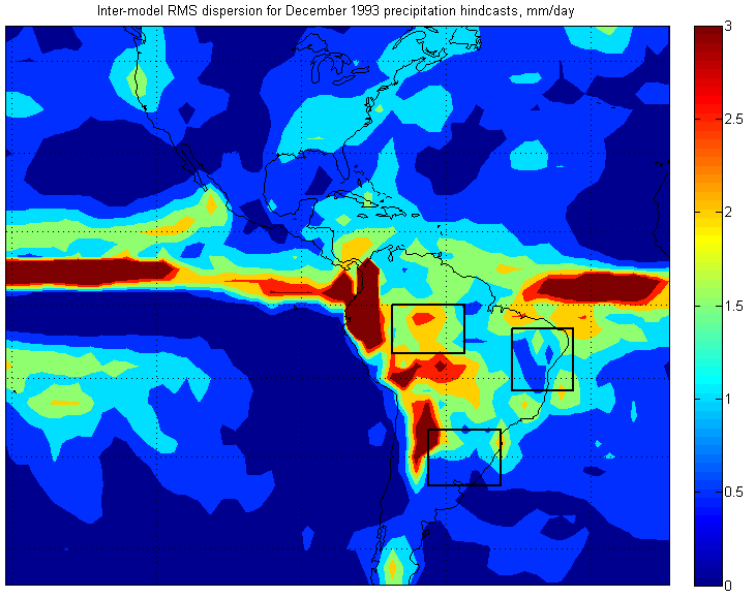


Figure 3.2: *Model root mean square dispersion (Mdisp) over the Pan-VAMOS region for December 1993 hindcasts, in mm/day.*

dispersion is highest when compared to the actual precipitation. This trend is visible for all years of the 1991-2001 period. Model dispersion varies little from one year to the next, meaning that dispersion is systematic. Only one noteworthy exception is found: in 1997, model dispersion was higher over the tropical Pacific and most of South America than for other years (not shown). This could be due to the exceptionally warm ENSO recorded that year.

A more detailed vision of model dispersion versus CMAP precipitation interannual standard deviation is given in figures 3.3, 3.4 and 3.5. These figures show year by year results for December, January and February over the three regions of interest, which are to be compared with interannual standard deviation averaged over the same regions. These amounts should also be compared with mean monthly precipitation amounts averaged over the regions, show in table 3.1.

| | **December** | **January** | **February** |
|---|---|---|---|
| **Core Amazon Region** | 6.81 | 8.28 | 9.08 |
| **Northeast Brazil (Nordeste)** | 3.62 | 3.82 | 3.63 |
| **La Plata Basin** | 4.48 | 4.88 | 5.00 |

Table 3.1: *Mean precipitation amounts in December, January and February 1991-2001 over the regions of study, in mm/day.*

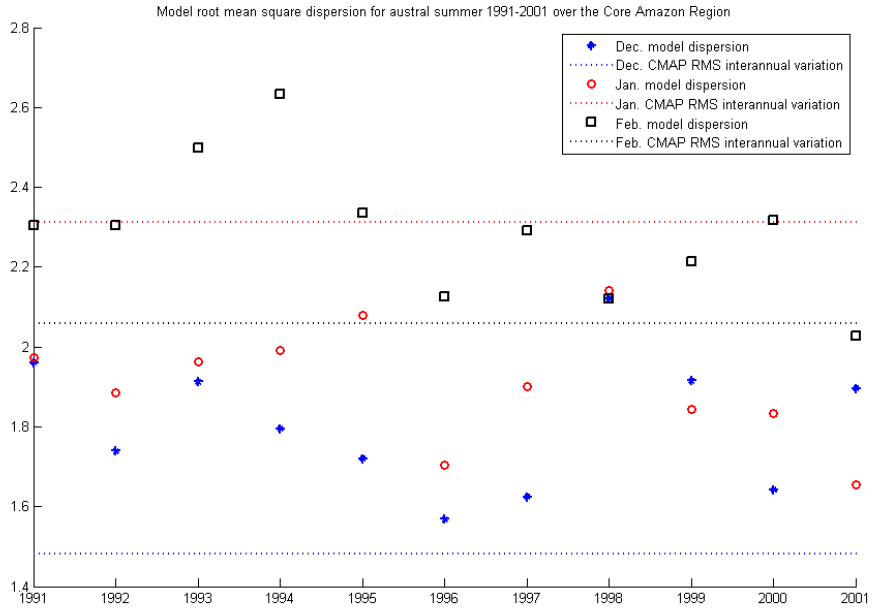


Figure 3.3: *Year by year December, January and February root mean square model dispersion (Mdisp) and CMAP monthly precipitation interannual standard deviation (CMAPstd) averaged over the Core Amazon Region for hindcasts started in November 1991 to 2001.*

Over the Amazon region (figure 3.3 page 48), results vary strongly depending on the month, but behavior is similar from one year to the next. A first observation is that model dispersion increases from December hindcasts to February hindcasts, which isn't surprising: all hindcasts are initialized in November, and prediction accuracy logically decreases with time, so models will tend to give increasingly different predictions for most fields. Another observation is that models have lower dispersion than CMAP interannual standard deviation only for January hindcasts. However, December interannual variation is very low (less than 1.5 mm/day) and model dispersion remains reasonable considering the total precipitation amounts over the region. After three months of hindcast running, model dispersion reaches values ranging from 2 to 2.7 mm/day, while interannual variations are slightly superior to 2.05 mm/day.

The same analysis but for the Brazilian North East (Nordeste) region is shown in figure 3.4 page 49. Once again, model dispersion increases with time, but model dispersion over the Nordeste doesn't have the same behaviour as over the Amazon region when compared to interannual variability. In December and January, model dispersion is for most years inferior to the CMAP standard deviation, with differences lower than 0.5 mm/day. In February, while CMAP standard deviation is similar to that of December (1.5 mm/day approximately), model dispersion values are above 2 mm/day. This shows that the models tend to differ on precipitation values for long-term hindcasts over the Nordeste regions, a possible source of growing errors from one month to the next.

For the La Plata Basin (figure 3.5 page 50), results are quite different. Model dispersion varies little

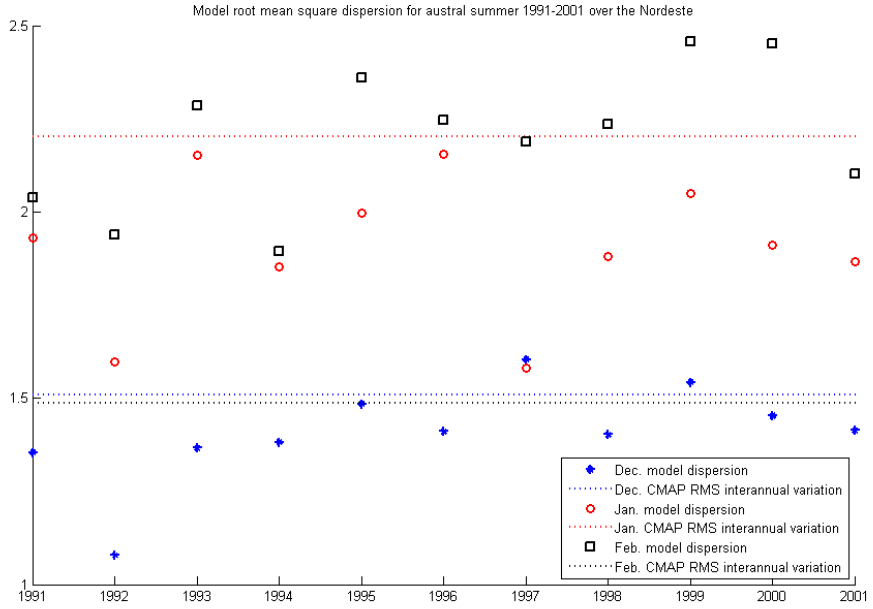


Figure 3.4: *Same as figure 3.3 but for the Brazilian North East region.*

between December and February in most cases, and values mostly range from 1.2 to 1.4 mm/day, and are lower than CMAP interannual standard deviation. However, interannual standard deviation was noticed to be quite high considering the average precipitation rates, and a lower model dispersion doesn't necessarily imply good model performances over the region.

### Model dispersion for boreal summer hindcasts

Figure 3.6 shows CMAP interannual standard deviation over the Pan-VAMOS region for the month of July. As in austral summer, standard deviation is higher over the regions of high precipitation (see figure 2.3 [d]) such as the ITCZ and Central America. Over the Inter-Americas zone, precipitation standard deviation values reach over 1.5 mm/day over the Bay of Campeche and southern Mexico, while total precipitation is around 5 mm/day. Over the Great Plains region, values above 1 mm/day are observed, reaching 2 mm/day to the north of the region, whereas average precipitation is often lower than over the Inter-Americas zone. This shows that the Great Plains region has very high precipitation variability from one year to the next, which may imply lower precipitation predictability. Over the US Southwest, precipitation standard deviation has an average of 0.5 mm/day, which is also quite significant when compared to average precipitation amounts. These results will be further discussed when evaluating model dispersion.

Figure 3.7 shows model root mean square dispersion (as calculated by equation 3.1) over the Pan VAMOS region for July 1994 hindcasts. When compared to CMAP precipitation standard deviation, it is clear that dispersion is very high over the US Southwest and Northern Mexico as well as over the Inter-Americas zone. When compared to CMAP precipitation means for the same month (figure 2.3 [d]), it appears that models

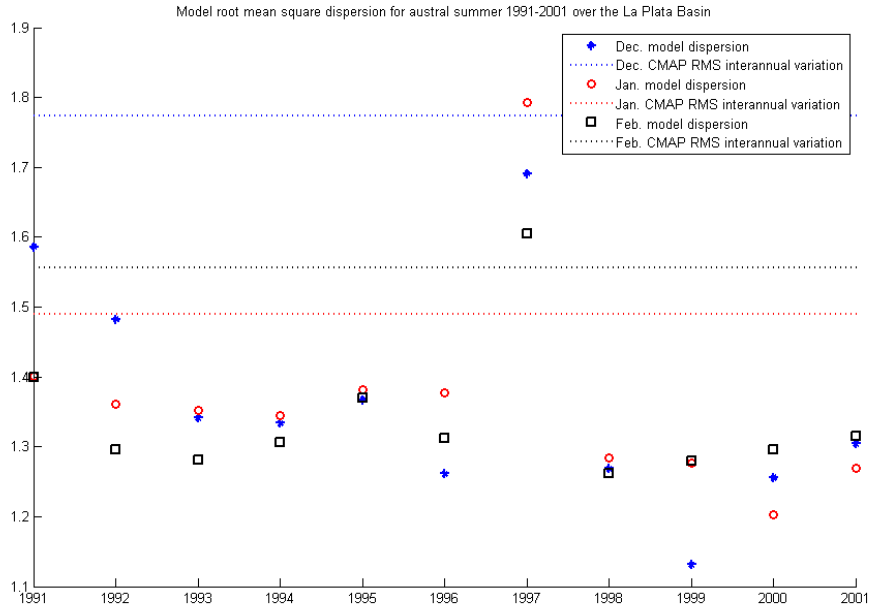


Figure 3.5: *Same as figure 3.3 but for the La Plata Basin.*

have high dispersion over some regions where precipitation is moderate. This suggests that some models have difficulties reproducing precipitation patterns over North America during the monsoon season.

In order to further assess these performances, regional graphs of year by year mean model dispersion compared with mean CMAP precipitation standard deviation values are shown in figures 3.8, 3.9 and 3.10. Mean monthly precipitation amounts over these regions for the 1991-2001 period are shown in table 3.2.

| | **June** | **July** | **August** |
|---|---|---|---|
| **Inter-Americas zone** | 6.68 | 5.68 | 6.40 |
| **US Southwest** | 1.09 | 1.67 | 2.08 |
| **Great Plains** | 3.61 | 2.90 | 2.57 |

Table 3.2: *Mean precipitation amounts in June, July and August 1991-2001 over the regions of study, in mm/day.*

Figure 3.8 confirms previous observations that model dispersion was very high compared to actual interannual variation. For every single month of the 1991-2001 boreal summers, dispersion between models is superior to interannual standard deviation. As stated before, CMAP standard deviation over the area is quite low considering the precipitation amounts, however, models greatly differ in their precipitation forecasts over the region (root mean square differences of up to 3.8 mm/day). Another striking observation is that on the contrary to previous observations concerning austral summer, model dispersion seems to decrease with

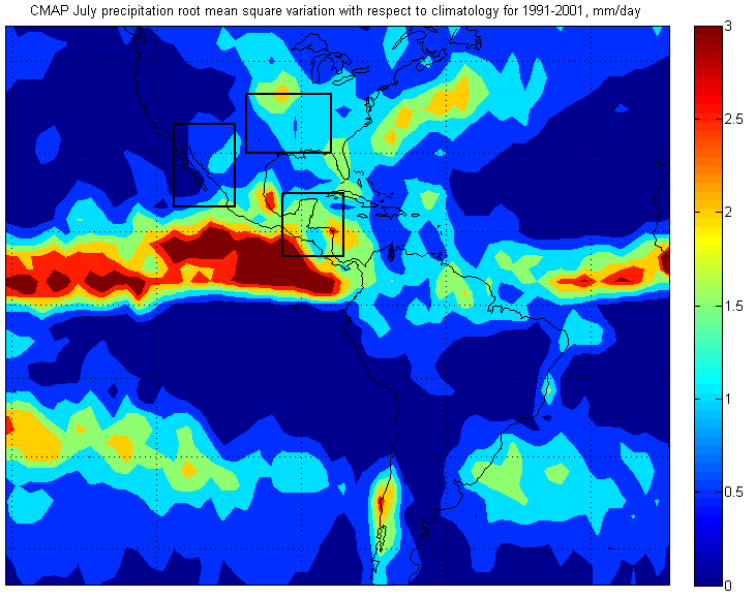


Figure 3.6: *CMAP interannual standard deviation for July precipitation over the Pan-VAMOS region, from 1991 to 2001, in mm/day.*

hindcast time length, August hindcasts agreeing more on precipitation values than June hindcasts.

Results for the US Southwest and Northern Mexico region are shown in figure 3.9, and vary little from one year to the next. CMAP precipitation interannual variation is very small, and therefore only June hindcasts have dispersion values comparable to the interannual standard deviation. July and August hindcasts have growing dispersion, reaching the double of CMAP standard deviation values for August in most years of study. Results must be interpreted with caution, since not all of the region of study is touched by the NAMS, and precipitation stays close to zero even during the NAMS peak season over some areas of the zone of study, whereas other areas witness important precipitation means. This could alter somewhat the significance of the results stated above.

Over the Great Plains region (figure 3.10), results seem quite chaotic. June hindcast dispersion is always lower than interannual precipitation variation, whereas July and August results are above. However, model dispersion decreases in general between July and August, following the precipitation variability trend.

In the following section, another method of evaluation of model performances using correlation coefficients is presented.

### 3.1.2 Correlation coefficients

In this section correlation coefficients are calculated in order to test existence of a linear relationship between hindcasts and observations for the 1991-2001 period over various regions. Both spatial and temporal

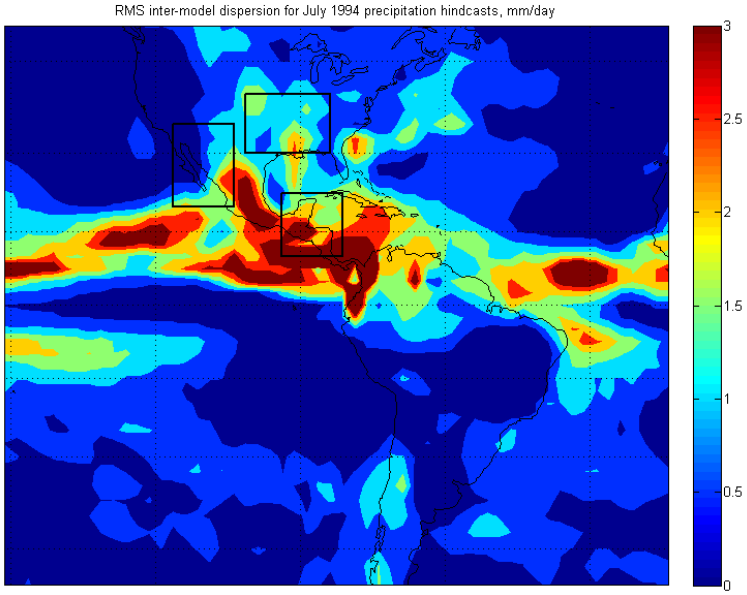


Figure 3.7: *Model root mean square dispersion (Mdisp) over the Pan-VAMOS region for July 1994 hindcasts, in mm/day.*

correlation coefficients and anomaly correlation coefficients were computed.

So as to make graphs easier to read, only three model performances are shown in most figures. The models studied are the DEMETER multi-model, constructed as the mean of all individual models ensemble hindcasts, the ECMWF model and the CNRM model. The ECMWF and CNRM models use different ocean and atmosphere component in their coupled models, with different resolutions, implying that they won't necessarily have the same responses. Both models are initialized using ERA-40 data. For all three models, the model studied is the mean of all nine ensembles generated in the DEMETER project.

### Spatial correlation over the SAMS regions

Spatial correlation coefficients are defined by equation 3.3, where n is the number of grid points in the studied region (n varies from 35 to 42 depending on the region size), $\overline{O}$ and $\overline{F}$ are the mean observation and forecast over the region, $O_i$ is the observed precipitation and $F_i$ the forecast precipitation over grid point i. These coefficients are sometimes called product moment correlation coefficients.

$$CC = \frac{\sum_{i=1}^{n} \left(O_i - \overline{O}\right) \cdot \left(F_i - \overline{F}\right)}{\sqrt{\sum_{i=1}^{n} \left(O_i - \overline{O}\right)^2} \cdot \sqrt{\sum_{i=1}^{n} \left(F_i - \overline{F}\right)^2}} \tag{3.3}$$

Spatial anomaly correlation coefficients are defined by equation 3.4, where $C_i$ is the value given by 1991-2001 climatology over grid point i for the month of study.

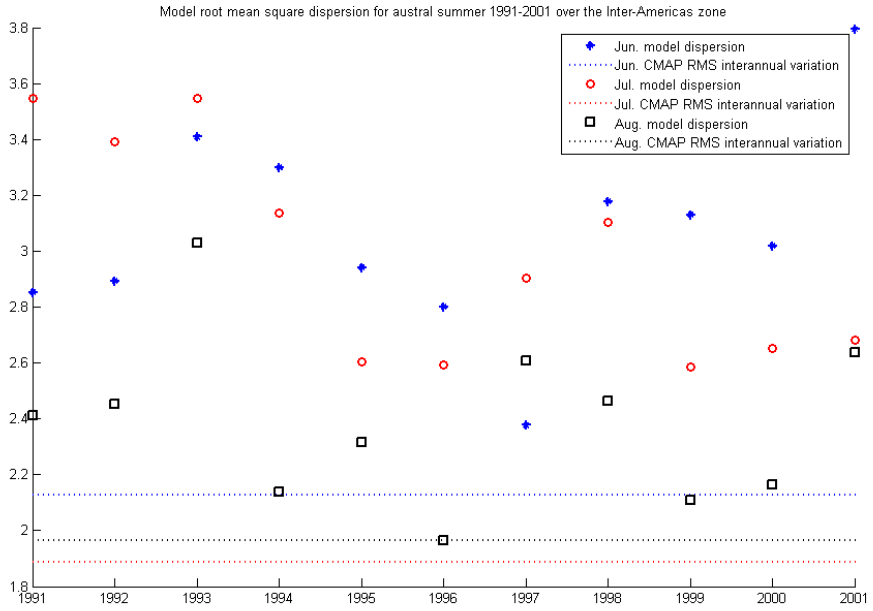


Figure 3.8: *Year by year June, July and August root mean square model dispersion (Mdisp) and CMAP monthly precipitation interannual standard deviation (CMAPstd) averaged over the Inter-Americas zone for hindcasts started in May 1991 to 2001.*

$$ACC = \frac{\sum_{i=1}^{n} (O_i - C_i) \cdot (F_i - C_i)}{\sqrt{\sum_{i=1}^{n} (O_i - C_i)^2} \cdot \sqrt{\sum_{i=1}^{n} (F_i - C_i)^2}} \tag{3.4}$$

The correlation coefficient measures how the forecast geographical distribution particularities (with respect to the mean forecast over the area of study) correspond to the observation's geographical distribution. For instance, if a particular grid point presents heavier rain than the other points, the CC measures if the forecast captures this phenomena or not. The ACC measures the same behaviour, but for the anomalies with respect to the mean climatology for each grid point. If a particular grid point had very high rain compared to the average precipitation over this point for the same month, then the ACC evaluates if the model reproduces this anomaly with respect to climatology or not. Both CC and ACC range from -1 to 1, 1 being the perfect score. It is important to note however that both scores do not take into account bias values, and forecasts with large bias errors can still have excellent scores for correlation. This makes these scores complementary to the ones presented in the previous section. CCs and ACCs were calculated for each summer month precipitation hindcast of the 1991-2001 period, and some results are presented in the following figures.

Figures 3.11 page 56 show year by year spatial correlation coefficients over the three regions of study for the month of December hindcasts started in November. Results are presented for the three models selected earlier.

Over the Core Amazon region (figure 3.11 [a]), correlation coefficients for the multi-model are higher than

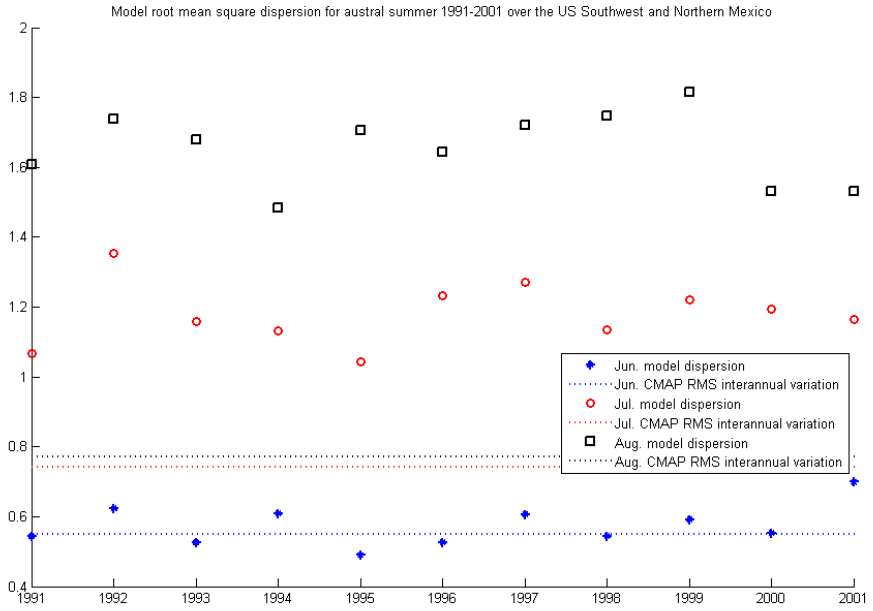


Figure 3.9: *Same as figure 3.8 but for the US Southwest and Northern Mexico region.*

0.5 save two years, 1998 and 1999. Improvement of the correlation coefficient values using the multi-model over independent models is noteworthy, since the multi-model geographical distribution has higher correlation with CMAP geographical distribution over this region than the two other models shown in a majority of years. Scores over the Brazilian Nordeste are yet higher (figure [b]). For the multi-model, correlation coefficients reach values close to 0.95 and are higher than 0.75 for every year of study. Once again, improvement using the multi-model is blatant, individual models having much more variation in correlation coefficient scores than the multi-model. The correlation coefficient values drop between the 1-month December hindcasts and the 3-month February hindcasts for the Nordeste region, however, performance over this region remains the best of all three zones for all hindcast months (not shown). Results over the La Plata Basin are strikingly worse. For most years, December hindcast correlation coefficients with respect to CMAP data range from -0.5 to 0.5, meaning that even the multi-model fails to capture geographical distribution of precipitation over this region.

These results should be further evaluated examining precipitation climatology for the month of December. Over the Nordeste region, precipitation in December as shown in figure 2.2 [c] shows that peak monsoon rainfall hasn't reached this region yet, and rainfall geographical distribution is quite homogeneous. On the contrary, over the La Plata Basin, a clear longitudinal distribution of precipitation can be seen, with rainfall amounts varying from 2.5 mm/day west of the boxed region to over 6 mm/day east of the boxed region. This geographical distribution may be harder to capture by the models than that of the Nordeste region. Over the Core Amazon region, precipitation amounts and a complex geographical distribution could also explain poorer correlation coefficients.

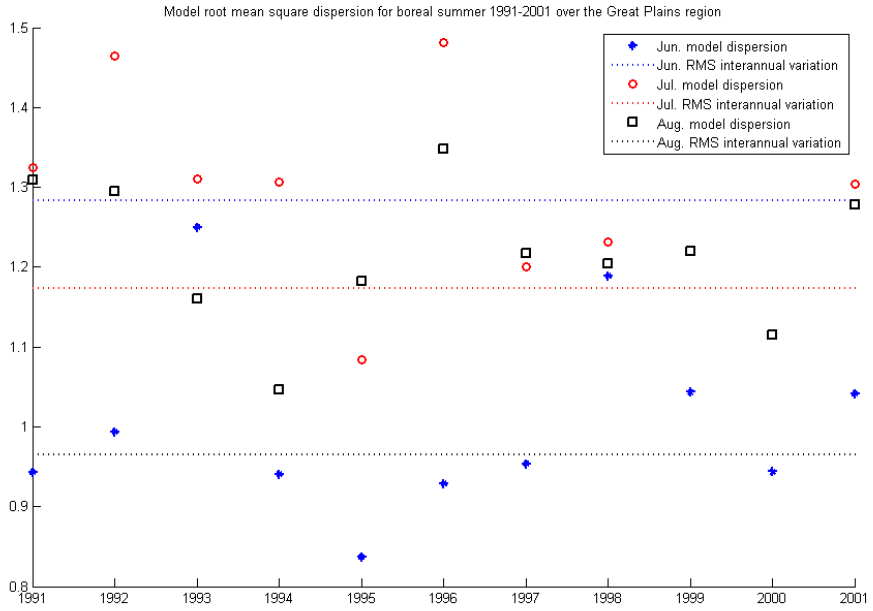


Figure 3.10: *Same as figure 3.8 but for the Great Plains region.*

To complete these results, anomaly correlation coefficients were also calculated. Results for December 1991-2001 are presented page 57.

Anomaly correlation coefficients for the three regions show poor model performance. While the models in general and the multi-model in particular seemed to capture fairly well particularities of geographical distribution of precipitation over two regions, the models don't seem to capture the anomalies in this distribution with respect to the 1991-2001 CMAP climatology for December precipitation. Moreover, the ACC values oscillate between negative and positive values.

In order to complete this study, temporal correlation coefficients were also calculated, in order to see if the same type of difficulties were observed.

### Temporal correlation over the SAMS regions

Temporal correlation coefficients are calculated over each grid point i according to equation 3.5, where y is the year of the hindcast starting date, $O_i^y$ is the CMAP precipitation observed and $F_i^y$ the hincast precipitation over point i in year y, and $\overline{O_i}$, $\overline{F_i}$ are the mean observation and forecasts over point i for the month of study over the 1991-2001 period.

$$CC_i = \frac{\sum_{y=1991}^{2001} \left(O_i^y - \overline{O_i}\right) \cdot \left(F_i^y - \overline{F_i}\right)}{\sqrt{\sum_{y=1991}^{2001} \left(O_i^y - \overline{O_i}\right)^2} \cdot \sqrt{\sum_{y=1991}^{2001} \left(F_i^y - \overline{F_i}\right)^2}} \tag{3.5}$$

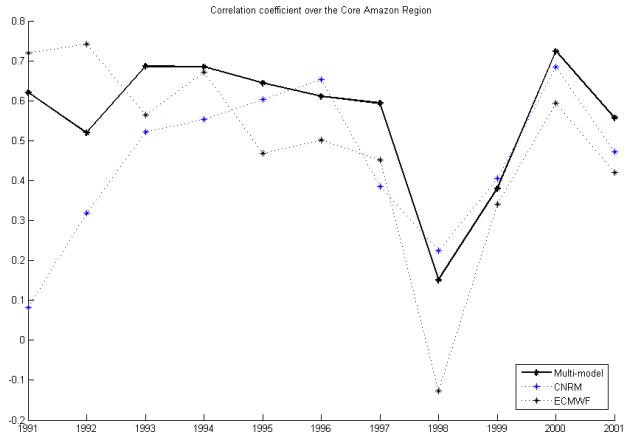


[a]

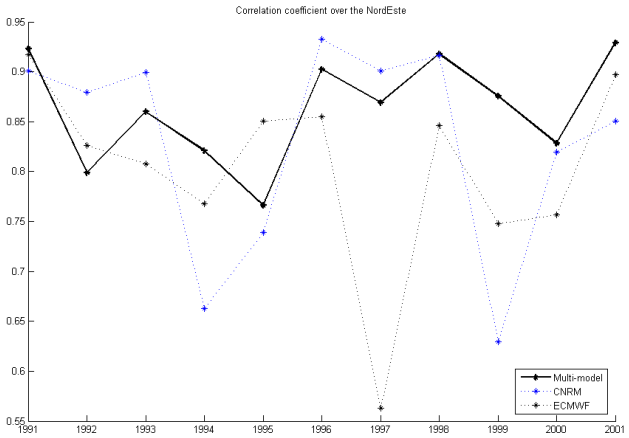


[b]

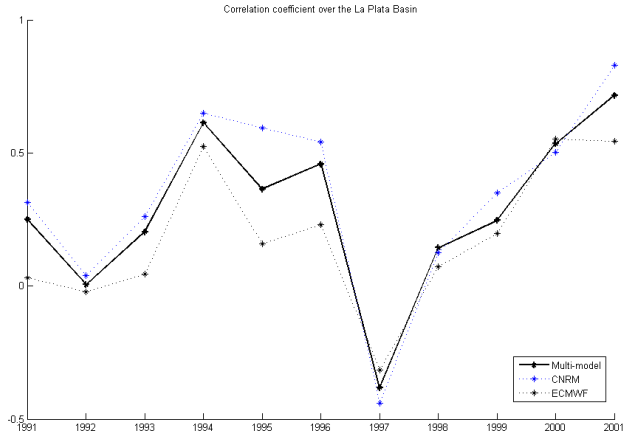


[c]

Figure 3.11: *Spatial correlation coefficients with respect to CMAP data for December hindcasts over the Core Amazon Region* [a] *, North East Brazil* [b] *and La Plata Basin* [c] *for hindcasts started in November 1991 to 2001.*

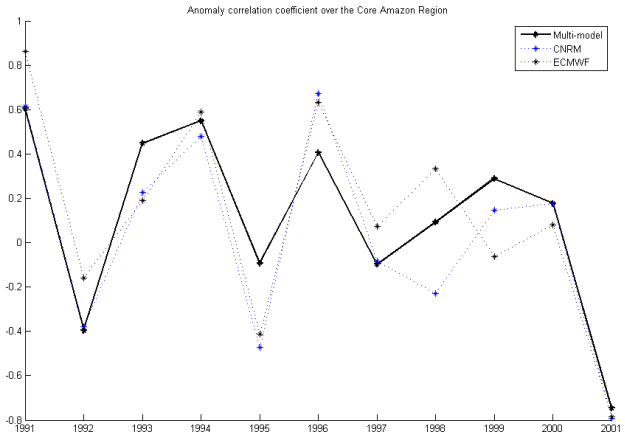


[a]

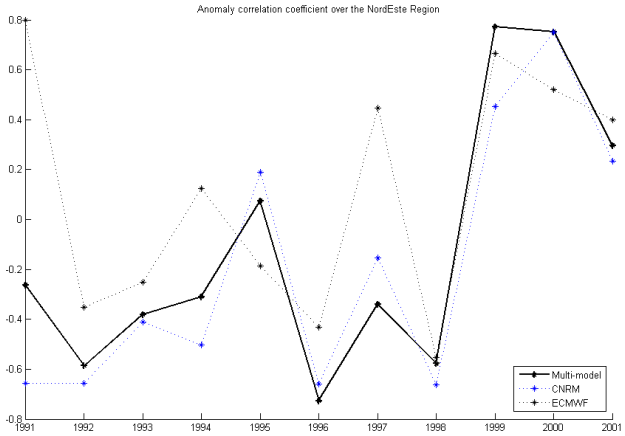


[b]

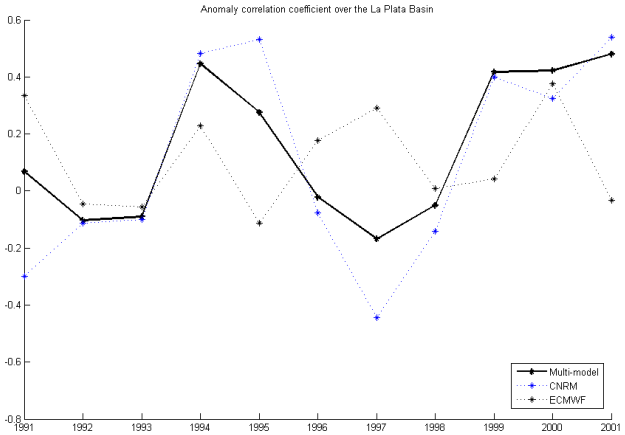


[c]

Figure 3.12: *Spatial anomaly correlation coefficients with respect to CMAP data for December hindcasts over the Core Amazon Region* [a] *, North East Brazil* [b] *and La Plata Basin* [c] *for hindcasts started in November 1991 to 2001.*

Correlation coefficients measure how models capture temporal variations in the field of study. Temporal anomaly correlation coefficients are calculated similarly over each grid point i using equation 3.6:

$$ACC_i = \frac{\sum_{y=1991}^{2001} (O_i^y - C_i) \cdot (F_i^y - C_i)}{\sqrt{\sum_{y=1991}^{2001} (O_i^y - C_i)^2} \cdot \sqrt{\sum_{y=1991}^{2001} (F_i^y - C_i)^2}} \tag{3.6}$$

$C_i$ is the climatological mean precipitation over point i, defined as the mean CMAP precipitation value for the month of study between 1991 and 2001. (In this study, $C_i$ corresponds to $\overline{O_i}$). Temporal ACC illustrate how models capture anomalies with respect to the climatological mean.

Results for austral summer were calculated over the Pan-VAMOS region, and results for the multi-model December hindcasts are shown in figure 3.13 page 59. So as to show only significant correlation coefficients, values between -0.3 and 0.3 were omitted on the graphs. A quick glance at the graphs show immediately that the multi-model has better scores for correlation coefficients than for anomaly correlation coefficients, meaning that it follows relatively well the observations, but has more trouble capturing strong anomalies with respect to climatology. Observing figure 3.13 with more attention, it appears that the correlation and anomaly correlation coefficients over the areas selected in this study are not significant, save over the La Plata Basin region. This result seems surprising, but the anomaly correlation coefficient map obtained here is similar to the one shown in Nobre et al.'s paper (figure 1 (a) in [Nobre et al., 2006]).

Another observation is that the highest correlation and anomaly correlation coefficients are found over the Pacific and Atlantic ITCZ, and over the North Atlantic Ocean off the U.S. East Coast. However, these regions have sustained rainfall (over 5 mm/day) during austral summer, as shown by figure 2.1 page 16. This rainfall is regular, making it more predictable than monsoon rainfall over the South American continent.

Individual model performances for correlation and anomaly correlation coefficients were also computed (not shown). The CNRM and ECMWF models have poorer scores than the multi-model, and regions where correlation exceeds 0.4 are smaller. However, the ECMWF model has higher anomaly correlation coefficients than the CNRM model for austral summer, particularly over the La Plata Basin and North America.

In the following sections, the same scores for boreal summer will be shown.

### Spatial correlation over the NAMS regions

Figure 3.14 page 60 shows spatial correlation coefficients (as defined by equation 3.3) for July precipitation hindcasts regarding CMAP data. The month of July was chosen so as to show performance for two-month hindcasts and show longer-term model performance (one-month hindcasts were presented in the austral summer study). Moreover, assessing performance for longer time periods enables to show model stability, and assess performances over more seasonal time scales.

The models presented are the same as in the austral summer study (CNRM, ECMWF and DEMETER multi-model). Over the Intra-Americas region (figure 3.14 [a]), all three models have scores higher than 0.4 for every year of interest, and the multi-model performs better than both individual models, with scores superior than 0.6 for every year. Values are generally similar from one month to the next over the Intra-Americas region, and general performance remains stable, but interannual variations for monthly correlation coefficients are quite different depending on the month of study (years when correlation is highest for June can show low correlation for July for instance). Over the U.S. Southwest and Northern Mexico (figure [b]), correlation coefficients are once again notably improved using the multi-model instead of individual models. However, both the CNRM and ECMWF models show high correlation coefficients (over 0.5) over this region for a majority of years during the 1991-2001 period. The multi-model thus performs very well over this region (over 0.65 save between 1996 and 1998). Performance over the Great Plains region is much less regular,

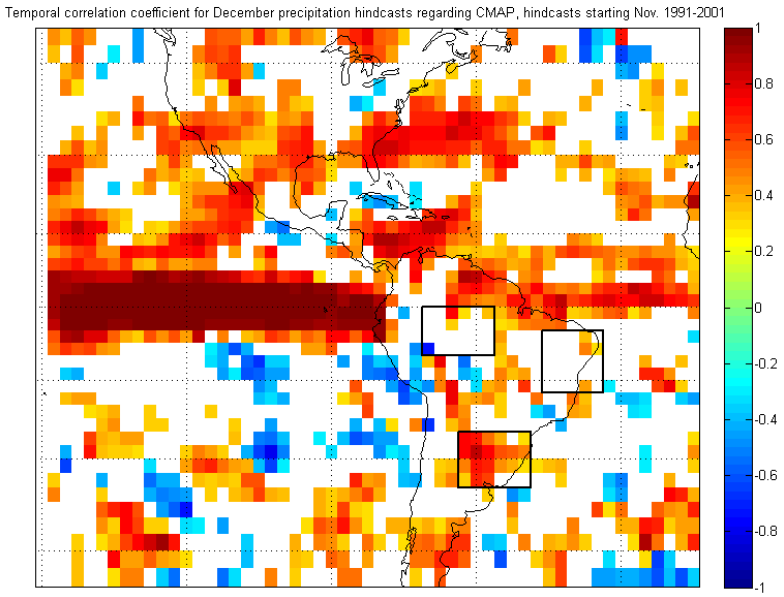


[a]

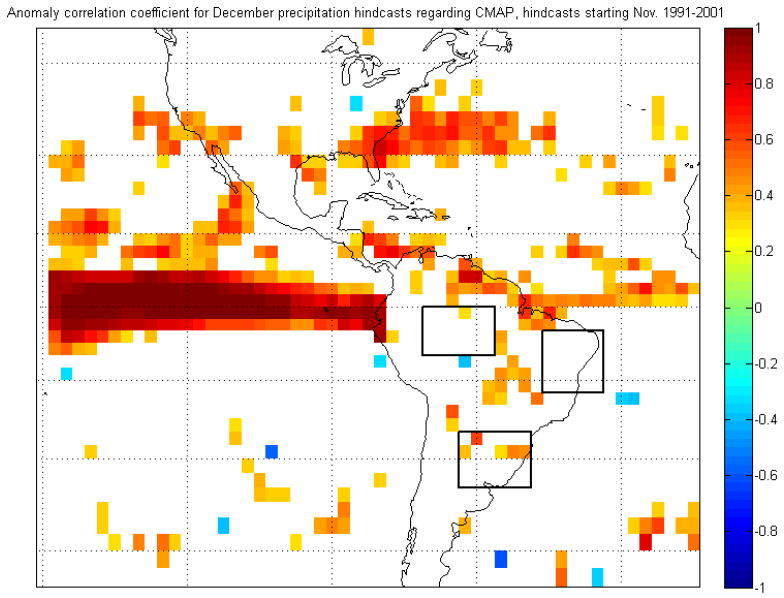


[b]

Figure 3.13: *Temporal correlation* [a] *and anomaly correlation* [b] *coefficients with respect to CMAP data for December hindcasts over the Pan-VAMOS region for mean of all ensembles multi-model hindcasts started in November 1991 to 2001. Values between -0.3 and 0.3 are not shaded in these graphs.*

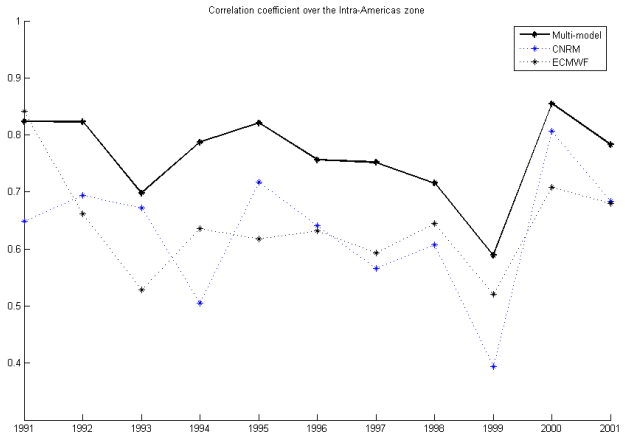


[a]

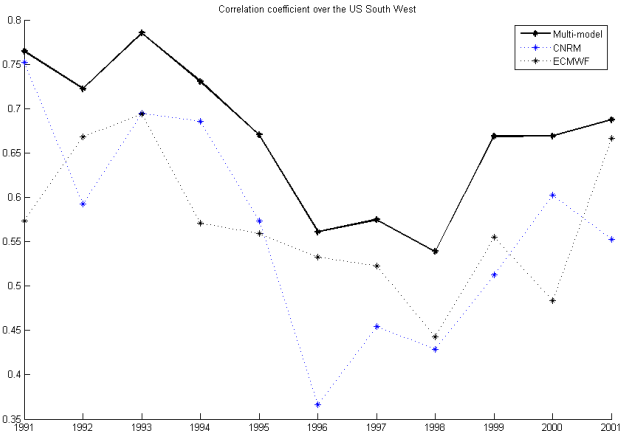


[b]

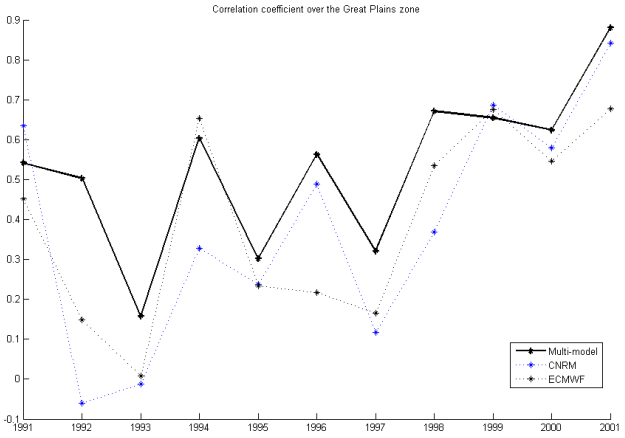


[c]

Figure 3.14: *Spatial correlation coefficients with respect to CMAP data for July precipitation hindcasts over the Intra-Americas Zone* [a] *, US South West and Northern Mexico* [b] *and US Great Plains region* [c] *for hindcasts started in May 1991 to 2001.*

with scores for the multi-model ranging from approximately 0.15 to close to 0.9, depending on the year. An oscillation between high and low correlation values is observed, but doesn't appear for June or August hindcasts (not shown). Both the ECMWF and the CNRM models exhibit similar year-to-year behaviour, but with slightly lower values than the multi-model. Mean score is higher for July than for June or August.

Once again, in order to modulate the importance of such scores, precipitation climatology over the regions of study should be examined for the month of July (see figure 2.3 [d]). Over the US Southwest, precipitation during July is still weak and varies from no rain at all to 3 mm/day in the southeastern corner of the boxed region. Precipitation has a much more complex geographical distribution over the Great Plains regions, with higher mean amounts and higher variation. Moreover, mean July CMAP precipitation geographical distribution varies from one year to the next (not shown). This could explain model performance variations. However, very few negative correlation values were found, and model performance therefore differs over the Great Plains region from performance over the South American La Plata Basin region, and is notably higher.

Figure 3.15 page 62 shows spatial anomaly correlation coefficients (see equation 3.4) over the three regions of interest for July precipitation hindcasts with respect to CMAP data. Climatology is defined as mean July precipitation from 1991 to 2001 as obtained by CMAP.

Despite good correlation coefficient scores over the North American Monsoon regions (US Southwest and Intra-Americas zone), anomaly correlation coefficients are poor over each region of study. For the Intra-Americas zone, anomaly correlation coefficients are over 0.4 for 4 years, below -0.4 for 2 years. For the other 5 years, anomaly correlation coefficients are not significant. Values vary from negative to positive from one year to the next, and negative values in July don't imply necessarily negative values in August or June, and vice-versa. The anomaly correlation coefficients therefore show the individual models and multi-model's difficulty to capture yearly anomalies with mean climatology. Over the US Southwest and Northern Mexico region, most scores range from -0.4 to 0.4, assessing poor model performance in anomaly pattern forecasting. Similar scores are found for August, and even less significant scores are found for June, where scores range from -0.2 to 0.2 (not shown). Similar results are obtained for the Great Plains region.

In order to further examine performance over these regions, and compare performance with other regions of the North and South American continents, temporal correlation coefficients were computed, and results are presented in the next paragraph.

#### Temporal correlation over the NAMS regions

Temporal correlation and anomaly correlation coefficients (see equations 3.5 and 3.6) for boreal summer were computed for the three models studied in this section, and results for the multi-model are presented in figure 3.16 page 63.

Results for correlation coefficients over the three regions confirm spatial correlation coefficient results: CCs are much higher over the Intra-Americas than over other regions. Models have lower temporal correlation performance over the US Southwest region than they had for spatial correlation. Over the Great Plains region, strong positive and negative values are found. As in austral summer, results for anomaly correlation coefficients are less significative than correlation coefficients. Over the Great Plains region, strong anomaly correlation coefficients are negative, indicating that models tend to inverse precipitation anomalies over some areas. This phenomena concerns only a small proportion of the grid points in this region.

Again, results obtained with these coefficients should be examined with mean precipitation data, and precipitation anomaly evolutions. Over the Intra-Americas zone, precipitation does vary from one year to the next, but with less relative inter-annual variance than over the Great Plains region or the US Southwest, where global models have been shown to encounter anomaly forecasting difficulties for drought or humid episodes due to low resolution [Mo et al., 2005].

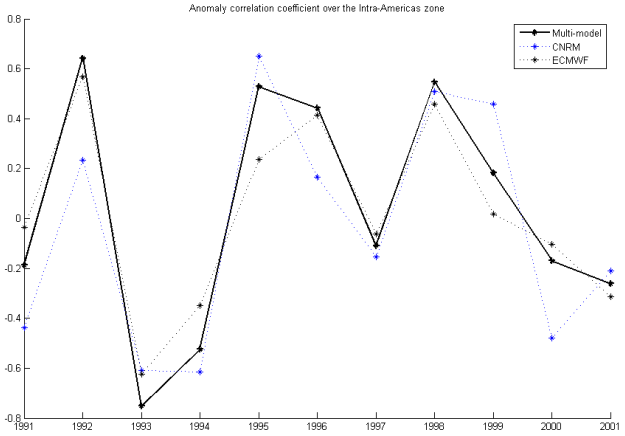


[a]

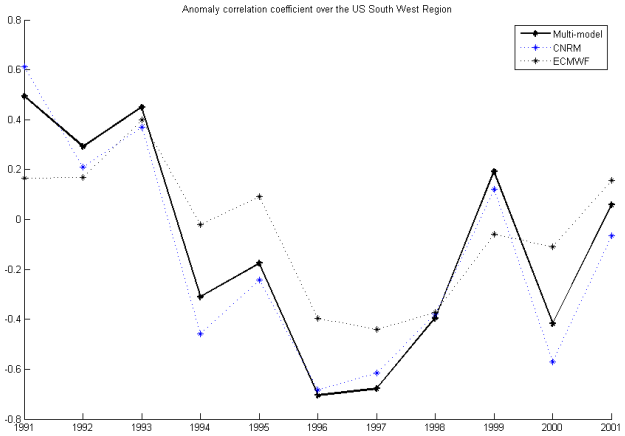


[b]

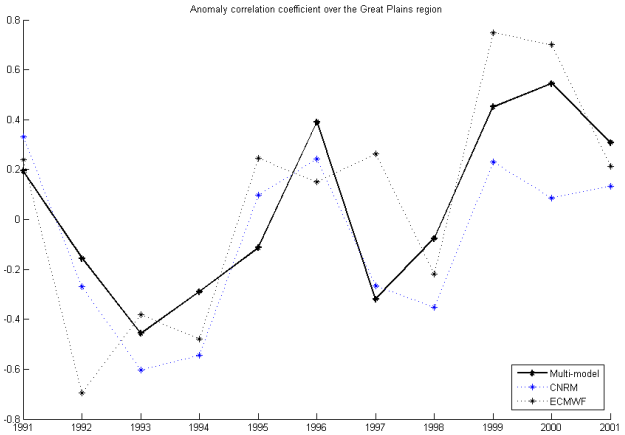


[c]

Figure 3.15: *Spatial anomaly correlation coefficients with respect to CMAP data for July precipitation hindcasts over the Intra-Americas Zone* [a] *, US South West and Northern Mexico* [b] *and Great Plains region for hindcasts started in May 1991 to 2001.*

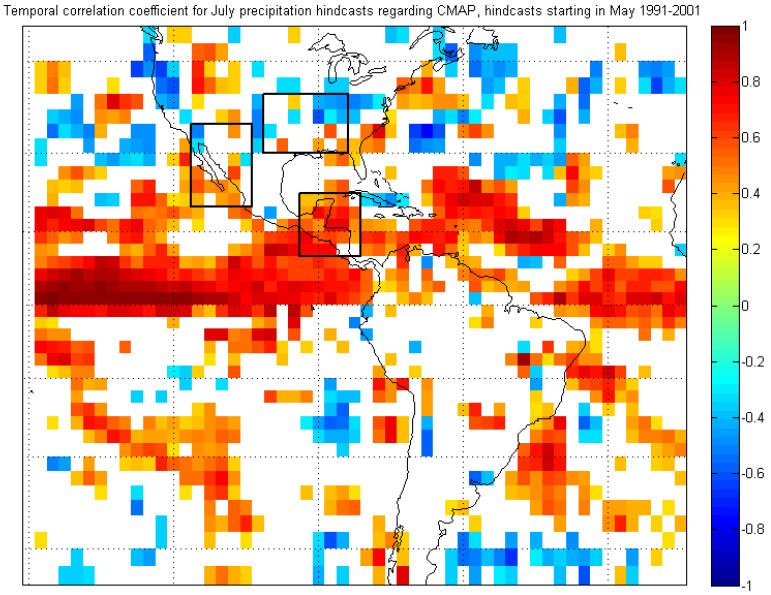


[a]

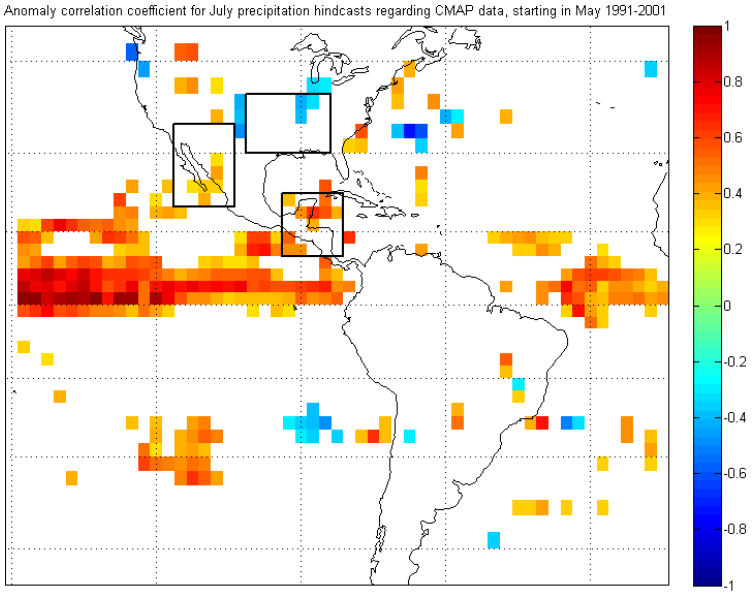


[b]

Figure 3.16: *Temporal correlation* [a] *and anomaly correlation* [b] *coefficients with respect to CMAP data for July hindcasts over the Pan-VAMOS region for mean of all ensembles multi-model hindcasts started in May 1991 to 2001.*

A general conclusion of this study of correlation coefficients and anomaly correlation coefficients over the Pan-VAMOS Region is that scores are generally lower and more chaotic in sub-tropical regions. This is consistent with the fact that tropical regions are subject to more predictable circulation systems, such as Hadley cells, whereas in higher latitudes, weather depends more on synoptic scale variations which are harder to predict and chaotic by nature.

## 3.2 Model performance for other fields

### 3.2.1 Correlation coefficients for 2 meter temperature hindcasts

In this section temporal and spatial correlation and anomaly correlation coefficients for 2 meter temperature hindcasts are presented. Calculations are similar to those detailed in equations 3.3, 3.4, 3.5 and 3.6, but relative to 2 meter temperature hindcasts. Monthly climatology is defined as mean monthly ERA-40 reanalysis 2 meter temperature over the period of study, and observations are also taken from monthly ERA-40 reanalysis.

All models performances for boreal and summer monthly hindcasts were studied, but as for the precipitation prediction skill, only three models (multi-model, CNRM and ECMWF) are shown on the spatial correlation graphs so as to make reading easier. The three months of each season of study (DJF and JJA) were also studied, but results are shown for the same month as in the precipitation forecast skill assessment.

#### Spatial correlation over the SAMS region

Figure 3.17 page 66 shows spatial correlation coefficients of December 2 meter temperature hindcasts over the three regions of South America studied in this report with respect to ERA-40 observations. As for precipitation hindcasts, correlation coefficients are mostly higher when using the multi-model, and individual models have highly variable performances from one year to the next. This is particularly striking over the Core Amazon region, where the CNRM and ECMWF models have almost opposite correlation coefficient variations from one year to the next. Highest scores are found over the Brazilian Nordeste, where the lowest multi-model correlation coefficient is reached in 1997 (over 0.7). This implies that geographical temperature variability over this region is well captured by the different models. Over the Core Amazon region, poorer scores indicated that individual models encounter problems in capturing these specificities. This seems surprising when examining average temperature over the region, since temperature seems to be quite homogeneous over this region (see DJF ERA-40 2 meter temperature climatology in figure 2.9), and varies much more over the La Plata Basin where spatial correlation coefficient results are higher than 0.75 for every multi-model hindcast. This is confirmed by monthly December ERA-40 2 meter temperature fields (not shown). Another point of interest is model behaviour during the 1997 El Niño episode. Over the Nordeste and the La Plata Basin regions, the ECMWF model correlation is significantly lower for this particular year than for other years of the 1991-2001 period. This also affects the multi-models' performance. However, looking back at figure 2.21 page 40, the ECMWF model has similar bias and RMSE than the CNRM model, and no link to SST anomaly predictions can be exhibited at this time.

Results for January and February are similar: January correlation coefficients are still higher over the Nordeste and La Plata Basin regions although they tend to decrease in comparison with December hindcasts, and interannual variation tends to increase. February multi-model hindcast correlation over the Core Amazon ranges from slightly negative to 0.8, while values over the La Plata Basin and the Nordeste remain fairly high (over 0.55 and 0.6 respectively). The high scores over the La Plata Basin do not mean however that models

forecast temperature correctly. Indeed, it was shown that models have high positive bias over the La Plata Basin for austral summer hindcasts.

Results should be compared to those calculated for precipitation hindcasts for the same month (figure 3.11 page 56). The ECMWF's peculiar behaviour in 1997 is also observed for precipitation hindcast spatial correlations over the Nordeste and La Plata Basin. Scores for precipitation and 2 meter temperature hindcasts for December over the Core Amazon region are similar, ranging from 0.4 to 0.75 in most cases, although inter-annual variations show different patterns. The high scores over the Nordeste for temperature are also seen for precipitation, demonstrating model ability to capture geographical particularities over this region in both fields. It has been shown earlier that this is not the case for anomaly correlation coefficients in precipitation, and 2 meter temperature results are now presented.

Figure 3.18 page 67 shows spatial anomaly correlation coefficients for December 2 meter temperature hindcasts over the same three regions. Scores are once again poorer than correlation coefficients over each region, with high variation from one year to the next. An important difference between ECMWF and CNRM scores and inter-annual variation can be seen, as for the correlation coefficients, although no model seems to outperform the other. The DEMETER multi-model seems to follow mainly CNRM anomaly correlation coefficients over the three regions.

If correlation coefficient results seemed encouraging over all three regions of study, anomaly correlation coefficient results make interpretation of these results harder. This could be due to the fact that monthly hindcasts and reference fields are used in these calculations, which would be more significant using daily fields. In any case these results demonstrate the high divergence between individual model performances, and the importance of using diverse scores when evaluating model performances.

### Temporal correlation over the SAMS region

Figure 3.19 page 68 shows temporal correlation and anomaly correlation coefficients for the multi-model hindcasts for December 2 meter precipitation with respect to ERA-40 data. Values between -0.3 and 0.3 were deleted in the graphs. The difference between both figures is mainly in coefficient values: these tend to be lower for anomaly correlation than for correlation, as for the spatial coefficients. However, when values are significant for both coefficients, they are of same sign. Unlike for spatial correlation, results are much better over the Core Amazon Region. However, monthly means of ERA-40 December 2 meter temperatures show that temperatures vary little from one year to the next over this region, with a mean anomaly range of less than 1 degree Celsius (not shown). The Nordeste region's mean 2 meter temperature for December has a mean anomaly range of 1.5° C, and correlation and anomaly correlation coefficients are lower than over the Core Amazon Region. Results over the La Plata Basin are poorer, the multi-model showing negative correlation and anomaly correlation results over some grid points to the north of the region, and positive correlation to the south. Anomaly correlation is insignificant or negative over the region. However, a higher range of mean temperature values (span of 2.5° C) could explain the model's difficulty to capture 2 meter temperature interannual variations.

Similar studies were led over the NAMS regions for boreal summer, and some results are presented in the next paragraphs.

### Spatial and temporal correlation over the NAMS regions

Spatial and temporal correlation and anomaly correlation coefficients were calculated over the NAMS regions. Results for spatial coefficients were similar to those noted for the SAMS regions: correlation coefficients for the multi-model were generally high (save over the Great Plains region) and quite stable from one year to

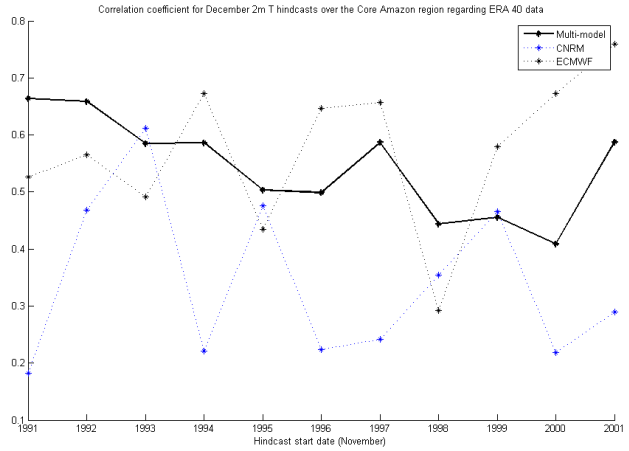


[a]

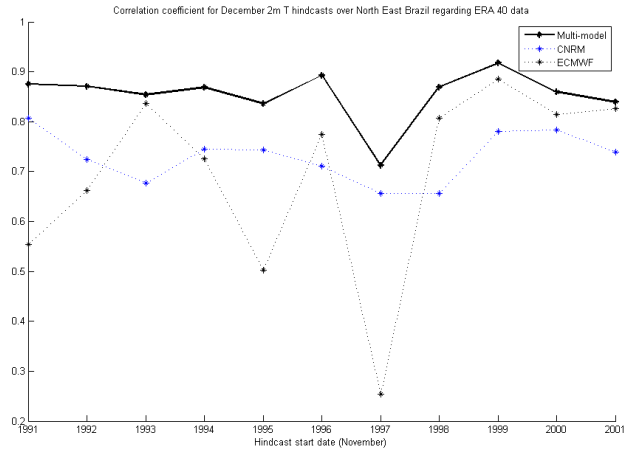


[b]

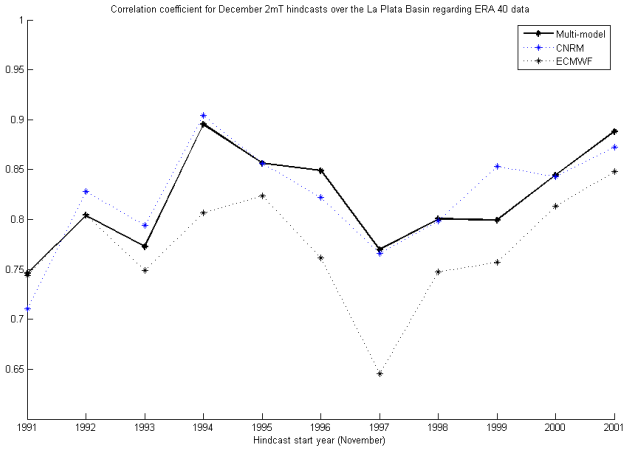


[c]

Figure 3.17: *Spatial correlation coefficients with respect to ERA-40 data for December 2 meter temperature hindcasts over the Core Amazon Region* [a] *, North East Brazil* [b] *and La Plata Basin* [c] *for hindcasts started in November 1991 to 2001.*

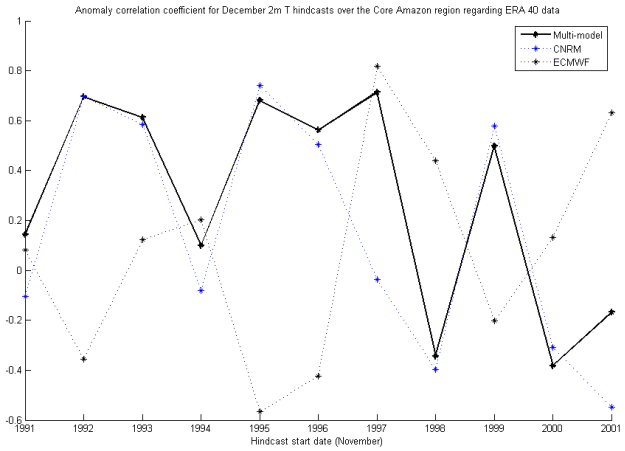


[a]

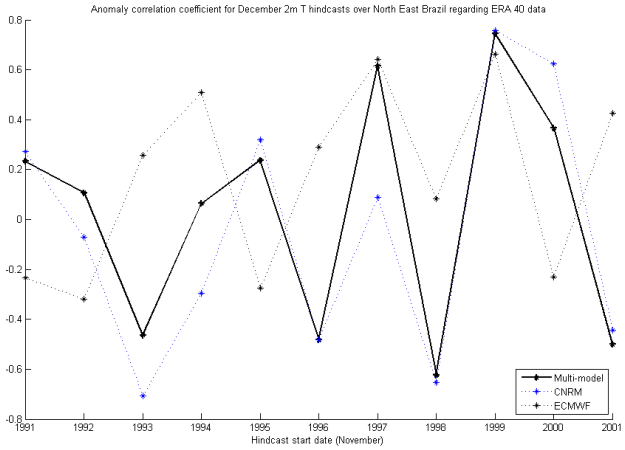


[b]

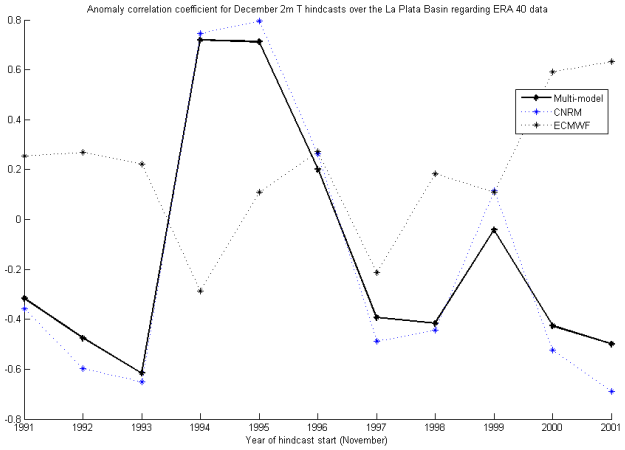


[c]

Figure 3.18: *Spatial anomaly correlation coefficients with respect to ERA-40 data for December 2 meter temperature hindcasts over the Core Amazon Region* [a] *, North East Brazil* [b] *and La Plata Basin* [c] *for hindcasts started in November 1991 to 2001.*

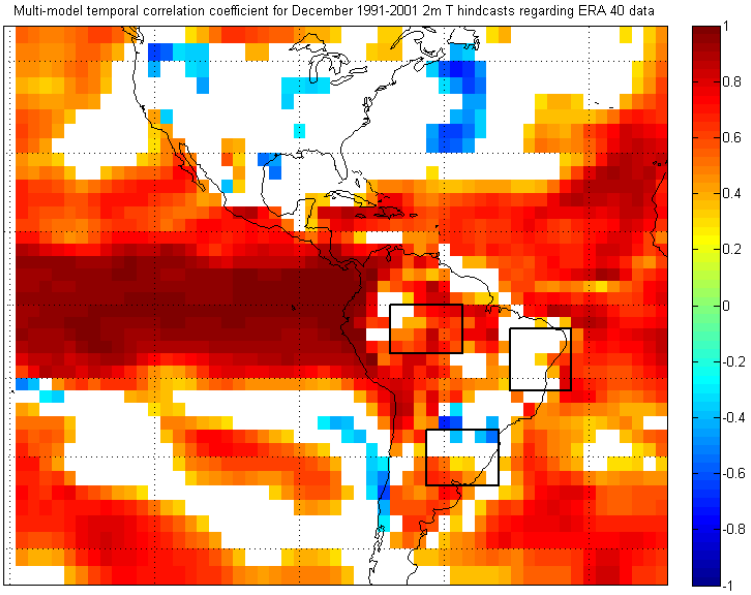


[a]

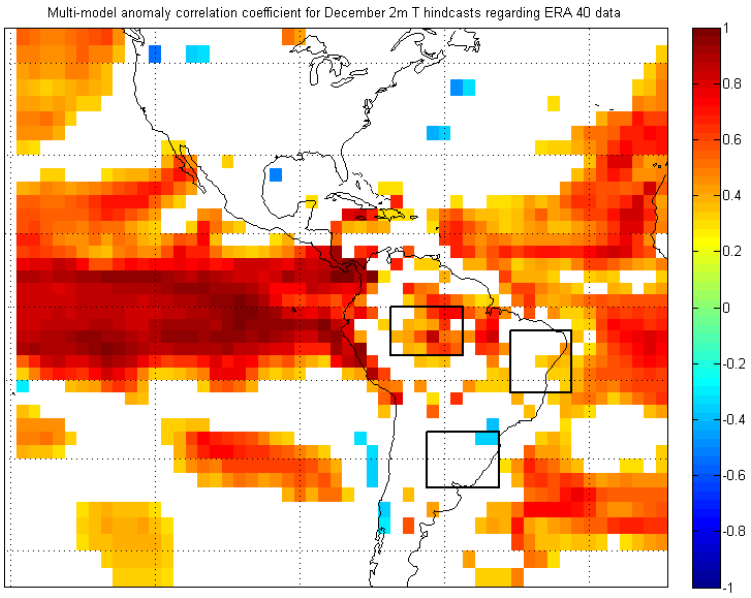


[b]

Figure 3.19: *Temporal correlation* [a] *and anomaly correlation* [b] *coefficients with respect to ERA-40 data for December 2 meter temperature hindcasts over the Pan-VAMOS region for mean of all ensembles multi-model hindcasts started in November 1991 to 2001. Values between -0.3 and 0.3 are not shaded on the graphs.*

the next, but anomaly correlation coefficients were much more chaotic with high oscillations (not shown). As for temporal coefficients, the same trend of higher correlation and anomaly correlation over the Tropics still holds for boreal summer, meaning that values over the Great Plains and US Southwest are often insignificant (lower than 0.3) whereas the multi-model performs relatively better over the Inter-Americas zone. However, ACCs were noticed to be lower over the NAMS regions than over the SAMS regions during austral summer. As seen before, areas with high ACCs are those with the highest CCs, and ACCs are lower in general than CCs.

### 3.2.2 Correlation coefficients for SST predictions

As seen earlier, SSTs play a significant role in local forcing and remote influence on precipitation patterns. Successfully predicting SSTs, particularly SST anomalies, is therefore of importance to avoid adding further error to precipitation predictions. Furthermore, in coupled ocean-atmosphere global circulation models, SSTs provide lower boundary forcing for the atmospheric component, and accurate SSTs are a pre-requisite to efficient seasonal forecasts. In this section, further assessment of the multi-model's performance in SST predictions during austral summer and austral spring is shown with monthly ACC maps illustrating the multi-models' temporal anomaly prediction skill.

#### Austral summer

Figure 3.20 page 70 shows temporal anomaly correlation coefficients over the Pan-VAMOS region for the multi-model SST hindcasts for austral summer. Anomaly correlation coefficients generally decrease with model run time. Over the El Niño 3.4 region, anomaly correlation coefficients are very high, with values between 0.9 and 1 for the December hindcasts and over 0.7 for February hindcasts. These results are similar to those presented in the DEMETER reference paper for the 1980-2001 1-month lead El Niño SST hindcast ACCs over El Niño 3.4 (table 2 in [Palmer et al., 2004]), even if slightly lower. This may be due to the fact that ACCs calculated in this report are uncentered, and using climatology based only on the 11 year period of study. Another region of interest during austral summer is the South Atlantic, since SSTs over some regions of the South Atlantic can be related to particular precipitation patterns over parts of South America. As shown earlier with the SST hindcast biases (figure 2.20 page 39), hindcast skill over this region is lower than over the Tropical Pacific. In particular, over the Western Subtropical South Atlantic region (boxed region in figure 3.20) ACCs are often lower than 0.3, and results worsen with hindcast run time. This implies that local SST anomalies east of the La Plata Basin region aren't captured correctly by the multi-model hindcasts, and could be one reason of model errors in precipitation hindcasts.

#### Austral spring

Other links between SSTs and austral summer precipitation were exhibited for austral spring SSTs, which are the fields of interest in this paragraph. Figures for September, October and November ACCs are shown in page 71. As for austral summer hindcasts, performance is higher over the El Niño 3.4 region and the Tropical Pacific in general than over the subtropical South Atlantic. Over the Pacific Ocean, the SST ACCs' geographical distribution seems more homogeneous than during austral summer, and ACCs over El Niño 3.4 are slightly lower for one-month hindcasts (September compared to December) but don't decrease as sharply as for austral summer. Also, the El Niño 3.4 region isn't the region of highest ACCs, but instead is a tongue of slightly lower anomaly correlation in a very high ACC region (over 0.9) located between 10 degrees North and 10 degrees South.

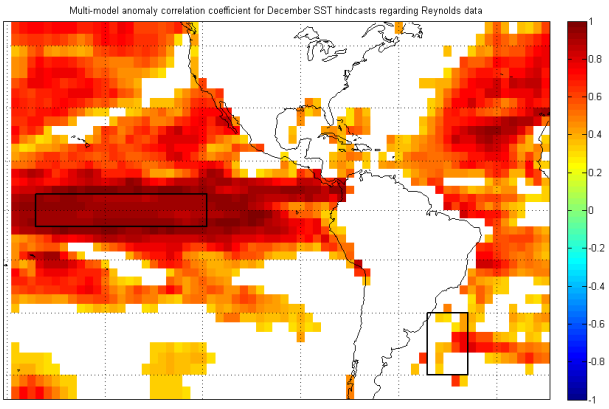


[a]

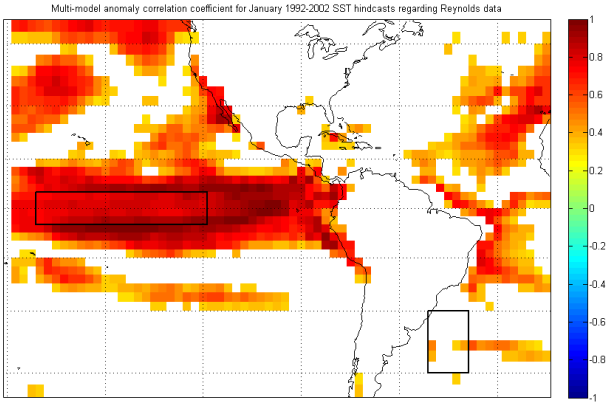


[b]

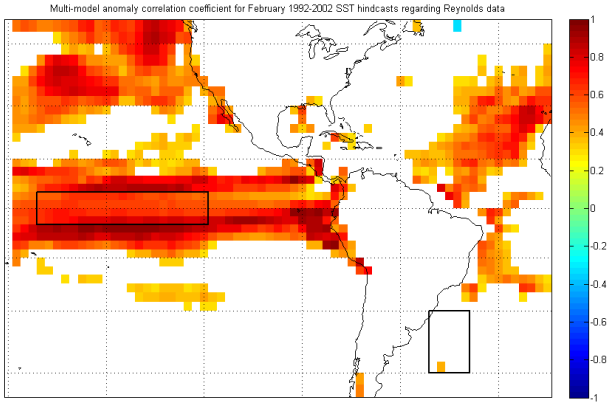


[c]

Figure 3.20: *Temporal anomaly correlation coefficients for December* [a] *January* [b] *and February* [c] *hindcasts with respect to Reynolds SST data over the Pan-VAMOS region. (Mean of all ensembles multi-model hindcasts started in November 1991 to 2001.)*

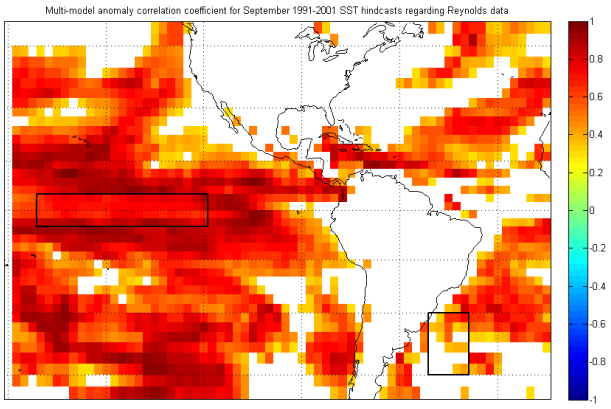


[a]

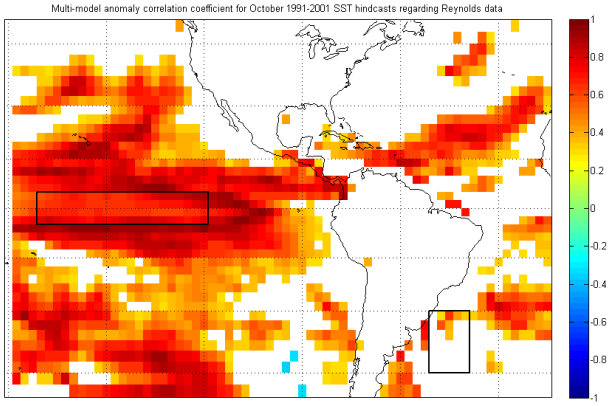


[b]

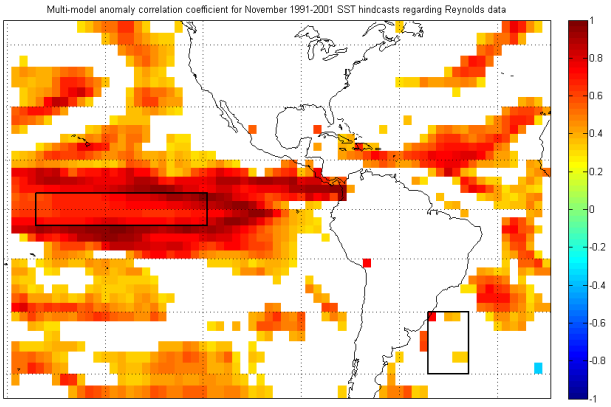


[c]

Figure 3.21: *Temporal anomaly correlation coefficients for September* [a] *October* [b] *and November* [c] *hindcasts with respect to Reynolds SST data over the Pan-VAMOS region. (Mean of all ensembles multi-model hindcasts started in August 1991 to 2001.)*

Over the South Atlantic, performance is slightly better than for austral summer. In any case, these results hint that models may have problems in resolving local sea surface temperature anomalies, which could affect precipitation hindcast performance.

## 3.3 Comparison with performances over the West African Monsoon region

In order to further assess DEMETER model performance over the NAMS and SAMS region, comparison with performance over another monsoon region is presented in this section. The West African Monsoon region was chosen for two main reasons: precipitation values are comparable to those over the NAMS region, and the DEMETER website provides statistical scores calculated for daily fields over the 1980-2001 period.

The DEMETER website shows statistical scores and indices over the West African region defined as the box delimited by 0° N to 20° N and 20° W to 25° E. These scores were calculated using the daily DEMETER hindcasts, but comparison with results for the monthly DEMETER hindcasts used in this project can give an idea of model performance over the American Monsoon systems relative to other monsoon systems.

### 3.3.1 Description of the West African Monsoon System

As shown by figure 1.1 in this report, the monsoon over the Sahel region, referred to as the West African Monsoon System (WAMS) in this report, has very similar characteristics (annual cycle and precipitation amounts) as NAMS. As in the NAMS, the onset of WAMS takes place during late April to June, which is a first rainy season over Guinean Africa. The ITCZ, along with maximum precipitation, are centered at a mean latitude of 5° N. The beginning of the WAMS peak season is characterized by an abrupt shift of the ITCZ's latitude from 5° N to 10° N. This is accompanied by sustained rains over the Sudano-Sahelian area, with maximum average pentad rainfall greater than 9 mm/day. The precipitation patterns are mainly zonal over the WAMS area. The monsoon system decreases in intensity after end of August [Sultan et al., 2005].

### 3.3.2 DEMETER multi-model performance in precipitation forecasting

Figure 3.22 page 73 shows CMAP mean June, July and August precipitation for the 1991-2001 period, the mean of monthly DEMETER multi-model hindcasts for the same period, and the bias between both in mm/day. Color scales are the same as in the NAMS and SAMS figures for easier comparison. The multi-model seems to capture well the zonal distribution of mean precipitation during the peak monsoon season, and the intensity of the ITCZ off the western coast of Guinea and Sierra Leone, it underestimates greatly precipitation intensity over Cameroon and Nigeria, resulting in a strong negative bias over this region. This result is comparable to the misplacing of the SACZ and highest precipitation zones over South America during SAMS. Bias values are generally lower over Western Africa while mean precipitation values are comparable.

Further assessment of hindcast performance over the West African region is presented in the ECMWF DEMETER website [DEMETER website]. Two figures obtained on this website are shown in figures 3.23 and 3.24. Figure 3.23 shows ensemble dispersion in precipitation anomaly hindcasts with reference to GPCP data. The GPCP dataset is another combined gauge-satellite dataset for precipitation field estimations. A first glance at the figure shows that ensemble dispersion ranges from less than 1 mm/day to over 2 mm/day during the 1980-2001 period. This is higher than the range of GPCP precipitation interannual anomalies (lower than 0.5 mm/day). This shows that as was noticed for monthly hindcasts over the NAMS and SAMS region, model dispersion often surpasses interannual variation. Another observation is that the ensemble

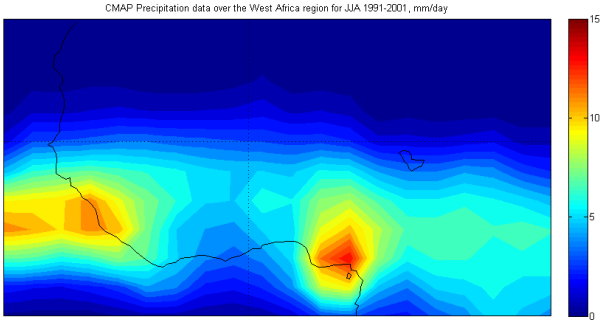


[a]

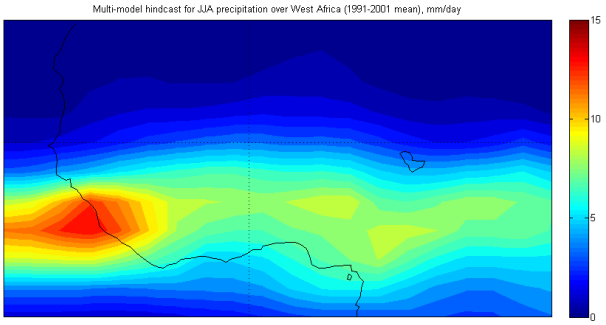


[b]

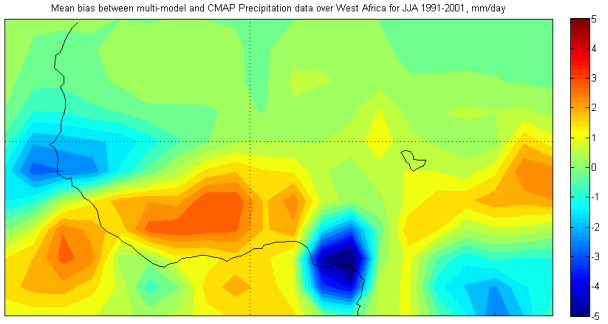


[c]

Figure 3.22: *Mean CMAP precipitation data* [a] *, multi-model hindcast for precipitation* [b] *and multi-model bias with respect to CMAP* [c] *for the West African Monsoon peak season (JJA) (mean of all ensembles monthly multi-model hindcasts started in May 1991 to 2001). Units are mm/day.*

mean (referred to as the multi-model in this report) fails to reproduce precipitation anomaly patterns over the region. Variations in GPCP mean anomalies and multi-model mean anomalies are poorly correlated, however the multi-models' averaged precipitation anomaly's bias with respect to GPCP data is higher than 0.5 mm/day for only one year of the 1980-2001 period. However, figure 3.22 [c] shows that both negative and positive bias regarding precipitation data is obtained over the West Africa region used in the calculations, so these errors can easily compensate and explain a fair "average" multi-model performance. Other scores are also given in this figure: the ratio of model standard deviation with GPCP standard deviation is close to 1, showing that model dispersion is equivalent to precipitation actual variation, as was stated before. Root mean square error of models is of 0.39 mm/day, which is much lower than the values calculated over the SAMS and NAMS region, which were around 2 mm/day for the La Plata Basin region and 1 mm/day for the Great Plains region for December hindcasts. However, comparison should be done with caution, since the region of interest here is much larger than the specific regions studied in the project, and daily hindcasts may have been used for calculations instead of monthly means.

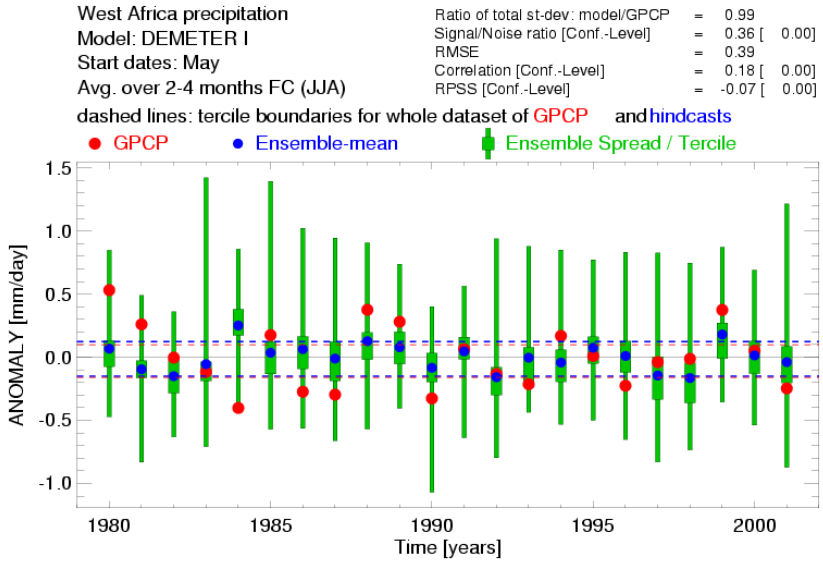


Figure 3.23: *Time series of the JJA precipitation hindcast performance, for hindcasts started in May 1980-2001. The multi-model ensembles' dispersion is shown by the box-and-whisker plot, each whisker representing a tercile of the ensembles. Blue and red dots are respectively the multi-model ensemble mean and the mean GPCP precipitation anomalies, and dashed lines mark the terciles of hindcast data (blue) and GPCP data (red). Other statistical score values are shown in the upper right corner.*

Figure 3.24 shows anomaly correlation coefficients calculated over West Africa for each JJA season. For all but three years of the 1980-2001 period, ACCs for the West African region are worth between -0.4 and 0.4, meaning low significance of model anomaly predictions. This is similar to results for monthly hindcasts for the 1991-2001 period over the NAMS and SAMS regions studied in this report.

More generally, models show similar scores when it comes to precipitation over the West African region than over NAMS or SAMS during the peak monsoon phases. Since calculations could have been done using daily hindcasts instead of monthly hindcasts, all scores may not be comparable, but no striking difference

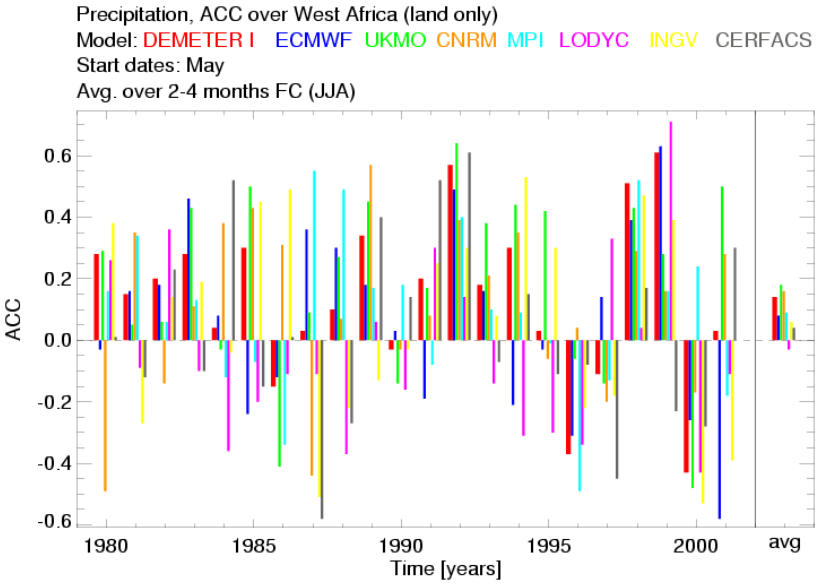


Figure 3.24: *Time series of anomaly correlation coefficients for the different model ensemble mean hindcasts regarding GPCP data, calculated over the West African region with the daily hindcast and precipitation values.*

in precipitation forecasting between these regions was found while examining the figures on the DEMETER website.

### 3.3.3 DEMETER multi-model performance in 2 meter temperature forecasting

Since other parameters were studied to assess multi-model performance over the SAMS and NAMS regions, similar assessment was examined for these parameters over West Africa. Figure 3.25 the mean multi-model hindcast bias with ERA-40 2 meter temperature for boreal summer 1991 to 2001 over West Africa. The multi-model captures the geographical distribution of 2 meter temperature over West Africa since bias doesn't exceed -1 to 1 degree in most regions. No particular pattern between 2 meter temperature bias and precipitation bias can be seen. This is confirmed by higher ACCs over West Africa, with an average of 0.4 (not shown).

Therefore, 2 meter temperature hindcasts seem to be more accurate over West Africa than over the NAMS and SAMS region. However, this does not necessarily imply better precipitation hindcasts, and proves that many other parameters than temperature can be responsible for poor precipitation forecasting.

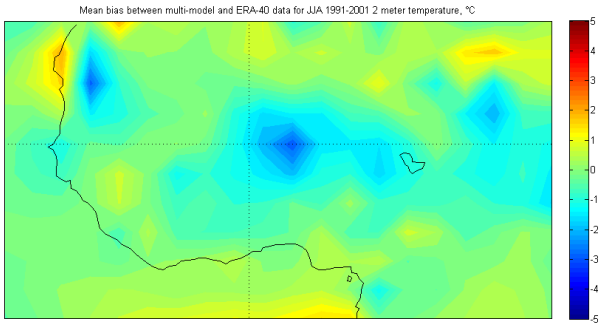


Figure 3.25: *Mean multi-model bias with respect to ERA-40 for the West African Monsoon peak season JJA (mean of all ensembles monthly multi-model hindcasts started in May 1991 to 2001). Units are in °C.*

# Part 4

# Conclusions and perspectives

In this project, DEMETER individual and multi-model performance during the peak monsoon seasons over the South and North America were assessed, using monthly mean hindcasts and reference data for the 1991-2001 period. An initial study of performances using bias and root mean square errors demonstrated that the multi-model technique, consisting in averaging all of the individual model ensembles, reduces both bias and root mean square error in precipitation and 2 meter temperature hindcasts with respect to reference data in comparison with the use of individual model ensemble means. Possible linkages between errors in 850 HPa circulation estimations, precipitation and 2 meter temperature predictions were exhibited over the La Plata Basin. General improvement using the multi-model is questionnable when it comes to SST predictions, since model dispersion is high, and excellent performances of some individual models are neutralized by high bias for other models when calculating the multi-model hindcast.

Further examination of model performances using more specific statistical scores exhibited a high dispersion between model hindcasts, which is often higher than the actual interannual variability of the field of study. This implies that the multi-model could experience some problems in capturing this interannual variability, signal being sometimes less important than noise. Spatial and temporal correlation and anomaly correlation coefficients were calculated for the multi-model and two individual models, showing that models correlation and anomaly correlation capabilities varied very highly depending on the region (for temporal coefficients) or the year (for spatial coefficients). These results are consistent with those shown on the DEMETER website, but should however be interpreted with caution, since they were calculated using monthly mean fields. They tend to show the difficulty in using global coupled models for efficient seasonal predictions.

This project encountered two major limitations: the short time period of study made interannual variability studies and temporal correlations difficult to evaluate or sometimes insignificant, and the use of monthly means considerably reduced the possibilities of score calculations. Further developments could therefore include the study of the DEMETER daily hindcast dataset with the same statistical scores, and the choice of a longer time period. Previous studies have shown that different multi-model ensemble combinations, such as a weighted superensemble with weights ajusted by linear regression [Yun et al., 2005] show higher performance than the unweighted ensemble mean studied in this project. Performance over the NAMS and SAMS region of such multi-models is yet to be assessed, however two conclusions from this project tend to suggest that this method is still very limited. One is that no particular individual model showed considerably better skill than others over each region of study, and the second limitation in using this technique comes from the very high model dispersion demonstrated in this report.

# Part 5

# Aknowledgements

The ECMWF DEMETER data and ERA-40 data used in this project were obtained from the ECMWF data server. The CMAP Monthly Precipitation Data was provided by the NCEP/CPC. Reynolds SSTs were downloaded from the PODAAC/JPL/NASA public FTP server.

I would particularly like to thank my tutor, Dra. Celeste SAULO, for her help and support during this project. She enabled me to progress in my comprehension of meteorology in general and to satisfy my curiosity by providing me with very interesting papers and her own personal insight on the subject. Special thanks also to Dr. Mario Nuñez and Hervé Le Treut who made this internship possible at the CIMA/CONICET in Buenos Aires. I would also like to thank Juan Ruiz and Paula Gonzalez for their help in using Matlab for data assimilation and plotting purposes, they were always ready to give a helping hand. Last but not least, I want to thank the "becarias" from the CIMA who were great companions during this internship, muchas gracias chicas para haber tolerado mi español muy malo, compartido el mate y sido tan simpaticas conmigo ! Nos vemos !

# Bibliography


[Vera et al., 2006] Vera, C., W. Higgins, J. Amador, T. Ambrizzi, R. Garreaud, D. Gochis, D. Gutzler, D. Lattenmaier, J. Marengo, C. R. Mechoso, J. Nogues-Paegle, P. L. Silva Dias and C. Zhang, 2006: Toward a Unified View of the American Monsoon System *Journal of Climate,* **19** 4977-5000.

[Higgins et al., 1997] Higgins, R. W., Y. Yao and X. L. Wang, 1997: Influence of the North American Monsoon System on the U.S. Summer Precipitation Regime *Journal of Climate,* **10** 2600-2622.

[Marengo et al., 2004] Marengo, Jose A., W. Soares, C. Saulo and M. Nicolini, 2004: Climatology of the Lower-Level Jet East of the Andes as Derived from the NCEP-NCAR Reanalyses: Characteristics and Temporal Variability *Journal of Climate,* **17** No. 12, 2261-2280.

[Nobre et al., 2006] Nobre, P., J.A. Marengo, I.F.A. Cavalcanti, G. Obregon, V. Barros, I. Camilloni, N. Campos and A. G. Ferreira, 2006: Seasonal-to-Decadal Predictability and Prediction of South American Climate*Journal of Climate,* **19** 5988-6004.

[Paegle and Mo, 1997] Julia Nogues-Paegle and Kingste C. Mo, 1997: Alternating Wet and Dry Conditions over South America during Summer *Monthly Weather Review,* **125** 279-291.

[Liebmann et al., 2004] Liebmann, Brant, G. N. Kiladis,C. Vera, C. Saulo and L. Carvalho, 2004: Subseasonal Variations of Rainfall in South America in the Vicinity of the Low-Level Jet East of the Andes and Comparison to Those in the South Atlantic Convergence Zone *Journal of Climate,* **17** 3829-3842.

[Grimm et al., 2007] Grimm, Alice M., J. Pal and F. Giorgi, 2007: Connection between Spring Conditions and Peak Summer Monsoon Rainfall in South America: Role of Soil Moisture, Surface Temperature, and Topography in Eastern Brazil. *Journal of Climate,* submitted 14 September 2006, revised 15 January 2007.

[Ferreira et al., 2006] Ferreira, Lorena J., C. Saulo, J. Ruiz and M. Seluchi, 2006: The Impact of Land Use Changes over the Low Level Circulation related to the Northwestern Argentinean Low *Proceedings of the 8th ICSHMO,* p. 1029-1035.

[Collini et al., 2006] Collini, Estela A., E. H. Berbery, V. Barros, 2006: Seasonal Dependence of Surface-Atmosphere Interactions for Subtropical South America *Proceedings of the 8th ICSHMO,* p. 999-1004.

[Gutzler et al., 2005] Gutzler, D. S., H.-K. Kim, R. W. Higgins, H.-M. Juang, M. Kanamitsu, K. Mitchell, K. Mo, P. Pegion, E. Ritchie, J.-K. Schemm, S. Schubert, Y. Song and R. Yang, 2005: The North American Monsoon Model Assessment Project: Integrating Numerical Modeling into a Field-based Process Study *Bulletin of the American Meteorological Society,* **86**, Issue 10, 1423-1429.

[Higgins and Gochis, 2007] Wayne Higgins and David Gochis, 2007: Synthesis of Results from the North American Monsoon Experiment (NAME) Process Study *Journal of Climate,* **20** Issue 9, 1601-1607.

[Kalnay, 2003] Atmospheric Modeling, Data Assimilation, and Predictability, *Cambridge University Press,* 2003. Pages used: **Chapter 1** section 1.7, pp 25-31; **Chapter 6** Atmosphere predictability and ensemble forecasting, pp 205-260.

[Palmer et al., 2004] Palmer, T. N., A. Alessandri, U. Andersen, P. Cantelaube, M. Davey, P. Délécluse, M. Déqué, E. Diez, F.J. Doblas-Reyes, H. Feddersen, R. Graham, S. Gualdi, J.-F. Guérémy, R. Hagedorn, M. Hoshen, N. Keenlyside, M. Latif, A. Lazar, E. Maisonnave, V. Marletto, A.P. Morse, B. Orfila, P. Rogel, J.-M. Terres and M.C. Thomson, 2004: Development of a European multi-model ensemble system for seasonal to inter-annual prediction (DEMETER) *Bulletin of the American Meteorological Society,* **85** 853-872.

[Seth et al., 2007] Seth, Anji, S. Rauscher, S. Camargo, J.H. Qian and J.S. Pal, 2007: RegCM3 regional climatologies for South America using reanalysis and ECHAM global model driving fields. *Climate Dynamics,* **28** No. 5, 461-480.

[Mo et al., 2005] Mo, Kingste C., J.-K. Schemm, H. M. H. Juang and R. Wayne Higgins, 2005: Impact of Model Resolution on the Prediction of Summer Precipitation over the United States and Mexico. *Journal of Climate,* **18** 3910-3927.

[Xie and Arkin, 1996] P. Xie and P. A. Arkin, 1996: Global precipitation: a 17-year monthly analysis based on gauge observations, satellite estimates, and numerical model outputs. *Bulletin of the American Meteorological Society,* **78** 2539-2558.

[Uppala et al., 2005] Uppala, S.M., Kållberg, P.W., Simmons, A.J. et al., 2005: The ERA-40 re-analysis. *Quart. J. R. Meteorol. Soc.,* **131** 2961-3012.

[Reynolds et al., 1994] Reynolds, R. W. and T. M. Smith, 1994: Improved global sea surface temperature analyses using optimum interpolation. *Journal of Climate,* **7** 929-948.

[IRI website] http://iri.columbia.edu/climate/ENSO/enso.html *The International Research Institute for Climate and Society website on ENSO.*

[Paegle and Mo, 2002] Julia Nogues-Paegle and Kingste Mo, 2002: Linkages between Summer Rainfall Variability over South America and Sea Surface Temperature Anomalies *Journal of Climate,* **15** 1389-1407.

[Doyle and Barros, 2002] Moira E. Doyle and Vicente R. Barros, 2002: Midsummer Low-Level Circulation and Precipitation in Subtropical South America and Related Sea Surface Temperature Anomalies in the South Atlantic *Journal of Climate,* **15** 3394-3410.

[Sultan et al., 2005] Sultan, Benjamin, C. Baron, M. Dingkhun, B. Sarr and S. Janicot, 2005: Agricultural impacts of large-scale variability of the West African monsoon. *Agricultural and Forest Meteorology,* **vol. 128** issues 1-2, 93-110.

[DEMETER website] http://www.ecmwf.int/research/demeter/ *Contains specific information on the DEMETER project, dataset and verification results.*

[Yun et al., 2005] Yun, W. T., L. Stefanova, A. K. Mitra, T. S. V. Vijaya Kumar, W. Dewar and T. N. Krishnamurti, 2005: A multi-model superensemble algorithm for seasonal climate prediction using DEMETER forecasts *Tellus,* A **57** 280-289.